DEGREE PROJECT IN ELECTRICAL ENGINEERING,
SECOND CYCLE, 30 CREDITS
STOCKHOLM, SWEDEN 2017

Robust Decentralized Control of Cooperative Multi-robot Systems

An inter-constraint Receding Horizon approach

ALEXANDROS FILOTHEOU

KTH ROYAL INSTITUTE OF TECHNOLOGY
SCHOOL OF ELECTRICAL ENGINEERING

MASTER'S DEGREE PROJECT

Robust Decentralized Control of Cooperative Multi-robot Systems: an inter-constraint Receding Horizon approach

Author

Alexandros Filotheou

Supervisor

Alexandros Nikou

Examiner

Prof. Dimos V. Dimarogonas

Stockholm, Sweden, June 2017

In partial satisfaction of the requirements for the degree of Master of Science

Degree Project in Automatic Control, Second Cycle (EL205X)

Automatic Control Department − School of Electrical Engineering

KTH Royal Institute of Technology

Abstract

In this work, a robust decentralized model predictive control regime for a team of cooperating robot systems is designed. Their assumed dynamics are in continuous time and non-linear. The problem involves agents whose dynamics are independent of one-another, and its solution couples their constraints as a means of capturing the cooperative behaviour required. Analytical proofs are given to show that, under the proposed control regime: (a) Subject to initial feasibility, the optimization solved at each step by each agent will always be feasible, irrespective of whether or not disturbances affect the agents. In the former case, recursive feasibility is established through successive restriction of each agent's constraints during the periodic solution to its respective optimization problem. (b) Each (sub)system can be stabilized to a desired configuration, either asymptotically when uncertainty is absent, or within a neighbourhood of it, when uncertainty is present, thus attenuating the affecting disturbance. In this context, disturbances are assumed to be additive and bounded. Simulations verify the efficacy of the proposed method over a range of different operating environments.

Contents

Introduction

Research into decentralized control of interacting systems has been well underway for the past three decades by academic, industrial or commercial, civilian or military parties. Decentralized Control schemes and strategies are now used in such areas as those concerned with controlling the trajectory and formation of mobile agents, the area of jurisdiction of an air traffic controller[1], or in the field of micro-robotics [2][3]. Focus has been given on research regarding unmanned autonomous vehicles − as in unmanned ground, underground and air vehicles, better known as UGV's, UUV's and UAV's [4][5][6][7]. In principle, all above areas are concerned with controlling a network of mobile agents under certain conditions, such as avoiding collisions with their environment or with one-another, and with the actuation forces applied to each agent having to satisfy certain constraints.

The nature of such problems is suitable for approach by the strategy of Model Predictive / Receding Horizon - Control since it can directly incorporate the consideration of such limitations, while being able to handle linear and non-linear, continuous-time or discrete-time underlying systems − see [8][9][10], and the thorough elementary review [11]. In principle, under this method, each agent solves a finite horizon optimal control problem (FHOCP) on-line given information on its configuration and that of its neighbours and, in general, information per-

taining to its environment. The optimization problem is posed in a way such that all relevant and necessary constraints are explicitly included. In decentralized approaches, the dynamics of each system may not be directly influencing the dynamics of other neighbouring systems (as a direct source of uncertainty for instance), but may only do so indirectly, as information on their state is incorporated in the cost function used, or in the constraints considered (such as in the case of maintaining a set distance between agents), or in both.

The literature on approaching the problem of decentralized stabilization of a compound system of neighbouring agents is large and evolving by branching out. In [7] ([12]), the authors consider agents modeled as discs whose sensing range is not unlimited, and whose dynamics are in continuous time and are described by the single (double) integrator. In this case, all agents are assigned a desired configuration that need not be known to any other agent than the one assigned to. The problem is approached by designing and utilizing decentralized navigation functions [13]. However, this method is problematic in that, in practice, it requires preposterously large actuation forces (up to 10^5), it may easily give rise to numerical instability, and it requires harsh assumptions on the initial conditions of the problem (for instance, when an agent needs to bypass an obstacle and the problem is symmetric, the method will direct it onto the obstacle instead of making it overtake it). In [14], the assignation regime is altered to a leader-follower configuration, leading to the added benefit of limiting the overall required sensor load, as resources are freed by having only leading/anchor agents being able to discern global positions or relative positions to landmarks. In this case the dynamics of both leaders and followers are based on the Laplacian consensus equation, and they directly include the state of neighbouring agents.

In [5], what is demonstrated in detail is a decentralized multi-agent MPC stabilization approach that couples agents chosen as neighbours during the solution of their optimization problems in the running cost but not through their constraints. An interesting compatibility constraint is introduced in order to keep a degree of consistency between an agent's states predicted by its neighbours and their real values. Plant-model mismatch or uncertainties are omitted. By contrast, in [15] and [4], robust centralized and decentralized control laws are designed for UAV's. In order to attenuate disturbances, they use a tightening of constraints regime that, in general contrast to this work, propagates among agents, instead of through

each of them. This work extends that of [16] in the multi-agent dimension, and it translates the constraints' tightening regime in the face of disturbances in the continuous-time case.

This work considers the stabilization of a network of multiple non-point agents whose dynamics are in continuous time and non-linear, whose sensing capabilities are not unlimited, in the absence and in the presence of additive bounded disturbances. In both cases, it designs control regimes which under sufficient conditions stabilize the compound multi-agent system. The problem is approached through the MPC framework in a decentralized manner in that each agent solves its own FHOCP, having availability of information on the current and planned actions of all agents within its sensing range. Agents needed to maintain connectivity with one-another are termed neighbours, and their determined interactivity ranges are explicitly defined through the constraints of the optimization problems that each of them solve.

This document is structured as follows: Chapter 1 introduces the notation used henceforth, and auxiliary prerequisites of the rest of the work. Chapter 2 poses its motivating problem. Part II is composed of the detailed feasibility and stability guarantee proofs for the cases of absent and present disturbances. Part III verifies the reality of the designed control regimes through simulations on four discrete scenarios, in ascending order of difficulty. Part IV concludes this work and poses relevant future directions of it. Appendix A is composed of proofs of various lemmas that this work introduces. Appendices B and C include the complete collection of results derived from the all determined simulations.

Part I

The problem

1

Preliminaries

1.1 Notation

The set of positive integers is denoted by $\mathbb{N}$. The real n-coordinate space, $n \in \mathbb{N}$, is denoted by $\mathbb{R}^n$; $\mathbb{R}^n_{\geq 0}$ and $\mathbb{R}^n_{>0}$ are the sets of real n-vectors with all elements nonnegative and positive, respectively. Given a set S, we denote by $|S|$ its cardinality. The notation $\|\mathbf{x}\|$ is used for the Euclidean norm of a vector $\mathbf{x} \in \mathbb{R}^n$; $\|\mathbf{x}\|_P$ denotes the $\boldsymbol{P}$-norm of $\mathbf{x}$. Given matrix $\boldsymbol{A}$, $\lambda_{\min}(\boldsymbol{A})$ and $\lambda_{\max}(\boldsymbol{A})$ denote the minimum and maximum eigenvalues of $\boldsymbol{A}$, respectively. Its minimum and maximum singular values are denoted by $\sigma_{\min}(\boldsymbol{A})$ and $\sigma_{\max}(\boldsymbol{A})$ respectively. Given two sets A and B, the operation $A \oplus B$ denotes the Minkowski addition, defined by $A \oplus B = \{\mathbf{a}+\mathbf{b},\ \mathbf{a} \in A, \mathbf{b} \in B\}$. Similarly, the Minkowski $-$ or Pontryagin difference is defined by $A \ominus B = \{\mathbf{a}-\mathbf{b},\ \mathbf{a} \in A, \mathbf{b} \in B\}$. $\boldsymbol{I_n} \in \mathbb{R}^{n \times n}$ and $\boldsymbol{0}_{m \times n} \in \mathbb{R}^{m \times n}$ are the unit matrix and the $m \times n$ matrix with all entries zeros respectively. The notation $\mathcal{B}(\mathbf{c}, r) \triangleq \{\mathbf{x} \in \mathbb{R}^3 : \|\mathbf{x}-\mathbf{c}\| \leq r\}$ is reserved for the 3D sphere of radius $r \in \mathbb{R}_{\geq 0}$ and center located at $\mathbf{c} \in \mathbb{R}^3$.

The vector expressing the coordinates of the origin of frame $\{j\}$ in frame $\{i\}$ is denoted by $\mathbf{p}_{j\triangleright i}$. When this vector is expressed in 3D space in a third frame, frame $\{k\}$, it is denoted by $\mathbf{p}^k_{j\triangleright i}$. The angular velocity of frame $\{j\}$ with respect to frame $\{i\}$, expressed in frame $\{k\}$ coordinates, is denoted by $\boldsymbol{\omega}^k_{j\triangleright i} \in \mathbb{R}^3$. We further denote by $\mathbf{q}_{j\triangleright i} \in \mathbb{T}^3$ the Euler angles representing the orientation of frame $\{j\}$ with respect to frame $\{i\}$, where $\mathbb{T}^3$ is the 3D torus. We also use the notation $\mathbb{M} = \mathbb{R}^3 \times \mathbb{T}^3$. For notational brevity, when a coordinate frame corresponds to the inertial frame of reference $\{\mathcal{O}\}$, we will omit its explicit notation (e.g., $\mathbf{p}_i = \mathbf{p}_{i\triangleright\mathcal{O}} = \mathbf{p}^{\mathcal{O}}_{i\triangleright\mathcal{O}}$, and $\boldsymbol{\omega}_i = \boldsymbol{\omega}_{i\triangleright\mathcal{O}} = \boldsymbol{\omega}^{\mathcal{O}}_{i\triangleright\mathcal{O}}$).

1.2 Auxiliary Prerequisites

This section features auxiliary and useful theorems, lemmas and definitions needed to support the advocated solutions in part II.

Lemma 1.2.1. [17] *The Grönwall-Bellman Inequality*
Let $\lambda : [a, b] \to \mathbb{R}$ be continuous and $\mu : [a, b] \to \mathbb{R}$ be continuous and non-negative. If a continuous function $y : [a, b] \to \mathbb{R}$ satisfies

$$y(t) \leq \lambda(t) + \int_a^t \mu(s)y(s)ds$$

for $a \leq t \leq b$, then on the same interval

$$y(t) \leq \lambda(t) + \int_a^t \lambda(s)\mu(s)e^{\int_s^t \mu(\tau)d\tau}ds$$

In particular, if $\lambda(t) \equiv \lambda$ is a constant, then

$$y(t) \leq \lambda e^{\int_a^t \mu(\tau)d\tau}ds$$

If $\lambda(t) \equiv \lambda$ and $\mu(t) \equiv \mu$ are both constants, then

$$y(t) \leq \lambda e^{\mu(t-a)}$$

Definition 1.2.1. [17] (*Class $\mathcal{K}$ function*)

A continuous function $\alpha : [0, a) \to [0, \infty)$ is said to belong to class $\mathcal{K}$ if

1. it is strictly increasing
2. $\alpha(0) = 0$

If $a = \infty$ and $\lim_{r\to\infty} \alpha(r) = \infty$, then function α is said to belong to class $\mathcal{K}_\infty$

Definition 1.2.2. [17] (*Class $\mathcal{KL}$ function*)

A continuous function $\beta : [0, a) \times [0, \infty) \to [0, \infty)$ is said to belong to class $\mathcal{KL}$ if

1. for a fixed s, the mapping $\beta(r, s)$ belongs to class $\mathcal{K}$ with respect to r
2. for a fixed r, the mapping $\beta(r, s)$ decreases with respect to s
3. $\lim_{s\to\infty} \beta(r, s) = 0$

Lemma 1.2.2. [18] (*A modification of Barbalat's lemma*)

Let f be a continuous, positive-definite function, and $\mathbf{x}$ be an absolutely continuous function in $\mathbb{R}$. If the following hold:

- $\|\mathbf{x}(\cdot)\| < \infty$
- $\|\dot{\mathbf{x}}(\cdot)\| < \infty$
- $\lim_{t\to\infty} \int_0^t f\big(\mathbf{x}(s)\big) ds < \infty$

then $\lim_{t\to\infty} \|\mathbf{x}(t)\| = 0$

Definition 1.2.3. [19] (*Input-to-State Stability*)
A nonlinear system $\dot{\mathbf{x}} = f(\mathbf{x}, \mathbf{u})$, $\mathbf{x} \in X$, $\mathbf{u} \in U$ with initial condition $\mathbf{x}(t_0)$ is said to be *locally Input-to-State Stable (ISS)* if there exist functions $\sigma \in \mathcal{K}$ and $\beta \in \mathcal{KL}$ and constants $k_1, k_2 \in \mathbb{R}_{>0}$ such that

$$\|\mathbf{x}(t)\| \leq \beta\big(\|\mathbf{x}(t_0)\|, t\big) + \sigma\big(\|\mathbf{u}\|_\infty\big), \ \forall t \geq 0$$

for all $\mathbf{x}(t_0) \in X$ and $\mathbf{u} \in U$ satisfying $\|\mathbf{x}(t_0)\| \leq k_1$ and $\sup_{t>0} \|\mathbf{u}(t)\| = \|\mathbf{u}\|_\infty \leq k_2$.

Remark 1.2.1. [16] A nonlinear system $\dot{\mathbf{x}} = f(\mathbf{x}, \mathbf{u})$, $\mathbf{x} \in X$, $\mathbf{u} \in U$ which is input-to-output stable, is asymptotically stable in the absence of disturbances $\mathbf{u}$, or if the disturbance is decaying. If the disturbance is merely bounded, then the evolution of the system is *ultimately bounded* in a set whose size depends on the bound of the disturbance.

Definition 1.2.4. [19] (*ISS Lyapunov function*)
A continuous function $V(\mathbf{x}) : \Psi \to \mathbb{R}_{\geq 0}$ for the nonlinear system $\dot{\mathbf{x}} = f(\mathbf{x}, \boldsymbol{\delta})$ is said to be a *ISS Lyapunov function* in Ψ if there are class $\mathcal{K}$ functions α_1, α_2, α_3 and σ, such that

$$\alpha_1\big(\|\mathbf{x}\|\big) \leq V\big(\mathbf{x}\big) \leq \alpha_2\big(\|\mathbf{x}\|\big), \ \forall \mathbf{x} \in \Psi$$

and

$$\frac{d}{dt} V\big(\mathbf{x}\big) \leq \sigma\big(\|\boldsymbol{\delta}\|\big) - \alpha_3\big(\|\mathbf{x}\|\big), \ \forall \mathbf{x} \in \Psi, \boldsymbol{\delta} \in \Delta$$

V is an ISS Lyapunov function if $\Psi = \mathbb{R}^n$, $\Delta = \mathbb{R}^m$, and α_1, α_2, α_3, $\sigma \in \mathcal{K}_\infty$.

Remark 1.2.2. With regard to definition (1.2.4), the statement

$$\frac{d}{dt}V\big(\mathbf{x}\big) \leq \sigma\big(\|\boldsymbol{\delta}\|\big) - \alpha_3\big(\|\mathbf{x}\|\big),\ \forall \mathbf{x} \in \Psi, \boldsymbol{\delta} \in \Delta$$

is equivalent to

$$V\big(\mathbf{x}(t_1)\big) - V\big(\mathbf{x}(t_0)\big) \leq \int_{t_0}^{t_1} \Big(\sigma\big(\|\boldsymbol{\delta}(t)\|\big) - \alpha_3\big(\|\mathbf{x}(t)\|\big)\Big)dt,\ \forall \mathbf{x} \in \Psi,\ \boldsymbol{\delta} \in \Delta,\ t \in [t_0, t_1]$$

Theorem 1.2.1. [19]
A nonlinear system $\dot{\mathbf{x}} = f(\mathbf{x}, \mathbf{u})$ is said to be *Input-to-State Stable* in Ψ if and only if it admits an ISS Lyapunov function in Ψ.

Definition 1.2.5. (*Positively Invariant Set*)
Consider a dynamical system $\dot{\mathbf{x}} = f(\mathbf{x})$, $\mathbf{x} \in \mathbb{R}^n$, and a trajectory $\mathbf{x}(t;\ \mathbf{x}_0)$, where $\mathbf{x}_0$ is the initial condition. The set $S = \{\mathbf{x} \in \mathbb{R}^n : \gamma(\mathbf{x}) = 0\}$, where γ is a valued function, is said to be *positively invariant* if the following holds:

$$\mathbf{x}_0 \in S \Rightarrow \mathbf{x}(t;\ \mathbf{x}_0) \in S,\ \forall t \geq t_0$$

Intuitively, this means that the set S is positively invariant if a trajectory of the system does not exit it once it enters it.

Definition 1.2.6. [20] (*Robust positively-invariant set*)
A set $\Psi \in \mathbb{R}^n$ is a robust positively invariant set for the nonlinear system $\dot{\mathbf{x}} = f(\mathbf{x}, \boldsymbol{\delta})$ if $f(\mathbf{x}, \boldsymbol{\delta}) \in \Psi$, for all $\mathbf{x} \in \Psi$ and for all $\boldsymbol{\delta} \in \Delta$.

The proofs of lemmas or properties whose reference is not cited are provided in appendix A.

1.3 Model Predictive control for non-linear continuous-time systems

The equations describing a model of a system are doubly powerful: they are *expressive* inasmuch as they are a collection of properties of the system, and they are *predictive*: they provide the ability to predict future values of relevant variables. A natural use for a model for control design purposes is the calculation of expected future values of the controlled variables as a function of possible control actions. This way, it is possible to choose a control action which is the optimal according to a given criterion, possibly while satisfying constraints on the controlled variables and control inputs. It is reasonable for a closed-form solution of the state-feedback law to be sought. Although this is possible when the system is linear and constraints are absent, it is impossible or infeasible in the general case. Fortunately, the problem can be bybassed altogether by solving an open-loop optimization problem periodically (or even aperiodically), applying a fragment of the resulting control input to the system, and repeating the process ad infinitum. Control approaches using this strategy (with variations) are referred to as *Model Predictive Control* (MPC), or *Receding Horizon Control*. In this context, the term horizon refers to the period of time or timesteps considered during the solution of the optimization problem.

In greater detail, in its pure form, the MPC strategy assumes the following form: at an initial sampling time t, the controller, having measurements of the states to be controlled, predicts the dynamic behaviour of the system over a prediction horizon T_p, that is until $t+T_p$, and determines the appropriate control input that minimizes a predetermined (open-loop) objective, typically under constraints involving the states and the inputs. The calculated input is then applied to the system until the next sampling time, at which time the above process is repeated. Hence the term "receding horizon" control.

When the system's dynamics are linear and there are is no system uncertainty (disturbances affecting the states of the system or model-plant mismatch) and no constraints are enforced, the input can be determined off-line by solving the optimization problem over an infinite horizon. In this case the input is applied to the open loop once, and the process is not repeated from then on. However, in general, systems may be non-linear, subject to disturbances,

partially descriptive, under constraints, while an infinite horizon approach may be practically infeasible. Hence, there are occasions when the optimization problem must be solved on-line under a finite time-horizon.

In its general form, nonlinear MPC (NMPC) possesses a unique usefulness in that it can directly incorporate nonlinear models for prediction, nonlinear constraints, and explicit constraints on the states of the system and its calculated/implemented inputs. Detailed descriptions and analyses of the NMPC strategy can be found in the notable [9] and [8].

2

Problem Formulation

2.1 System Model

Consider a set $\mathcal{V}$ of N rigid bodies, $\mathcal{V} = \{1, 2, \ldots, N\}$, $|\mathcal{V}| = N \geq 2$, operating in a workspace $W \subseteq \mathbb{R}^3$. A coordinate frame $\{i\}, i \in \mathcal{V}$ is attached to the center of mass of each body. The workspace is assumed to be modeled as a bounded sphere $\mathcal{B}\big(\mathbf{p}_W, r_W\big)$ expressed in an inertial frame $\{\mathcal{O}\}$.

We consider that over time t each agent $i \in \mathcal{V}$ occupies the space of a sphere $\mathcal{B}\big(\mathbf{p}_i(t), r_i\big)$, where $\mathbf{p}_i : \mathbb{R}_{\geq 0} \to \mathbb{R}^3$ is the position of the agent's center of mass, and $r_i < r_W$ is the radius of the agent's body. We denote by $\mathbf{q}_i(t) : \mathbb{R}_{\geq 0} \to \mathbb{T}^3$, the Euler angles representing the agents' orientation with respect to the inertial frame $\{\mathcal{O}\}$, with $\mathbf{q}_i \triangleq [\phi_i, \theta_i, \psi_i]^\top$, where $\phi_i, \psi_i \in [-\pi, \pi]$ and $\theta_i \in [-\frac{\pi}{2}, \frac{\pi}{2}]$. We define

$$\mathbf{x}_i(t) \triangleq [\mathbf{p}_i(t)^\top, \mathbf{q}_i(t)^\top]^\top, \ \mathbf{x}_i(t) : \mathbb{R}_{\geq 0} \to \mathbb{R}^3 \times \mathbb{T}^3 \equiv \mathbb{M}$$

$$\mathbf{v}_i(t) \triangleq [\dot{\mathbf{p}}_i(t)^\top, \boldsymbol{\omega}_i(t)^\top]^\top,\ \mathbf{v}_i(t) : \mathbb{R}_{\geq 0} \to \mathbb{R}^3 \times \mathbb{R}^3 \equiv \mathbb{R}^6$$

and model the motion of agent i under continuous second order dynamics:

$$\dot{\mathbf{x}}_i(t) = \boldsymbol{J}_i^{-1}(\mathbf{x}_i)\mathbf{v}_i(t), \tag{2.1a}$$

$$\mathbf{u}_i(t) = \boldsymbol{M}_i(\mathbf{x}_i)\dot{\mathbf{v}}_i(t) + \boldsymbol{C}_i(\mathbf{x}_i, \dot{\mathbf{x}}_i)\mathbf{v}_i(t) + \mathbf{g}_i(\mathbf{x}_i) \tag{2.1b}$$

In equation (2.1a), $\boldsymbol{J}_i : \mathbb{T}^3 \to \mathbb{R}^{6\times 6}$ is a Jacobian matrix that maps the non-orthogonal Euler angle rates to the orthogonal angular velocities $\mathbf{v}_i$:

$$\boldsymbol{J}_i(\mathbf{x}_i) = \begin{bmatrix} \boldsymbol{I}_3 & \boldsymbol{0}_{3\times 3} \\ \boldsymbol{0}_{3\times 3} & \boldsymbol{J}_q(\mathbf{x}_i) \end{bmatrix},\ \text{where } \boldsymbol{J}_q(\mathbf{x}_i) = \begin{bmatrix} 1 & 0 & \sin\theta_i \\ 0 & \cos\phi_i & -\cos\theta_i \sin\phi_i \\ 0 & \sin\phi_i & \cos\phi_i \cos\theta_i \end{bmatrix}$$

Matrix $\boldsymbol{J}_i$ is singular when $det(\boldsymbol{J}_i) = \cos\theta_i = 0 \Leftrightarrow \theta_i = \pm\frac{\pi}{2}$. The control scheme proposed in this thesis guarantees that this is always avoided, and hence equation (2.1a) is well defined.
In equation (2.1b), $\boldsymbol{M}_i : \mathbb{M} \to \mathbb{R}^{6\times 6}$ is the symmetric and positive definite *inertia matrix*, $\boldsymbol{C}_i : \mathbb{M} \times \mathbb{R}^6 \to \mathbb{R}^{6\times 6}$ is the *Coriolis matrix* and $\mathbf{g}_i : \mathbb{M} \to \mathbb{R}^6$ is the *gravity vector*. Finally, $\mathbf{u}_i \in \mathbb{R}^6$ is the control input vector representing the 6D generalized *actuation force* acting on the agent.
However, access to measurements of, or knowledge about these matrices and vectors was not hitherto considered. At this point we make the following assumption:

Assumption 2.1.1. (*Measurements and Access to Information from an Inter-agent Perspective*)

1. Agent i has access to measurements $\mathbf{p}_i, \mathbf{q}_i, \dot{\mathbf{p}}_i, \boldsymbol{\omega}_i, \forall i \in \mathcal{V}$, that is, vectors $\mathbf{x}_i, \mathbf{v}_i$ pertaining to himself,

2. Agent i has a (upper-bounded) sensing range d_i such that

$$d_i > \max\{r_i + r_j : \forall i, j \in \mathcal{V}, i \neq j\}$$

3. the inertia $\boldsymbol{M}_i$ and Coriolis $\boldsymbol{C}_i$ vector fields are bounded and unknown for all $i \in \mathcal{V}$

4. the gravity vectors $\mathbf{g}$ are bounded and known for all $i \in \mathcal{V}$

The consequence of points 1 and 2 of assumption (2.1.1) is that by defining the set of agents j that are within the sensing range of agent i at time t as

$$\mathcal{R}_i(t) \triangleq \{j \in \mathcal{V} : \mathbf{p}_j(t) \in \mathcal{B}\big(\mathbf{p}_i(t), d_i\big)\}$$

or equivalently

$$\mathcal{R}_i(t) \triangleq \{j \in \mathcal{V} : \|\mathbf{p}_i(t) - \mathbf{p}_j(t)\| \leq d_i\}$$

agent i also knows at each time instant t all

$$\mathbf{p}_{j\triangleright i}(t), \mathbf{q}_{j\triangleright i}(t), \dot{\mathbf{p}}_{j\triangleright i}(t), \boldsymbol{\omega}_{j\triangleright i}(t)$$

Therefore, agent i assumes access to all measurements

$$\mathbf{p}_j(t), \mathbf{q}_j(t), \dot{\mathbf{p}}_j(t), \boldsymbol{\omega}_j(t), \ \forall j \in \mathcal{R}_i(t), t \in \mathbb{R}_{\geq 0}$$

of all agents $j \in \mathcal{R}_i(t)$ by virtue of being able to calculate them using knowledge of its own $\mathbf{p}_i(t)$, $\mathbf{q}_i(t)$, $\dot{\mathbf{p}}_i(t)$, $\boldsymbol{\omega}_i(t)$.

In the workspace there is a set $\mathcal{L}$ of L *static obstacles*, $\mathcal{L} = \{1, 2, \ldots, L\}$, $L = |\mathcal{L}|$, also modeled as spheres, with centers at positions $\mathbf{p}_\ell \in \mathbb{R}^3$ with radii $r_\ell \in \mathbb{R}$, $\ell \in \mathcal{L}$. Thus, the obstacles are modeled by spheres $\mathcal{B}\big(\mathbf{p}_\ell, r_\ell\big)$, $\ell \in \mathcal{L}$. Their position and size in 3D space is assumed to be known a priori to each agent. The geometry of two agents i and j as well as an obstacle ℓ in workspace W is depicted in Fig. 2.1.

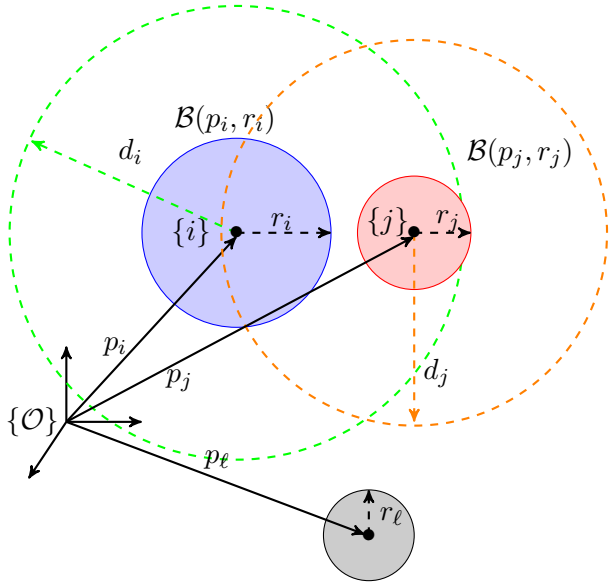

Figure 2.1: Illustration of two agents $i, j \in \mathcal{V}$ and a static obstacle $\ell \in \mathcal{L}$ in the workspace; $\{\mathcal{O}\}$ is the inertial frame, $\{i\}, \{j\}$ are the frames attached to the agents' center of mass, $\mathbf{p}_i, \mathbf{p}_j, \mathbf{p}_\ell \in \mathbb{R}^3$ are the positions of the centers of mass of agents i, j and obstacle ℓ respectively, expressed in frame $\{\mathcal{O}\}$. r_i, r_j, r_ℓ are the radii of the agents i, j and the obstacle ℓ respectively. d_i, d_j with $d_i > d_j$ are the agents' sensing ranges. In this figure, agents i and j are neighbours, since the center of mass of agent j is within the sensing range of agent i and vice versa: $\mathbf{p}_j \in \mathcal{B}\big(\mathbf{p}_i(t), d_i\big)$ and $\mathbf{p}_i \in \mathcal{B}\big(\mathbf{p}_j(t), d_j\big)$. Furthermore, the configuration between the two agents and the obstacle is a collision-free configuration.

Let us now define the distance between any two agents i, j at time t as $d_{ij,a}(t)$; that between agent i and obstacle ℓ as $d_{i\ell,o}(t)$; and that between an agent i and the origin of the workspace W as $d_{i,W}(t)$, with $d_{ij,a}, d_{i\ell,o}, d_{i,W} : \mathbb{R}^3 \to \mathbb{R}_{\geq 0}$:

$$d_{ij,a}(t) \triangleq \|\mathbf{p}_i(t) - \mathbf{p}_j(t)\|$$

$$d_{i\ell,o}(t) \triangleq \|\mathbf{p}_i(t) - \mathbf{p}_\ell\|$$

$$d_{i,W}(t) \triangleq \|\mathbf{p}_W - \mathbf{p}_i(t)\|$$

as well as constants

$$\underline{d}_{ij,a} \triangleq r_i + r_j$$

$$\underline{d}_{i\ell,o} \triangleq r_i + r_\ell$$

$$\overline{d}_{i,W} \triangleq r_W - r_i$$

$\forall i, j \in \mathcal{V}$, $i \neq j$, $\ell \in \mathcal{L}$. The latter stand for the minimum distance between two *agents*, the minimum distance between an *agent* and an *obstacle*, and the maximum distance between an *agent* and the origin of the workspace, respectively. They arise spatially as physical limitations and will be utilized in forming collision-avoidance constraints.

Based on these definitions, we will now define the concept of a *collision-free configuration*:

Definition 2.1.1. (*Collision-free Configuration*)

A collision-free configuration between

- any two agents $i, j \in \mathcal{V}$ is when $d_{ij,a}(t) > \underline{d}_{ij,a}$
- an agent $i \in \mathcal{V}$ and an obstacle $\ell \in \mathcal{L}$ is when $d_{il,o}(t) > \underline{d}_{il,o}$
- an agent $i \in \mathcal{V}$ and the workspace W boundary, is when $d_{i,W}(t) < \overline{d}_{i,W}$

at a generic time instant $t \in \mathbb{R}_{\geq 0}$. When all three conditions are met, we will simply refer to the overall configuration as a collision-free configuration.

2.2 Initial Conditions

We assume that at time $t = 0$ *all* agents are in a *collision-free configuration*, i.e.

$$d_{ij,a}(0) > \underline{d}_{ij,a}$$

$$d_{il,o}(0) > \underline{d}_{il,o}$$

$$d_{i,W}(0) < \overline{d}_{i,W}$$

$\forall i \in \mathcal{V}, \ell \in \mathcal{L}$. Before declaring further assumptions that relate to the initial conditions of the system's configuration, we have to give the definition of the *neighbour set* $\mathcal{N}_i$ of a generic agent $i \in \mathcal{V}$:

Definition 2.2.1. (*Neighbours Set*)
Agents $j \in \mathcal{N}_i$ are defined as the *neighbours* of agent $i \in \mathcal{V}$. The set $\mathcal{N}_i$ is composed of the indices of agents $j \in \mathcal{V}$ which

1. are within the sensing range of agent i at time $t = 0$, i.e. $j \in \mathcal{R}_i(0)$, *and*
2. are *intended* to be kept within the sensing range of agent i at all times $t \in \mathbb{R}_{>0}$

Therefore, while the composition of the set $\mathcal{R}_i(t)$ evolves and varies through time in general, the set $\mathcal{N}_i$ *should* remain invariant over time[1].
It is not necessary that all agents are assigned a set of agents with whom they should maintain connectivity; however, if *all* agents were neighbour-less, then the concept of *cooperation* between them would be void, since in that case the problem would break down into $|\mathcal{V}|$ individual problems of smaller significance or interest, while weakening the "multi-agent" perspective as well. Therefore, we assume that $\sum_i |\mathcal{N}_i| > 0$.
It is further assumed that $\mathcal{N}_i$ is given at $t = 0$, and that neighbouring relations are reciprocal, i.e. agent i is a neighbour of agent j if and only if j is a neighbour of i:

$$j \in \mathcal{N}_i \Leftrightarrow i \in \mathcal{N}_j, \ \forall i, j \in \mathcal{V}, i \neq j$$

Furthermore, it is assumed that at time $t = 0$ the Jacobians $\boldsymbol{J}_i$ are well-defined $\forall i \in \mathcal{V}$, and that the system (2.1) enjoys a continuous solution for all initial conditions. The assumptions which concern the initial conditions of the problem are formally summarized in assumption 2.2.1:

Assumption 2.2.1. (*Initial Conditions Assumption*)
At time $t = 0$

1. the sets $\mathcal{N}_i$ are known for all $i \in \mathcal{V}$ and $\sum_i |\mathcal{N}_i| > 0$

[1] This reason, and the fact that the proposed control scheme guarantees that $\mathcal{N}_i$ *will* remain invariant over time, is why we do not refer to this set as $\mathcal{N}_i(t)$.

2. all agents are in a collision-free configuration with each other, the obstacles $\ell \in \mathcal{L}$ and the workspace W boundary

3. all agents are in a singularity-free configuration:

$$-\frac{\pi}{2} < \theta_i(0) < \frac{\pi}{2},\ \forall i \in \mathcal{V}$$

2.3 Objective

Given the aforementioned structure of the system, the objective to be pursued is the *stabilization of all agents* $i \in \mathcal{V}$ starting from an initial configuration abiding by assumption (2.2.1) to a desired feasible configuration $\mathbf{x}_{i,des}, \mathbf{v}_{i,des}$, while satisfying all communication constraints, i.e. sustaining connectivity between neighbouring agents, and avoiding collisions between agents, obstacles, and the workspace boundary. The concept of a *desired feasible configuration* or *feasible steady-state configuration* is given in definition (2.3.1).

Definition 2.3.1. (*Feasible Steady-state Configuration*)
The desired steady-state configuration $\mathbf{x}_{i,des}$ of agents $\forall i \in \mathcal{V}, j \in \mathcal{N}_i$ is *feasible* if and only if

1. it is a collision-free configuration according to definition (2.1.1)

2. it does not result in violation of the communication constraints between neighbouring agents i, j, i.e. the following inequalities hold true simultaneously:

$$\|\mathbf{p}_{i,des} - \mathbf{p}_{j,des}\| < d_i$$

$$\|\mathbf{p}_{i,des} - \mathbf{p}_{j,des}\| < d_j$$

At this point we must address an issue that refers to the feasibility of the problem's solution and relates to the avoidance of collisions from an intra-environmental perspective. Namely, we demand that a solution be feasible if and only if the agent with the largest radius is able to pass through the spaces demarcated by (a) the two least distant obstacles, and (b) the obstacle closest to the boundary of the workspace and the boundary of the workspace itself. To this end, we formalize the relevant notions in definition (2.3.2).

Definition 2.3.2. (*Intra-environmental Arrangement*)

Let us define $\underline{d}_{\ell'\ell}$

$$\underline{d}_{\ell'\ell} \triangleq \min\{\|\mathbf{p}_\ell - \mathbf{p}_{\ell'}\| + r_\ell + r_{\ell'} : \ell, \ell' \in \mathcal{L}, \ell \neq \ell'\},$$

as the distance between the two least distant obstacles in the workspace, $\underline{d}_{\ell,W}$

$$\underline{d}_{\ell,W} \triangleq \min\{r_W - (\|\mathbf{p}_W - \mathbf{p}_\ell\| + r_\ell) : \ell \in \mathcal{L}\},$$

as the distance between the least distant obstacle from the boundary of the workspace and the boundary itself, and D

$$D \triangleq \min\{\underline{d}_{\ell'\ell}, \underline{d}_{\ell,W}\}$$

as the least of these two distances.

Given these notions, we can state an assumption on the feasibility of a solution to the problem that this work addresses:

Assumption 2.3.1. (*Intra-environmental Arrangement of Obstacles*)

All obstacles $\ell \in \mathcal{L}$ are situated inside the workspace W in such a way that

$$D > 2r_i,\ i \in \mathcal{V} : r_i = max\{r_j\}\ \forall j \in \mathcal{V}$$

where D is defined in Definition (2.3.2).

The designed desirable control scheme should provide feasible control inputs $\mathbf{u}_i$ per agent $i \in \mathcal{V}$, that is, inputs that abide by the input constraints $\mathcal{U}_i$:

Definition 2.3.3. (*Feasible Control Input*) The control input $\mathbf{u}_i(\cdot)$ is called feasible when it abides by its respective constraint:

$$\mathbf{u}_i(t) \in \mathcal{U}_i = \{\mathbf{u}_i(t) \in \mathbb{R}^6 : \|\mathbf{u}_i(t)\| \leq \overline{u}_i\}$$

Overall then, the objective of each agent i is for $\lim_{t\to\infty} \|\mathbf{x}_i(t) - \mathbf{x}_{i,des}\| = 0$. If we design feasible control inputs $\mathbf{u}_i \in \mathcal{U}_i$, $\forall i \in \mathcal{V}$ such that the signal $\lim_{t\to\infty} \mathbf{x}_i(t) = \mathbf{x}_{i,des}$ with dynamics given in (2.1), constrained under assumptions (2.1.1), (2.2.1), and (2.3.1) satisfies $\lim_{t\to\infty} \|\mathbf{x}_i(t) - \mathbf{x}_{i,des}\| = 0$, while all system related signals remain bounded in their respective regions, − if all of the above are achieved, then problem (2.4) has been solved.

2.4 Problem Statement

Due to the fact that the agents are not dimensionless and their communication capabilities are limited, given feasible steady-state configurations $\mathbf{p}_{i,des}, \mathbf{q}_{i,des}$, the control protocol should for all agents $i \in \mathcal{V}$ guarantee that:

1. the desired positions $\mathbf{p}_{i,des}$ are achieved in finite time
2. the desired angles $\mathbf{q}_{i,des}$ are achieved in finite time
3. connectivity between neighbouring agents $j \in \mathcal{N}_i$ is maintained at all times

Furthermore, for all agents $i \in \mathcal{V}$, obstacles $\ell \in \mathcal{L}$ and the workspace boundary W, it should guarantee for all $t \in \mathbb{R}_{\geq 0}$ that:

1. all agents avoid collisions with each other
2. all agents avoid collisions with all obstacles
3. all agents avoid collisions with the workspace boundary
4. singularity of the Jacobian matrices $\boldsymbol{J}_i$ is avoided

5. all input control signals are bounded in their respective regions

Therefore, all neighboring agents of agent i must remain within a distance less than d_i to him for all $i \in \mathcal{V} : |\mathcal{N}_i| \neq 0$, and all agents $i, j \in \mathcal{V}, i \neq j$ must remain within distance greater than $\underline{d}_{ij,a}$ with one another.

Formally, the control problem under the aforementioned constraints is formulated as follows:

Problem 2.4.1. Consider N agents modeled as bounded spheres $\mathcal{B}(\mathbf{p}_i, r_i)$, $i \in \mathcal{V}, N = |\mathcal{V}|$, that operate in workspace W that is also modeled as a bounded sphere $\mathcal{B}(\mathbf{p}_W, r_W)$. W features $|\mathcal{L}|$ spherical obstacles in its interior, also modeled as bounded spheres $\mathcal{B}(\mathbf{p}_\ell, r_\ell), \ell \in \mathcal{L}$.

All agents $i \in \mathcal{V}$ are governed by the dynamics (2.1), and the compound system of agents, obstacles and the workspace is subject to assumptions (2.1.1), (2.2.1), (2.3.1). Given desired *feasible* steady-state agent configurations $\mathbf{x}_{i,des}$ according to definition (2.3.1), $\forall i \in \mathcal{V}$, design feasible decentralized control laws $\mathbf{u}_i(t)$ according to definition (2.3.3), such that $\forall i \in \mathcal{V}$ and for all times $t \in \mathbb{R}_{\geq 0}$, the following hold:

1. Position and orientation configuration is achieved in steady-state

$$\lim_{t \to \infty} \|\mathbf{x}_i(t) - \mathbf{x}_{i,des}\| = 0$$

2. Inter-agent collisions are avoided

$$\|\mathbf{p}_i(t) - \mathbf{p}_j(t)\| = d_{ij,a}(t) > \underline{d}_{ij,a}, \forall j \in \mathcal{V} \backslash \{i\}$$

3. Inter-agent connectivity loss between neighbouring agents is avoided

$$\|\mathbf{p}_i(t) - \mathbf{p}_j(t)\| = d_{ij,a}(t) < d_i, \forall j \in \mathcal{N}_i, \forall i : |\mathcal{N}_i| \neq 0$$

4. Agent-with-obstacle collisions are avoided

$$\|\mathbf{p}_i(t) - \mathbf{p}_\ell(t)\| = d_{i\ell,o}(t) > \underline{d}_{i\ell,o}, \forall \ell \in \mathcal{L}$$

5. Agent-with-workspace-boundary collisions are avoided

$$\|\mathbf{p}_W - \mathbf{p}_i(t)\| = d_{i,W}(t) < \overline{d}_{i,W}$$

6. All maps $\boldsymbol{J}_i$ are well defined

$$-\frac{\pi}{2} < \theta_i(t) < \frac{\pi}{2}$$

7. The control laws $\mathbf{u}_i(t)$ abide by their respective input constraints

$$\mathbf{u}_i(t) \in \mathcal{U}_i$$

Part II

Advocated Solutions

3

Disturbance-free Stabililization

The purpose to be saught in this chapter is the steering of each agent $i \in \mathcal{V}$ into a desired configuration in 12D space while conforming to the requirements posed by the problem. Here, the real system and its model are equivalent: no model-reality mismatches exist, and no disturbances act on the real system. At first, the model of system (2.1) will be formalized. Next, the error model and *its* constraints will be expressed. Then, the optimization problem to be solved periodically will be posed; it will equip us with the optimum feasible input that steers the system towards achieving its intended collision-free steady-state configuration while avoiding the pitfall of violating its constraints. This will lead to the proof of stability of the compound closed-loop system of agents $i \in \mathcal{V}$ under the proposed control regime.

3.1 Formalizing the system's model

We begin by rewriting the decoupled non-linear time-invariant system equations (2.1a), (2.1b) for a generic agent $i \in \mathcal{V}$ in state-space form:

$$\dot{\mathbf{x}}_i(t) = \boldsymbol{J}_i^{-1}(\mathbf{x}_i)\mathbf{v}_i(t)$$

$$\dot{\mathbf{v}}_i(t) = -\boldsymbol{M}_i^{-1}(\mathbf{x}_i)\boldsymbol{C}_i(\mathbf{x}_i, \dot{\mathbf{x}}_i)\mathbf{v}_i(t) - \boldsymbol{M}_i^{-1}(\mathbf{x}_i)\mathbf{g}_i(\mathbf{x}_i) + \boldsymbol{M}_i^{-1}(\mathbf{x}_i)\mathbf{u}_i(t)$$

where the inversion of $\boldsymbol{M}_i$ is possible due to it being positive-definite $\forall i \in \mathcal{V}$. Denoting by $\mathbf{z}_i(t)$

$$\mathbf{z}_i(t) \triangleq \begin{bmatrix} \mathbf{x}_i(t) \\ \mathbf{v}_i(t) \end{bmatrix}, \ \mathbf{z}_i(t) : \mathbb{R}_{\geq 0} \to \mathbb{R}^9 \times \mathbb{T}^3$$

and $\dot{\mathbf{x}}_i(t)$ and $\dot{\mathbf{v}}_i(t)$ by

$$\dot{\mathbf{x}}_i(t) = f_{i,x}(\mathbf{z}_i, \mathbf{u}_i)$$

$$\dot{\mathbf{v}}_i(t) = f_{i,v}(\mathbf{z}_i, \mathbf{u}_i)$$

we get the compact representation of the system's model

$$\dot{\mathbf{z}}_i(t) = \begin{bmatrix} f_{i,x}(\mathbf{z}_i, \mathbf{u}_i) \\ f_{i,v}(\mathbf{z}_i, \mathbf{u}_i) \end{bmatrix} = f_i\big(\mathbf{z}_i(t), \mathbf{u}_i(t)\big)$$

The state evolution of agent i is modeled by a system of non-linear continuous-time differential equations of the form

$$\dot{\mathbf{z}}_i(t) = f_i\big(\mathbf{z}_i(t), \mathbf{u}_i(t)\big)$$

$$\mathbf{z}_i(0) = \mathbf{z}_{i,0}$$

$$\mathbf{z}_i(t) \subset \mathbb{R}^9 \times \mathbb{T}^3$$

$$\mathbf{u}_i(t) \subset \mathbb{R}^6 \tag{3.3}$$

where state $\mathbf{z}_i$ is directly measurable as per assumption (2.1.1).

We define the set $\mathcal{Z}_{i,t} \subset \mathbb{R}^9 \times \mathbb{T}^3$ as the set that captures all the *state* constraints on the system posed by the problem (2.4) at $t \in \mathbb{R}_{\geq 0}$. Therefore $\mathcal{Z}_{i,t}$ is such that:

$$\begin{aligned}\mathcal{Z}_{i,t} \triangleq \big\{\mathbf{z}_i(t) \in \mathbb{R}^9 \times \mathbb{T}^3 : \|\mathbf{p}_i(t) - \mathbf{p}_j(t)\| > \underline{d}_{ij,a}, \forall j \in \mathcal{R}_i(t),\\ \|\mathbf{p}_i(t) - \mathbf{p}_j(t)\| < d_i, \forall j \in \mathcal{N}_i,\\ \|\mathbf{p}_i(t) - \mathbf{p}_\ell\| > \underline{d}_{i\ell,o}, \forall \ell \in \mathcal{L},\\ \|\mathbf{p}_W - \mathbf{p}_i(t)\| < \overline{d}_{i,W},\\ -\frac{\pi}{2} < \theta_i(t) < \frac{\pi}{2}\big\}\end{aligned}$$

3.2 The error model

A feasible desired configuration $\mathbf{z}_{i,des} \in \mathbb{R}^9 \times \mathbb{T}^3$ is assigned to each agent $i \in \mathcal{V}$, with the aim of agent i achieving it in steady-state: $\lim_{t\to\infty} \|\mathbf{z}_i(t) - \mathbf{z}_{i,des}\| = 0$. The interior of the norm of this expression denotes the state error of agent i:

$$\mathbf{e}_i(t) : \mathbb{R}_{\geq 0} \to \mathbb{R}^9 \times \mathbb{T}^3,\ \mathbf{e}_i(t) = \mathbf{z}_i(t) - \mathbf{z}_{i,des}$$

The error dynamics are denoted by $g_i(\mathbf{e}_i, \mathbf{u}_i)$:

$$\dot{\mathbf{e}}_i(t) = \dot{\mathbf{z}}_i(t) - \dot{\mathbf{z}}_{i,des} = \dot{\mathbf{z}}_i(t) = f_i\big(\mathbf{z}_i(t), \mathbf{u}_i(t)\big) = g_i\big(\mathbf{e}_i(t), \mathbf{u}_i(t)\big) \tag{3.4}$$

with $\mathbf{e}_i(0) = \mathbf{z}_i(0) - \mathbf{z}_{i,des}$.

In order to translate the constraints that are dictated for the state $\mathbf{z}_i(t)$ into constraints regarding the error state $\mathbf{e}_i(t)$, we define the set $\mathcal{E}_{i,t} \subset \mathbb{R}^9 \times \mathbb{T}^3$ as:

$$\mathcal{E}_{i,t} \triangleq \big\{\mathbf{e}_i(t) \in \mathbb{R}^9 \times \mathbb{T}^3 : \mathbf{e}_i(t) \in \mathcal{Z}_{i,t} \ominus \mathbf{z}_{i,des}\big\}$$

as the set that captures all constraints on the error state with dynamics (3.4) dictated by problem (2.4).

On functions g_i we make the following assumption:

Assumption 3.2.1. (g_i *is Lipschitz continuous in* $\mathcal{E}_{i,t} \times \mathcal{U}_i$)
Suppose that $\mathbf{e}_1, \mathbf{e}_2 \in \mathcal{E}_{i,t}$ and $\mathbf{u} \in \mathcal{U}_i$. Functions g_i are Lipschitz continuous in $\mathcal{E}_{i,t} \times \mathcal{U}_i$ with Lipschitz constants L_{g_i}:

$$\big\|g_i\big(\mathbf{e}_1, \mathbf{u}\big) - g_i\big(\mathbf{e}_2, \mathbf{u}\big)\big\| \leq L_{g_i}\big\|\mathbf{e}_1 - \mathbf{e}_2\big\|$$

If we design control laws $\mathbf{u}_i \in \mathcal{U}_i$, $\forall i \in \mathcal{V}$ such that the error signal $\mathbf{e}_i(t)$ with dynamics given in (3.4), constrained under $\mathbf{e}_i(t) \in \mathcal{E}_{i,t}$, satisfies $\lim_{t\to\infty} \|\mathbf{e}_i(t)\| = 0$, while all system related signals remain bounded in their respective regions,– if all of the above are achieved, then problem (2.4) has been solved.

In order to achieve this task, we employ a Nonlinear Receding Horizon scheme.

3.3 The optimization problem

Consider a sequence of sampling times $\{t_k\}_{k\geq 0}$, with a constant sampling time h, $0 < h < T_p$, where T_p is the finite time-horizon, such that $t_{k+1} = t_k + h$. In sampling data NMPC, a finite-horizon open-loop optimal control problem (FHOCP) is solved at discrete sampling time instants t_k based on the then-current state error measurement $\mathbf{e}_i(t_k)$. The solution is an optimal control signal $\overline{\mathbf{u}}_i^\star(t)$, computed over $t \in [t_k, t_k + T_p]$. This signal is applied to the open-loop system in between sampling times t_k and t_{k+1}.

At a generic time t_k then, agent i solves the following optimization problem:

Problem 3.3.1.

Find

$$\overline{\mathbf{u}}_i^\star(\cdot;\ \mathbf{e}_i(t_k)) \triangleq \underset{\overline{\mathbf{u}}_i(\cdot)}{\operatorname{argmin}} \quad J_i\big(\mathbf{e}_i(t_k), \overline{\mathbf{u}}_i(\cdot)\big) \tag{3.5}$$

where

$$J_i\big(\mathbf{e}_i(t_k), \overline{\mathbf{u}}_i(\cdot)\big) \triangleq \int_{t_k}^{t_k+T_p} F_i\big(\overline{\mathbf{e}}_i(s), \overline{\mathbf{u}}_i(s)\big)ds + V_i\big(\overline{\mathbf{e}}_i(t_k+T_p)\big)$$

subject to:

$$\dot{\overline{\mathbf{e}}}_i(s) = g_i\big(\overline{\mathbf{e}}_i(s), \overline{\mathbf{u}}_i(s)\big), \quad \overline{\mathbf{e}}_i(t_k) = \mathbf{e}_i(t_k) \tag{3.6}$$

$$\overline{\mathbf{u}}_i(s) \in \mathcal{U}_i, \quad \overline{\mathbf{e}}_i(s) \in \mathcal{E}_{i,s}, \quad s \in [t_k, t_k+T_p]$$

$$\overline{\mathbf{e}}_i(t_k+T_p) \in \Omega_i$$

The notation $\bar{\cdot}$ is used to distinguish predicted states which are internal to the controller, as opposed to their actual values, because the predicted values will not be equal to the actual closed-loop values. This means that $\overline{\mathbf{e}}_i(\cdot)$ is the solution to (3.6) driven by the control input $\overline{\mathbf{u}}_i(\cdot) : [t_k, t_k+T_p] \to \mathcal{U}_i$ with initial condition $\mathbf{e}_i(t_k)$.

The applied input signal is a portion of the optimal solution to an optimization problem where information on the states of the neighbouring agents of agent i is taken into account only in the constraints considered in the optimization problem. These constraints pertain to the set of its neighbours $\mathcal{N}_i$ and, in total, to the set of all agents within its sensing range $\mathcal{R}_i$. Regarding these, we make the following assumption:

Assumption 3.3.1. (*Access to Predicted Information from an Inter-agent Perspective*)

Considering the context of Receding Horizon Control, when at time t_k agent i solves a finite horizon optimization problem, he has access to[a]

1. measurements of the states[b]
   - $\mathbf{z}_j(t_k)$ of all agents $j \in \mathcal{R}_i(t_k)$ within its sensing range at time t_k
   - $\mathbf{z}_{j'}(t_k)$ of all of its neighbouring agents $j' \in \mathcal{N}_i$ at time t_k
2. the *predicted states*
   - $\overline{\mathbf{z}}_j(\tau)$ of all agents $j \in \mathcal{R}_i(t_k)$ within its sensing range

- $\bar{\mathbf{z}}_{j'}(\tau)$ of all of its neighbouring agents $j' \in \mathcal{N}_i$

across the entire horizon $\tau \in (t_k, t_k + T_p]$

[a] Although $\mathcal{N}_i \subseteq \mathcal{R}_i$, we make the distinction between the two because all agents $j \in \mathcal{R}_i$ need to avoid collision with agent i, but only agents $j' \in \mathcal{N}_i$ need to remain within the sensing range of agent i.

[b] as per assumption (2.1.1)

Remark 3.3.1. The justification for this assumption is the following: considering that $\mathcal{N}_i \subseteq \mathcal{R}_i$, that the state vectors $\mathbf{z}_j$ are comprised of 12 real numbers that are encoded by 4 bytes, and that sampling occurs with a frequency f for all agents, the overall downstream bandwidth required by each agent is

$$BW_d = 12 \times 32 \text{ [bits]} \times |\mathcal{R}_i| \times \frac{T_p}{h} \times f \text{ [sec}^{-1}\text{]}$$

Given a conservative sampling time $f = 100$ Hz and a horizon of $\frac{T_p}{h} = 100$ timesteps, the wireless protocol IEEE 802.11n-2009 (a standard for present-day devices) can accommodate up to

$$|\mathcal{R}_i| = \frac{600 \text{ [Mbit} \cdot \text{sec}^{-1}\text{]}}{12 \times 32\text{[bit]} \times 10^4\text{[sec}^{-1}\text{]}} \approx 16 \cdot 10^2 \text{ agents}$$

within the range of one agent. We deem this number to be large enough for practical applications for the approach of assuming access to the predicted states of agents within the range of one agent to be legal.

In other words, each time an agent solves its own individual optimization problem, he knows the (open-loop) state predictions that have been generated by the solution of the optimization problem of all agents within its range at that time, for the next T_p timesteps. This assumption is crucial to satisfying the constraints regarding collision aversion and connectivity maintenance between neighbouring agents. We assume that the above pieces of information are (a) always available and accurate, and (b) exchanged without delay. We encapsulate these pieces of information in four stacked vectors:

$$\mathbf{z}_{\mathcal{R}_i}(t_k) \triangleq col[\mathbf{z}_j(t_k)], \forall j \in \mathcal{R}_i(t_k)$$

$$\mathbf{z}_{\mathcal{N}_i}(t_k) \triangleq col[\mathbf{z}_j(t_k)], \forall j \in \mathcal{N}_i$$

$$\overline{\mathbf{z}}_{\mathcal{R}_i}(\tau) \triangleq col[\overline{\mathbf{z}}_j(\tau)], \forall j \in \mathcal{R}_i(\tau), \tau \in [t_k, t_k + T_p]$$

$$\overline{\mathbf{z}}_{\mathcal{N}_i}(\tau) \triangleq col[\overline{\mathbf{z}}_j(\tau)], \forall j \in \mathcal{N}_i, \tau \in [t_k, t_k + T_p]$$

These are taken into consideration during the solution to the optimization problem as follows: when agent i solves his own optimization problem, *his predicted configuration at time* $\tau \in [t_k, t_k+T_p]$ *is constrained by the predicted configuration of its neighbouring and perceivable*[1] *agents at the same time instant* τ. The form of the inter-agent constraint regime is necessary to be such, as each agent is constrained not by constant values, but by the trajectories of its associated agents, which are time-varying in nature.

Formally then, $\mathcal{E}_{i,s} = \{\mathbf{e}_i(s) : \mathbf{e}_i(s) \in \mathcal{Z}_{i,s} \ominus \mathbf{z}_{i,des}\}$, for $s \in [t_k, t_k + T_p]$, where, for $s = t_k$:

$$\begin{aligned}\mathcal{Z}_{i,t_k} = \big\{\mathbf{z}_i(t_k) \in \mathbb{R}^9 \times \mathbb{T}^3 : &\|\mathbf{p}_i(t_k) - \mathbf{p}_{\mathcal{R}_i}(t_k)\| > \underline{d}_{ij,a}, \forall j \in \mathcal{R}_i(t_k)\\ &\|\mathbf{p}_i(t_k) - \mathbf{p}_{\mathcal{N}_i}(t_k)\| < d_i, \forall j \in \mathcal{N}_i,\\ &\|\mathbf{p}_i(t_k) - \mathbf{p}_\ell\| > \underline{d}_{i\ell,o}, \forall \ell \in \mathcal{L},\\ &\|\mathbf{p}_W - \mathbf{p}_i(t_k)\| < \overline{d}_{i,W},\\ &-\frac{\pi}{2} < \theta_i(t_k) < \frac{\pi}{2}\big\}\end{aligned}$$

and, for $s \in (t_k, t_k + T_p]$:

$$\begin{aligned}\mathcal{Z}_{i,s} = \big\{\mathbf{z}_i(s) \in \mathbb{R}^9 \times \mathbb{T}^3 : &\|\overline{\mathbf{p}}_i(s) - \overline{\mathbf{p}}_{\mathcal{R}_i}(s)\| > \underline{d}_{ij,a}, \forall j \in \mathcal{R}_i(s)\\ &\|\overline{\mathbf{p}}_i(s) - \overline{\mathbf{p}}_{\mathcal{N}_i}(s)\| < d_i, \forall j \in \mathcal{N}_i,\\ &\|\overline{\mathbf{p}}_i(s) - \mathbf{p}_\ell\| > \underline{d}_{i\ell,o}, \forall \ell \in \mathcal{L},\\ &\|\mathbf{p}_W - \overline{\mathbf{p}}_i(s)\| < \overline{d}_{i,W},\end{aligned}$$

[1] agents within its sensing range

$$-\frac{\pi}{2} < \overline{\theta}_i(s) < \frac{\pi}{2}\}$$

The denotations $\mathbf{p}_{\mathcal{R}_i}(t_k)$, $\mathbf{p}_{\mathcal{N}_i}(t_k)$, $\overline{\mathbf{p}}_{\mathcal{R}_i}(s)$, and $\overline{\mathbf{p}}_{\mathcal{N}_i}(s)$ serve as to point to the column vectors $\mathbf{z}_{\mathcal{R}_i}(t_k)$, $\mathbf{z}_{\mathcal{N}_i}(t_k)$, $\overline{\mathbf{z}}_{\mathcal{R}_i}(s)$, and $\overline{\mathbf{z}}_{\mathcal{N}_i}(s)$ respectively, of which they are components, and whose notation they abide by as per our established denotation. Figure (3.1) depicts the designed inter-agent (and intra-horizon) constraint regime.

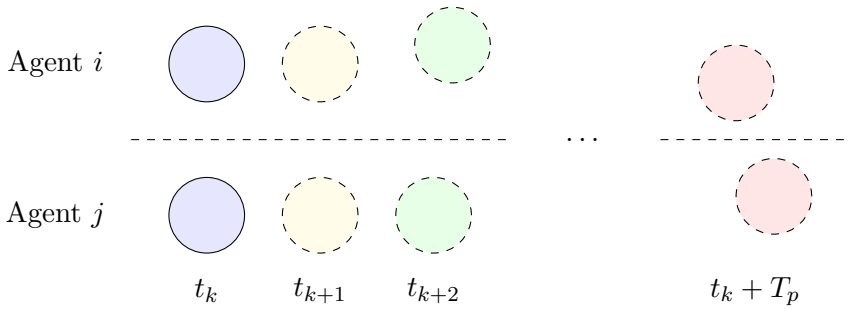

Figure 3.1: The inter-agent constraint regime for two agents, i, j. Fully outlined circles denote measured configurations, while partly outlined circles denote predicted configurations. During the solution to the individual optimization problems, the predicted configuration of each agent at each timestep is constrained by the predicted configuration of the other agent at the same timestep (hence the homologously identical colours at each discrete timestep).

The functions $F_i : \mathcal{E}_{i,s} \times \mathcal{U}_i \to \mathbb{R}_{\geq 0}$ and $V_i : \Omega_i \to \mathbb{R}_{\geq 0}$ are defined as

$$F_i\big(\overline{\mathbf{e}}_i(t), \overline{\mathbf{u}}_i(t)\big) \triangleq \overline{\mathbf{e}}_i(t)^\top \boldsymbol{Q}_i \overline{\mathbf{e}}_i(t) + \overline{\mathbf{u}}_i(t)^\top \boldsymbol{R}_i \overline{\mathbf{u}}_i(t) \tag{3.8}$$

$$V_i\big(\overline{\mathbf{e}}_i(t)\big) \triangleq \overline{\mathbf{e}}_i(t)^\top \boldsymbol{P}_i \overline{\mathbf{e}}_i(t) \tag{3.9}$$

Matrices $\boldsymbol{R}_i \in \mathbb{R}^{6\times 6}$ and $\boldsymbol{Q}_i, \boldsymbol{P}_i \in \mathbb{R}^{12\times 12}$ are symmetric and positive definite. The running costs F_i are upper- and lower-bounded by class $\mathcal{K}_\infty$ functions:

Lemma 3.3.1. (*F_i is lower- and upper-bounded by class $\mathcal{K}_\infty$ functions*)
Let functions $\alpha_1, \alpha_2 \in \mathcal{K}_\infty$ and F_i be defined by (3.8). Then, for all $\mathbf{e}_i \in \mathcal{E}_{i,s}$

$$\alpha_1\big(\|\mathbf{e}_i\|\big) \leq F_i\big(\mathbf{e}_i, \mathbf{u}_i\big) \leq \alpha_2\big(\|\mathbf{e}_i\|\big)$$

Lemma 3.3.2. (F_i is Lipschitz continuous in $\mathcal{E}_{i,s} \times \mathcal{U}_i$)

Suppose that $\mathbf{e}_1, \mathbf{e}_2 \in \mathcal{E}_{i,s}$, $\mathbf{u}_i \in \mathcal{U}_i$ and that F_i is defined by (3.8). The running costs F_i are Lipschitz continuous in $\mathcal{E}_{i,s} \times \mathcal{U}_i$:

$$\big|F_i(\mathbf{e}_1, \mathbf{u}_i) - F_i(\mathbf{e}_2, \mathbf{u}_i)\big| \leq L_{F_i}\|\mathbf{e}_1 - \mathbf{e}_2\|$$

with Lipschitz constant $L_{F_i} = 2\sigma_{max}(\boldsymbol{Q}_i)\overline{\varepsilon}_i$, where $\overline{\varepsilon}_i = \sup_{\mathbf{e}_i \in \mathcal{E}_{i,s}} \|\mathbf{e}_i\|$

The terminal set $\Omega_i \subseteq \mathcal{E}_{i,t_k+T_p}$ is an admissible, positively invariant set according to definition (1.2.5) for system (3.4) such that

$$\Omega_i = \{\mathbf{e}_i \in \mathcal{E}_{i,t_k+T_p} : V_i(\mathbf{e}_i) \leq \varepsilon_{\Omega_i}\}$$

where ε_{Ω_i} is an arbitrarily small but fixed positive real scalar.

With regard to the terminal penalty function V_i, the following lemma will prove to be useful in guaranteeing the convergence of the solution to the optimal control problem to the terminal region Ω_i:

Lemma 3.3.3. (V_i is Lipschitz continuous in Ω_i)

Suppose that $\mathbf{e}_1, \mathbf{e}_2 \in \Omega_i$, and that V_i is defined by (3.9). The terminal penalty function V_i is Lipschitz continuous in Ω_i

$$\big|V_i(\mathbf{e}_1) - V_i(\mathbf{e}_2)\big| \leq L_{V_i}\|\mathbf{e}_1 - \mathbf{e}_2\|$$

with Lipschitz constant $L_{V_i} = 2\sigma_{max}(\boldsymbol{P}_i)\overline{\varepsilon}_{i,\Omega_i}$

where $\overline{\varepsilon}_{i,\Omega_i} = \sup_{\mathbf{e}_i \in \Omega_i} \|\mathbf{e}_i\|$

Furthermore, V_i is lower- and upper-bounded by class $\mathcal{K}_\infty$ functions.

Lemma 3.3.4. (*V_i is lower- and upper-bounded by class $\mathcal{K}_\infty$ functions in Ω_i*)

Let $\alpha_1, \alpha_2 \in \mathcal{K}_\infty$, $\mathbf{e}_i \in \Omega_i$ and let V_i be defined by (3.9). Then

$$\alpha_1\big(\|\mathbf{e}_i\|\big) \leq V_i(\mathbf{e}_i) \leq \alpha_2\big(\|\mathbf{e}_i\|\big)$$

The solution to the optimal control problem (3.5) at time t_k is an optimal control input, denoted by $\overline{\mathbf{u}}_i^\star(\cdot;\ \mathbf{e}_i(t_k))$, which is applied to the open-loop system until the next sampling instant $t_k + h$, with $h \in (0, T_p)$:

$$\mathbf{u}_i(t) = \overline{\mathbf{u}}_i^\star\big(t;\ \mathbf{e}_i(t_k)\big),\ t \in [t_k, t_k + h] \tag{3.10}$$

At time t_{k+1} a new finite horizon optimal control problem is solved in the same manner, leading to a receding horizon approach.

The control input $\mathbf{u}_i(\cdot)$ is of feedback form, since it is recalculated at each sampling instant based on the then-current state. The solution to equation (3.4) − the model of the real system, starting at time t_1, from an initial condition $\mathbf{e}_i(t_1) = \overline{\mathbf{e}}_i(t_1)$, by application of the control input $\mathbf{u}_i : [t_1, t_2] \to \mathcal{U}_i$ is denoted by

$$\mathbf{e}_i\big(t;\ \mathbf{u}_i(\cdot), \mathbf{e}_i(t_1)\big),\ t \in [t_1, t_2]$$

On the existence of solutions to (3.4) we assume the following:

Assumption 3.3.2. The system (3.4) has a *continuous solution* for any $\mathbf{e}_i(0) \in \mathcal{E}_{i,0}$ and any *piecewise continuous* input $\mathbf{u}_i(\cdot) : [0, T_p] \to \mathcal{U}_i$.

The states of the open-loop system (3.6) − the predicted states obey the following notation:

Remark 3.3.2. The *predicted* state of the system (3.4) at time $\tau \geq t_k$, based on the measurement of the state at time t_k, $\mathbf{e}_i(t_k)$, by application of the control input (3.10), is denoted by

$$\overline{\mathbf{e}}_i\big(\tau;\ \mathbf{u}_i(\tau), \mathbf{e}_i(t_k)\big)$$

The closed-loop system for which stability is to be guaranteed is

$$\mathbf{e}_i(\tau) = g_i\big(\mathbf{e}_i(\tau), \overline{\mathbf{u}}_i^{\star}(\tau)\big),\ \tau \geq t_0 = 0 \tag{3.11}$$

where $\overline{\mathbf{u}}_i^{\star}(\tau) = \overline{\mathbf{u}}_i^{\star}(\tau;\ \mathbf{e}_i(t_k))$, $\tau \in [t_k, t_k + h)$ and $t_0 = 0$.

We can now give the definition of an *admissible input* for the FHOCP (3.3.1):

Definition 3.3.1. (*Admissible input for the FHOCP* (3.3.1))

A control input $\mathbf{u}_i : [t_k, t_k + T_p] \to \mathbb{R}^6$ for a state $\mathbf{e}_i(t_k)$ is called *admissible* for the problem (3.3.1) if all the following hold:

1. $\mathbf{u}_i(\cdot)$ is piecewise continuous
2. $\mathbf{u}_i(\tau) \in \mathcal{U}_i,\ \forall \tau \in [t_k, t_k + T_p]$
3. $\overline{\mathbf{e}}_i\big(\tau;\ \mathbf{u}_i(\cdot), \mathbf{e}_i(t_k)\big) \in \mathcal{E}_{i,\tau},\ \forall \tau \in [t_k, t_k + T_p]$
4. $\overline{\mathbf{e}}_i\big(t_k + T_p;\ \mathbf{u}_i(\cdot), \mathbf{e}_i(t_k)\big) \in \Omega_i$

In other words, $\mathbf{u}_i$ is admissible if it conforms to the constraints on the input and its application yields states that conform to the prescribed state constraints of problem (3.3.1) along the entire horizon $[t_k, t_k + T_p]$, and the terminal predicted state conforms to the terminal constraint.

3.4 Stabilization: Feasibility and Convergence

Under these considerations, we can now state the theorem that relates to the guaranteeing of the stability of the compound system of agents $i \in \mathcal{V}$, when each of them is assigned a desired position which results in feasible displacements:

Theorem 3.4.1. Suppose that

1. the terminal region $\Omega_i \subseteq \mathcal{E}_{i,s}$ is closed with $\mathbf{0} \in \Omega_i \ \forall s \in \mathbb{R}_{\geq 0}$
2. a solution to the optimal control problem (3.5) is feasible at time $t = 0$, that is, assumptions (2.1.1), (2.2.1), and (2.3.1) hold at time $t = 0$
3. assumptions (3.2.1), (3.3.1), and (3.3.2) hold
4. there exists an admissible control input $h_i(\mathbf{e}_i) : [t_k + T_p, t_{k+1} + T_p] \to \mathcal{U}_i$ such that for all $\mathbf{e}_i \in \Omega_i$ and $\forall \tau \in [t_k + T_p, t_{k+1} + T_p]$:
   (a) $\mathbf{e}_i(\tau) \in \Omega_i$
   (b) $\dfrac{\partial V_i}{\partial \mathbf{e}_i} g_i\big(\mathbf{e}_i(\tau), h_i\big(\mathbf{e}_i(\tau)\big)\big) + F_i\big(\mathbf{e}_i(\tau), h_i\big(\mathbf{e}_i(\tau)\big)\big) \leq 0$

then the closed loop system (3.11) under the control input (3.10) converges to the set Ω_i when $t \to \infty$.

Proof. The proof of the above theorem consists of two parts: in the first, recursive feasibility is established, that is, initial feasibility is shown to imply subsequent feasibility; in the second part, and based on the first , it is shown that the error state $\mathbf{e}_i(t)$ converges to the terminal set Ω_i.

Feasibility analysis Consider a sampling instant t_k for which a solution $\overline{\mathbf{u}}_i^{\star}\big(\cdot;\ \mathbf{e}_i(t_k)\big)$ to (3.5) exists. Suppose now a time instant t_{k+1} such that[2] $t_k < t_{k+1} < t_k + T_p$, and consider that the optimal control signal calculated at t_k is comprised of the following two portions:

[2]It is not strictly necessary that $t_{k+1} = t_k + h$ here, however it is necessary for the following that $t_{k+1} - t_k \leq h$

$$\overline{\mathbf{u}}_i^{\star}\big(\cdot;\ \mathbf{e}_i(t_k)\big) = \begin{cases} \overline{\mathbf{u}}_i^{\star}\big(\tau_1;\ \mathbf{e}_i(t_k)\big), & \tau_1 \in [t_k, t_{k+1}] \\ \\ \overline{\mathbf{u}}_i^{\star}\big(\tau_2;\ \mathbf{e}_i(t_k)\big), & \tau_2 \in [t_{k+1}, t_k + T_p] \end{cases} \tag{3.12}$$

Both portions are admissible since the calculated optimal control input is admissible, and hence they both conform to the input constraints. As for the resulting predicted states, they satisfy the state constraints, and, crucially: $\overline{\mathbf{e}}_i\big(t_k + T_p;\ \overline{\mathbf{u}}_i^{\star}(\cdot), \mathbf{e}_i(t_k)\big) \in \Omega_i$. Furthermore, according to assumption (3) of the theorem, there exists an admissible (and certainly not guaranteed optimal) input $h_i(\mathbf{e}_i)$ that renders Ω_i invariant over $[t_k + T_p, t_{k+1} + T_p]$.
Given the above facts, we can construct an admissible input $\widetilde{\mathbf{u}}_i(\cdot)$ starting at time t_{k+1} by sewing together the second portion of (3.12) and the input $h_i(\mathbf{e}_i)$:

$$\widetilde{\mathbf{u}}_i(\tau) = \begin{cases} \overline{\mathbf{u}}_i^{\star}\big(\tau;\ \mathbf{e}_i(t_k)\big), & \tau \in [t_{k+1}, t_k + T_p] \\ \\ h_i\big(\mathbf{e}_i(\tau)\big), & \tau \in (t_k + T_p, t_{k+1} + T_p] \end{cases} \tag{3.13}$$

The control input $\widetilde{\mathbf{u}}_i(\cdot)$ is admissible as a composition of admissible control inputs. This means that feasibility of a solution to the optimization problem at time t_k implies feasibility at time $t_{k+1} > t_k$, and, thus, since at time $t = 0$ a solution is assumed to be feasible, a solution to the optimal control problem is feasible for all $t \geq 0$.

Convergence analysis The second part of the proof involves demonstrating the convergence of the state $\mathbf{e}_i$ to the terminal set Ω_i. In order for this to be proved, it must be shown that a proper value function decreases along closed-loop trajectories starting at some initial time t_k. We consider the *optimal* cost $J_i^{\star}\big(\mathbf{e}_i(t)\big)$ as a candidate Lyapunov function:

$$J_i^{\star}\big(\mathbf{e}_i(t)\big) \triangleq J_i\Big(\mathbf{e}_i(t), \overline{\mathbf{u}}_i^{\star}\big(\cdot;\ \mathbf{e}_i(t)\big)\Big)$$

and, in particular, our goal is to show that that this cost decreases over consecutive sampling instants $t_{k+1} = t_k + h$, i.e. $J_i^{\star}\big(\mathbf{e}_i(t_{k+1})\big) - J_i^{\star}\big(\mathbf{e}_i(t_k)\big) \leq 0$.

In order not to wreak notational havoc, let us define the following terms:

- $\mathbf{u}_{0,i}(\tau) \triangleq \overline{\mathbf{u}}_i^\star\big(\tau;\ \mathbf{e}_i(t_k)\big)$ as the *optimal* input that results from the solution to problem (3.3.1) based on the measurement of state $\mathbf{e}_i(t_k)$, applied at time $\tau \geq t_k$
- $\mathbf{e}_{0,i}(\tau) \triangleq \overline{\mathbf{e}}_i\big(\tau;\ \overline{\mathbf{u}}_i^\star\big(\cdot;\ \mathbf{e}_i(t_k)\big), \mathbf{e}_i(t_k)\big)$ as the *predicted* state at time $\tau \geq t_k$, that is, the state that results from the application of the above input $\overline{\mathbf{u}}_i^\star\big(\cdot;\ \mathbf{e}_i(t_k)\big)$ to the state $\mathbf{e}_i(t_k)$, at time τ
- $\mathbf{u}_{1,i}(\tau) \triangleq \widetilde{\mathbf{u}}_i(\tau)$ as the *admissible* input at $\tau \geq t_{k+1}$ (see eq. (3.13))
- $\mathbf{e}_{1,i}(\tau) \triangleq \overline{\mathbf{e}}_i\big(\tau;\ \widetilde{\mathbf{u}}_i(\cdot), \mathbf{e}_i(t_{k+1})\big)$ as the *predicted* state at time $\tau \geq t_{k+1}$, that is, the state that results from the application of the above input $\widetilde{\mathbf{u}}_i(\cdot)$ to the state $\mathbf{e}_i\big(t_{k+1};\ \overline{\mathbf{u}}_i^\star\big(\cdot;\ \mathbf{e}_i(t_k)\big), \mathbf{e}_i(t_k)\big)$, at time τ

Remark 3.4.1. Given that no model mismatch or disturbances exist, for the predicted and actual states at time $\tau_1 \geq \tau_0 \in \mathbb{R}_{\geq 0}$ it holds that:

$$\mathbf{e}_i\big(\tau_1;\ \mathbf{u}_i(\cdot), \mathbf{e}_i(\tau_0)\big) = \mathbf{e}_i(\tau_0) + \int_{\tau_0}^{\tau_1} g_i\big(\mathbf{e}_i(s;\ \mathbf{e}_i(\tau_0)), \mathbf{u}_i(s)\big) ds$$

$$\overline{\mathbf{e}}_i\big(\tau_1;\ \mathbf{u}_i(\cdot), \mathbf{e}_i(\tau_0)\big) = \mathbf{e}_i(\tau_0) + \int_{\tau_0}^{\tau_1} g_i\big(\overline{\mathbf{e}}_i(s;\ \mathbf{e}_i(\tau_0)), \mathbf{u}_i(s)\big) ds$$

Before beginning to prove convergence, it is worth noting that while the cost

$$J_i\Big(\mathbf{e}_i(t), \overline{\mathbf{u}}_i^\star\big(\cdot;\ \mathbf{e}_i(t)\big)\Big)$$

is optimal (in the sense that it is based on the optimal input, which provides its minimum realization), a cost that is based on a plainly admissible (and thus, without loss of generality, sub-optimal) input $\mathbf{u}_i \neq \overline{\mathbf{u}}_i^\star$ will result in a configuration where

$$J_i\Big(\mathbf{e}_i(t), \mathbf{u}_i\big(\cdot;\ \mathbf{e}_i(t)\big)\Big) \geq J_i\Big(\mathbf{e}_i(t), \overline{\mathbf{u}}_i^\star\big(\cdot;\ \mathbf{e}_i(t)\big)\Big)$$

Let us now begin our investigation on the difference between the cost that results from the application of the feasible input $\mathbf{u}_{1,i}$, which we shall denote by $\overline{J}_i\big(\mathbf{e}_i(t_{k+1})\big)$, and the optimal cost $J_i^\star\big(\mathbf{e}_i(t_k)\big)$. We remind ourselves that $J_i\big(\mathbf{e}_i(t), \overline{\mathbf{u}}_i(\cdot)\big) = \int_t^{t+T_p} F_i\big(\overline{\mathbf{e}}_i(s), \overline{\mathbf{u}}_i(s)\big) ds +$

$V_i\big(\overline{\mathbf{e}}_i(t+T_p)\big)$:

$$\overline{J}_i\big(\mathbf{e}_i(t_{k+1})\big) - J_i^\star\big(\mathbf{e}_i(t_k)\big) = V_i\big(\mathbf{e}_{1,i}(t_{k+1}+T_p)\big) + \int_{t_{k+1}}^{t_{k+1}+T_p} F_i\big(\mathbf{e}_{1,i}(s), \mathbf{u}_{1,i}(s)\big)ds$$

$$-V_i\big(\mathbf{e}_{0,i}(t_k+T_p)\big) - \int_{t_k}^{t_k+T_p} F_i\big(\mathbf{e}_{0,i}(s), \mathbf{u}_{0,i}(s)\big)ds$$

Considering that $t_k < t_{k+1} < t_k + T_p < t_{k+1} + T_p$, we break down the two integrals above in between these intervals:

$$\begin{aligned}
&\overline{J}_i\big(\mathbf{e}_i(t_{k+1})\big) - J_i^\star\big(\mathbf{e}_i(t_k)\big) = \\
&\quad V_i\big(\mathbf{e}_{1,i}(t_{k+1}+T_p)\big) + \int_{t_{k+1}}^{t_k+T_p} F_i\big(\mathbf{e}_{1,i}(s), \mathbf{u}_{1,i}(s)\big)ds + \int_{t_k+T_p}^{t_{k+1}+T_p} F_i\big(\mathbf{e}_{1,i}(s), \mathbf{u}_{1,i}(s)\big)ds \\
&\quad -V_i\big(\mathbf{e}_{0,i}(t_k+T_p)\big) - \int_{t_k}^{t_{k+1}} F_i\big(\mathbf{e}_{0,i}(s), \mathbf{u}_{0,i}(s)\big)ds - \int_{t_{k+1}}^{t_k+T_p} F_i\big(\mathbf{e}_{0,i}(s), \mathbf{u}_{0,i}(s)\big)ds
\end{aligned} \tag{3.14}$$

Since no model mismatch or disturbances are present, consulting with remark (3.4.1) and substituting for $\tau_0 = t_k$ and $\tau_1 = t_{k+1}$ yields:

$$\mathbf{e}_i\big(t_{k+1};\ \overline{\mathbf{u}}_i^\star\big(\cdot;\ \mathbf{e}_i(t_k)\big), \mathbf{e}_i(t_k)\big) = \mathbf{e}_i(t_k) + \int_{t_k}^{t_{k+1}} g_i\big(\mathbf{e}_i(s;\ \mathbf{e}_i(t_k)), \overline{\mathbf{u}}_i^\star(s)\big)ds$$

$$\overline{\mathbf{e}}_i\big(t_{k+1};\ \overline{\mathbf{u}}_i^\star\big(\cdot;\ \mathbf{e}_i(t_k)\big), \mathbf{e}_i(t_k)\big) = \mathbf{e}_i(t_k) + \int_{t_k}^{t_{k+1}} g_i\big(\overline{\mathbf{e}}_i(s;\ \mathbf{e}_i(t_k)), \overline{\mathbf{u}}_i^\star(s)\big)ds$$

Subtracting the second expression from the first, we get

$$\begin{aligned}
&\mathbf{e}_i\big(t_{k+1}; \overline{\mathbf{u}}_i^\star\big(\cdot;\ \mathbf{e}_i(t_k)\big), \mathbf{e}_i(t_k)\big) - \overline{\mathbf{e}}_i\big(t_{k+1};\ \overline{\mathbf{u}}_i^\star\big(\cdot;\ \mathbf{e}_i(t_k)\big), \mathbf{e}_i(t_k)\big) \\
&\qquad = \int_{t_k}^{t_{k+1}} g_i\big(\mathbf{e}_i(s;\ \mathbf{e}_i(t_k)), \overline{\mathbf{u}}_i^\star(s)\big)ds - \int_{t_k}^{t_{k+1}} g_i\big(\overline{\mathbf{e}}_i(s;\ \mathbf{e}_i(t_k)), \overline{\mathbf{u}}_i^\star(s)\big)ds \\
&\qquad = \int_{t_k}^{t_{k+1}} \Big(g_i\big(\mathbf{e}_i(s;\ \mathbf{e}_i(t_k)), \overline{\mathbf{u}}_i^\star(s)\big) - g_i\big(\overline{\mathbf{e}}_i(s;\ \mathbf{e}_i(t_k)), \overline{\mathbf{u}}_i^\star(s)\big) \Big)ds
\end{aligned}$$

Taking norms on either side yields

$$\begin{aligned}
&\left\|\mathbf{e}_i\big(t_{k+1};\ \overline{\mathbf{u}}_i^\star\big(\cdot;\ \mathbf{e}_i(t_k)\big),\mathbf{e}_i(t_k)\big)-\overline{\mathbf{e}}_i\big(t_{k+1};\ \overline{\mathbf{u}}_i^\star\big(\cdot;\ \mathbf{e}_i(t_k)\big),\mathbf{e}_i(t_k)\big)\right\| \\
&\qquad=\left\|\int_{t_k}^{t_{k+1}}\Big(g_i\big(\mathbf{e}_i(s;\ \mathbf{e}_i(t_k)),\overline{\mathbf{u}}_i^\star(s)\big)-g_i\big(\overline{\mathbf{e}}_i(s;\ \mathbf{e}_i(t_k)),\overline{\mathbf{u}}_i^\star(s)\big)\Big)ds\right\| \\
&\qquad\le\int_{t_k}^{t_{k+1}}\left\|g_i\big(\mathbf{e}_i(s;\ \mathbf{e}_i(t_k)),\overline{\mathbf{u}}_i^\star(s)\big)-g_i\big(\overline{\mathbf{e}}_i(s;\ \mathbf{e}_i(t_k)),\overline{\mathbf{u}}_i^\star(s)\big)\right\|ds \\
&\qquad\le L_{g_i}\int_{t_k}^{t_{k+1}}\left\|\mathbf{e}_i\big(s;\ \overline{\mathbf{u}}_i^\star\big(\cdot;\ \mathbf{e}_i(t_k)\big),\mathbf{e}_i(t_k)\big)-\overline{\mathbf{e}}_i\big(s;\ \overline{\mathbf{u}}_i^\star\big(\cdot;\ \mathbf{e}_i(t_k)\big),\mathbf{e}_i(t_k)\big)\right\|ds
\end{aligned}$$

since g_i is Lipschitz continuous in $\mathcal{E}_{i,s}$ with Lipschitz constant L_{g_i}. Reformulation yields

$$\begin{aligned}
&\left\|\mathbf{e}_i\big(t_k+h;\ \overline{\mathbf{u}}_i^\star\big(\cdot;\ \mathbf{e}_i(t_k)\big),\mathbf{e}_i(t_k)\big)-\overline{\mathbf{e}}_i\big(t_k+h;\ \overline{\mathbf{u}}_i^\star\big(\cdot;\ \mathbf{e}_i(t_k)\big),\mathbf{e}_i(t_k)\big)\right\| \\
&\qquad\le L_{g_i}\int_0^h\left\|\mathbf{e}_i\big(t_k+s;\ \overline{\mathbf{u}}_i^\star\big(\cdot;\ \mathbf{e}_i(t_k)\big),\mathbf{e}_i(t_k)\big)-\overline{\mathbf{e}}_i\big(t_k+s;\ \overline{\mathbf{u}}_i^\star\big(\cdot;\ \mathbf{e}_i(t_k)\big),\mathbf{e}_i(t_k)\big)\right\|ds
\end{aligned}$$

By applying the Grönwall-Bellman inequality we obtain zero as an upper bound for the norm of the difference between the two states. Since any norm cannot be negative, we conclude that

$$\left\|\mathbf{e}_i\big(t_{k+1};\ \overline{\mathbf{u}}_i^\star\big(\cdot;\ \mathbf{e}_i(t_k)\big),\mathbf{e}_i(t_k)\big)-\overline{\mathbf{e}}_i\big(t_{k+1};\ \overline{\mathbf{u}}_i^\star\big(\cdot;\ \mathbf{e}_i(t_k)\big),\mathbf{e}_i(t_k)\big)\right\|=0$$

which means that

$$\mathbf{e}_i\big(t_{k+1};\ \overline{\mathbf{u}}_i^\star\big(\cdot;\ \mathbf{e}_i(t_k)\big),\mathbf{e}_i(t_k)\big)=\overline{\mathbf{e}}_i\big(t_{k+1};\ \overline{\mathbf{u}}_i^\star\big(\cdot;\ \mathbf{e}_i(t_k)\big),\mathbf{e}_i(t_k)\big)$$

In between times t_{k+1} and t_k+T_p, the constructed admissible input $\widetilde{\mathbf{u}}_i(\cdot)$ is equal to the optimal input $\overline{\mathbf{u}}_i^\star\big(\cdot;\ \mathbf{e}_i(t_k)\big)$ (see eq. 3.13), which means that $\mathbf{u}_{1,i}(\tau)=\mathbf{u}_{0,i}(\tau)$ in the interval $\tau\in[t_{k+1},t_k+T_p]$. Since the initial conditions at $t=t_{k+1}$ are equal and

the control laws are also equal, so will the predicted states over the same interval:

$$\overline{\mathbf{e}}_i\big(\tau;\ \widetilde{\mathbf{u}}_i(\cdot), \mathbf{e}_i(t_{k+1})\big) = \overline{\mathbf{e}}_i\big(\tau;\ \overline{\mathbf{u}}_i^{\star}(\cdot), \overline{\mathbf{e}}_i(t_{k+1})\big),\ \tau \in [t_{k+1}, t_k + T_p] \tag{3.15}$$

Using our notation then, in the same interval $[[t_{k+1}, t_k + T_p]$: $\mathbf{e}_{1,i}(\cdot) = \mathbf{e}_{0,i}(\cdot)$. Coupled with the fact that in the same interval $\mathbf{u}_{1,i}(\tau) = \mathbf{u}_{0,i}(\tau)$, the following equality holds over $[t_{k+1}, t_k + T_p]$:

$$F_i\big(\mathbf{e}_{1,i}(s), \mathbf{u}_{1,i}(s)\big) = F_i\big(\mathbf{e}_{0,i}(s), \mathbf{u}_{0,i}(s)\big),\ s \in [t_{k+1}, t_k + T_p]$$

Integrating this equality over the interval where it is valid yields

$$\int_{t_{k+1}}^{t_k+T_p} F_i\big(\mathbf{e}_{1,i}(s), \mathbf{u}_{1,i}(s)\big)ds = \int_{t_{k+1}}^{t_k+T_p} F_i\big(\mathbf{e}_{0,i}(s), \mathbf{u}_{0,i}(s)\big)ds$$

This means that these two integrals with ends over the interval $[t_{k+1}, t_k + T_p]$ featured in the right-hand side of eq. (3.14) vanish, and thus the cost difference becomes

$$\begin{aligned}\overline{J}_i\big(\mathbf{e}_i(t_{k+1})\big) - J_i^{\star}\big(\mathbf{e}_i(t_k)\big) = V_i\big(\mathbf{e}_{1,i}(t_{k+1} + T_p)\big) + \int_{t_k+T_p}^{t_{k+1}+T_p} F_i\big(\mathbf{e}_{1,i}(s), \mathbf{u}_{1,i}(s)\big)ds \\ - V_i\big(\mathbf{e}_{0,i}(t_k + T_p)\big) - \int_{t_k}^{t_{k+1}} F_i\big(\mathbf{e}_{0,i}(s), \mathbf{u}_{0,i}(s)\big)ds\end{aligned} \tag{3.16}$$

During the course of arriving at the above result, we have concluded that, in the absence of disturbances, the remark (3.4.2) holds.

Remark 3.4.2. In the absence of disturbances, the following equality holds over the entire horizon $t \in [t_k, t_k + T_p]$:

$$\mathbf{e}_i\big(t;\ \overline{\mathbf{u}}_i^{\star}\big(\cdot;\ \mathbf{e}_i(t_k)\big), \mathbf{e}_i(t_k)\big) = \overline{\mathbf{e}}_i\big(t;\ \overline{\mathbf{u}}_i^{\star}\big(\cdot;\ \mathbf{e}_i(t_k)\big), \mathbf{e}_i(t_k)\big)$$

We turn our attention to the first integral in the above expression, and we note that $[t_{k+1}+T_p, t_k+T_p]$, is exactly the the interval where assumption (3b) of the theorem holds. Hence, we integrate the expression found in the assumption over the interval $[t_k+T_p, t_{k+1}+T_p]$, for the controls and states applicable in it:

$$\int_{t_k+T_p}^{t_{k+1}+T_p}\left(\frac{\partial V_i}{\partial \mathbf{e}_{1,i}}g_i\big(\mathbf{e}_{1,i}(s),\mathbf{u}_{1,i}(s)\big)+F_i\big(\mathbf{e}_{1,i}(s),\mathbf{u}_{1,i}(s)\big)\right)ds\leq 0$$

$$\int_{t_k+T_p}^{t_{k+1}+T_p}\frac{d}{ds}V_i\big(\mathbf{e}_{1,i}(s)\big)ds+\int_{t_k+T_p}^{t_{k+1}+T_p}F_i\big(\mathbf{e}_{1,i}(s),\mathbf{u}_{1,i}(s)\big)ds\leq 0$$

$$V_i\big(\mathbf{e}_{1,i}(t_{k+1}+T_p)\big)-V_i\big(\mathbf{e}_{1,i}(t_k+T_p)\big)+\int_{t_k+T_p}^{t_{k+1}+T_p}F_i\big(\mathbf{e}_{1,i}(s),\mathbf{u}_{1,i}(s)\big)ds\leq 0$$

$$V_i\big(\mathbf{e}_{1,i}(t_{k+1}+T_p)\big)+\int_{t_k+T_p}^{t_{k+1}+T_p}F_i\big(\mathbf{e}_{1,i}(s),\mathbf{u}_{1,i}(s)\big)ds\leq V_i\big(\mathbf{e}_{1,i}(t_k+T_p)\big)$$

The left-hand side expression is the same as the first two terms in the right-hand side of equality (3.16). We can introduce the third one by subtracting it from both sides:

$$V_i\big(\mathbf{e}_{1,i}(t_{k+1}+T_p)\big)+\int_{t_k+T_p}^{t_{k+1}+T_p}F_i\big(\mathbf{e}_{1,i}(s),\mathbf{u}_{1,i}(s)\big)ds-V_i\big(\mathbf{e}_{0,i}(t_k+T_p)\big)$$

$$\leq V_i\big(\mathbf{e}_{1,i}(t_k+T_p)\big)-V_i\big(\mathbf{e}_{0,i}(t_k+T_p)\big)$$

$$\leq \Big|V_i\big(\mathbf{e}_{1,i}(t_k+T_p)\big)-V_i\big(\mathbf{e}_{0,i}(t_k+T_p)\big)\Big|$$

since $x\leq|x|,\forall x\in\mathbb{R}$.

By revisiting lemma (3.3.3), the above inequality becomes

$$V_i\big(\mathbf{e}_{1,i}(t_{k+1}+T_p)\big)+\int_{t_k+T_p}^{t_{k+1}+T_p}F_i\big(\mathbf{e}_{1,i}(s),\mathbf{u}_{1,i}(s)\big)ds-V_i\big(\mathbf{e}_{0,i}(t_k+T_p)\big)$$

$$\leq L_{V_i}\big\|\mathbf{e}_{1,i}(t_k+T_p)-\mathbf{e}_{0,i}(t_k+T_p)\big\|$$

However, as we witnessed in (3.15), in the interval $[t_{k+1}, t_k + T_p]$: $\mathbf{e}_{1,i}(\cdot) = \mathbf{e}_{0,i}(\cdot)$, hence the right-hand side of the inequality equals zero:

$$V_i\big(\mathbf{e}_{1,i}(t_{k+1}+T_p)\big) + \int_{t_k+T_p}^{t_{k+1}+T_p} F_i\big(\mathbf{e}_{1,i}(s), \mathbf{u}_{1,i}(s)\big)ds - V_i\big(\mathbf{e}_{0,i}(t_k+T_p)\big) \leq 0$$

By subtracting the fourth term needed to complete the right-hand side expression of (3.16), i.e. $\int_{t_k}^{t_{k+1}} F_i\big(\mathbf{e}_{0,i}(s), \mathbf{u}_{0,i}(s)\big)ds$ from both sides we get

$$V_i\big(\mathbf{e}_{1,i}(t_{k+1}+T_p)\big) + \int_{t_k+T_p}^{t_{k+1}+T_p} F_i\big(\mathbf{e}_{1,i}(s), \mathbf{u}_{1,i}(s)\big)ds$$

$$-V_i\big(\mathbf{e}_{0,i}(t_k+T_p)\big) - \int_{t_k}^{t_{k+1}} F_i\big(\mathbf{e}_{0,i}(s), \mathbf{u}_{0,i}(s)\big)ds \leq -\int_{t_k}^{t_{k+1}} F_i\big(\mathbf{e}_{0,i}(s), \mathbf{u}_{0,i}(s)\big)ds$$

The left-hand side of this inequality is now equal to the cost difference $\overline{J}_i\big(\mathbf{e}_i(t_{k+1})\big) - J_i^\star\big(\mathbf{e}_i(t_k)\big)$.

Hence, the cost difference becomes bounded by

$$\overline{J}_i\big(\mathbf{e}_i(t_{k+1})\big) - J_i^\star\big(\mathbf{e}_i(t_k)\big) \leq -\int_{t_k}^{t_{k+1}} F_i\big(\mathbf{e}_{0,i}(s), \mathbf{u}_{0,i}(s)\big)ds$$

F_i is a positive-definite function as a sum of a positive-definite $\|\mathbf{u}_i\|^2_{\boldsymbol{R}_i}$ and a positive semi-definite function $\|\mathbf{e}_i\|^2_{\boldsymbol{Q}_i}$. If we denote by $m_i = \lambda_{min}(\boldsymbol{Q}_i, \boldsymbol{R}_i) \geq 0$ the minimum eigenvalue between those of matrices $\boldsymbol{R}_i$, $\boldsymbol{Q}_i$, this means that

$$F_i\big(\mathbf{e}_{0,i}(s), \mathbf{u}_{0,i}(s)\big) \geq m_i \|\mathbf{e}_{0,i}(s)\|^2$$

By integrating the above between our interval of interest $[t_k, t_{k+1}]$ we get

$$\int_{t_k}^{t_{k+1}} F_i\big(\mathbf{e}_{0,i}(s), \mathbf{u}_{0,i}(s)\big) \geq \int_{t_k}^{t_{k+1}} m_i \|\mathbf{e}_{0,i}(s)\|^2 ds$$

or

$$-\int_{t_k}^{t_{k+1}} F_i\big(\mathbf{e}_{0,i}(s), \mathbf{u}_{0,i}(s)\big) \leq -m_i \int_{t_k}^{t_{k+1}} \|\mathbf{e}_{0,i}(s)\|^2 ds$$

This means that the cost difference is upper-bounded by a class $\mathcal{K}$ function

$$\overline{J}_i\big(\mathbf{e}_i(t_{k+1})\big) - J_i^\star\big(\mathbf{e}_i(t_k)\big) \leq -m_i \int_{t_k}^{t_{k+1}} \|\mathbf{e}_{0,i}(s)\|^2 ds \leq 0$$

and, since the cost $\overline{J}_i\big(\mathbf{e}_i(t_{k+1})\big)$ is (in general) sub-optimal: $J_i^\star\big(\mathbf{e}_i(t_{k+1})\big) - \overline{J}_i\big(\mathbf{e}_i(t_{k+1})\big) \leq 0$:

$$J_i^\star\big(\mathbf{e}_i(t_{k+1})\big) - J_i^\star\big(\mathbf{e}_i(t_k)\big) \leq -m_i \int_{t_k}^{t_{k+1}} \|\mathbf{e}_{0,i}(s)\|^2 ds \tag{3.17}$$

With this milestone result established, we need to trace the time t_k back to $t_0 = 0$ in order to prove that the closed-loop system is stable at all times $t \in \mathbb{R}_{\geq 0}$.

The integral of $\|\mathbf{e}_{0,i}(\tau)\|^2$ over the interval $[t_0, t_{k+1}]$, $t_0 < t_k < t_{k+1}$ can be decomposed into the addition of two integrals with limits ranging from (a) t_0 to t_k and (b) t_k to t_{k+1}:

$$\int_{t_0}^{t_{k+1}} \|\mathbf{e}_{0,i}(s)\|^2 ds = \int_{t_0}^{t_k} \|\mathbf{e}_{0,i}(s)\|^2 ds + \int_{t_k}^{t_{k+1}} \|\mathbf{e}_{0,i}(s)\|^2 ds$$

By rearranging terms, this means that

$$\int_{t_k}^{t_{k+1}} \|\mathbf{e}_{0,i}(s)\|^2 ds = \int_{t_0}^{t_{k+1}} \|\mathbf{e}_{0,i}(s)\|^2 ds - \int_{t_0}^{t_k} \|\mathbf{e}_{0,i}(s)\|^2 ds$$

making the optimal cost difference between the consecutive sampling times t_k and t_{k+1} in (3.17)

$$J_i^\star\big(\mathbf{e}_i(t_{k+1})\big) - J_i^\star\big(\mathbf{e}_i(t_k)\big) \leq -m_i \int_{t_0}^{t_{k+1}} \|\mathbf{e}_{0,i}(s)\|^2 ds + m_i \int_{t_0}^{t_k} \|\mathbf{e}_{0,i}(s)\|^2 ds$$

Similarly, the optimal cost difference between the sampling times t_{k-1} and t_k is

$$J_i^\star\big(\mathbf{e}_i(t_k)\big) - J_i^\star\big(\mathbf{e}_i(t_{k-1})\big) \leq -m_i \int_{t_0}^{t_k} \|\mathbf{e}_{0,i}(s)\|^2 ds + m_i \int_{t_0}^{t_{k-1}} \|\mathbf{e}_{0,i}(s)\|^2 ds$$

and we can apply this rationale all the way back to the cost difference between t_0 and t_1. Summing all the inequalities between the pairs of consecutive sampling times (t_0, t_1), (t_1, t_2), ..., (t_{k-1}, t_k), we get

$$J_i^\star\big(\mathbf{e}_i(t_k)\big) - J_i^\star\big(\mathbf{e}_i(t_0)\big) \leq -m_i \int_{t_0}^{t_k} \|\mathbf{e}_{0,i}(s)\|^2 ds$$

Hence, for $t_0 = 0$

$$J_i^\star\big(\mathbf{e}_i(t_k)\big) - J_i^\star\big(\mathbf{e}_i(0)\big) \leq -m_i \int_{0}^{t_k} \|\mathbf{e}_{0,i}(s)\|^2 ds \leq 0 \tag{3.18}$$

which implies that the value function $J_i^\star\big(\mathbf{e}_i(t_k)\big)$ in non-increasing for all sampling times:

$$J_i^\star\big(\mathbf{e}_i(t_k)\big) \leq J_i^\star\big(\mathbf{e}_i(0)\big),\ \forall t_k \in \mathbb{R}_{\geq 0}$$

Let us now define the function $\Xi_i\big(\mathbf{e}_i(t)\big)$:

$$\Xi_i\big(\mathbf{e}(t)\big) \triangleq J_i^\star\big(\mathbf{e}_i(\tau)\big),\ t \in \mathbb{R}_{\geq 0}$$

where $\tau = max\{t_k : t_k \leq t\}$ – i.e. the immediately previous to t sampling time. Then the above inequality reforms into

$$\Xi_i\big(\mathbf{e}(t)\big) \leq \Xi_i\big(\mathbf{e}_i(0)\big),\ t \in \mathbb{R}_{\geq 0}$$

Since $\Xi_i\big(\mathbf{e}_i(0)\big)$ is bounded (as composition of bounded parts), this implies that $\Xi_i\big(\mathbf{e}(t)\big)$ is also bounded. The signals $\mathbf{e}_i(t) \in \mathcal{E}_{i,s}$ and $\mathbf{u}_i(t) \in \mathcal{U}_i$ are also bounded. According to (3.4), this means that $\dot{\mathbf{e}}_i(t)$ is bounded as well. From inequality (3.18) we then have

$$\Xi_i\big(\mathbf{e}_i(t)\big) \leq \Xi_i\big(\mathbf{e}_i(0)\big) - m_i \int_{0}^{\tau} \|\mathbf{e}_{0,i}(s)\|^2 ds$$

which, due to the fact that $\tau \leq t$, is equivalent to

$$\Xi_i\big(\mathbf{e}_i(t)\big) \leq \Xi_i\big(\mathbf{e}_i(0)\big) - m_i \int_{0}^{t} \|\mathbf{e}_{0,i}(s)\|^2 ds,\ t \in \mathbb{R}_{\geq 0}$$

Solving for the integral we get

$$\int_0^t \|\mathbf{e}_{0,i}(s)\|^2 ds \leq \frac{1}{m_i}\Big(\Xi_i\big(\mathbf{e}_i(0)\big) - \Xi_i\big(\mathbf{e}_i(t)\big)\Big),\ t \in \mathbb{R}_{\geq 0}$$

Both $\Xi_i\big(\mathbf{e}_i(0)\big)$ and $\Xi_i\big(\mathbf{e}_i(t)\big)$ are bounded, and therefore so is their difference, which means that the integral $\int_0^t \|\mathbf{e}_{0,i}(s)\|^2 ds$ and its limit when $t \to \infty$ are bounded as well. Lemma (1.2.2) assures us that under these conditions for the error and its dynamics, which are fulfilled in our case, the error

$$\lim_{t\to\infty} \|\mathbf{e}_{0,i}(t)\| = 0 \Leftrightarrow$$

$$\lim_{t\to\infty} \left\|\overline{\mathbf{e}}_i\Big(t;\ \overline{\mathbf{u}}_i^{\star}\big(\cdot;\ \mathbf{e}_i(t_k)\big), \mathbf{e}_i(t_k)\Big)\right\| = 0,\ \forall t_k \in \mathbb{R}_{\geq 0}$$

which, given remark (3.4.2), and dropping the initial condition, means that

$$\lim_{t\to\infty} \|\mathbf{e}_i(t)\| = 0$$

which implies that

$$\lim_{t\to\infty} \mathbf{e}_i(t) \in \Omega_i$$

Therefore, the closed-loop trajectory of the error state $\mathbf{e}_i$ converges to the terminal set Ω_i as $t \to \infty$.

In turn, this means that the system (3.3) converges to $\mathbf{z}_{i,des}$ while simultaneously conforming to all constraints $\mathcal{Z}_{i,t}$, as $t \to \infty$. This conclusion holds for all $i \in \mathcal{V}$, and hence, the compound system of agents $\mathcal{V}$ is stable in $\mathcal{Z}_{i,t}$. ■

4

Stabilization in the face of Disturbances

The purpose to be saught in this chapter is the steering of each agent $i \in \mathcal{V}$ into a desired configuration in 12D space while conforming to the requirements posed by the problem. Here, the real system and its model are *not* equivalent: we consider that additive disturbances act on the real system. At first, the model of the perturbed system (2.1) will be formalized. Next, the error model and *its* constraints will be expressed. We will then pose the optimization problem to be solved periodically: it will equip us with the optimum feasible input that steers the system towards achieving its intended configuration regardless of the introduced uncertainty, provided that it is bounded by a certain value. This will lead to the proof of this statement, i.e. that the compound closed-loop system of agents $i \in \mathcal{V}$ is stable under the proposed control regime, provided that the disturbance is bounded.

4.1 The perturbed model

In the following, we assume that the real system is subject to bounded additive disturbances $\boldsymbol{\delta}_i$ such that $\boldsymbol{\delta}_i \in \Delta_i \subset \mathbb{R}^9 \times \mathbb{T}^3$, where Δ_i is a compact set containing the origin. The real system is described by:

$$\begin{aligned}
\dot{\mathbf{z}}_i(t) &= f_i^R\big(\mathbf{z}_i(t), \mathbf{u}_i(t)\big) \qquad (4.1)\\
&= f_i\big(\mathbf{z}_i(t), \mathbf{u}_i(t)\big) + \boldsymbol{\delta}_i(t)\\
\mathbf{z}_i(0) &= \mathbf{z}_{i,0}\\
\mathbf{z}_i(t) &\subset \mathbb{R}^9 \times \mathbb{T}^3\\
\mathbf{u}_i(t) &\subset \mathbb{R}^6\\
\boldsymbol{\delta}_i(t) &\in \Delta_i \subset \mathbb{R}^9 \times \mathbb{T}^3,\ t \in \mathbb{R}_{\geq 0}\\
\sup_{t \in \mathbb{R}_{\geq 0}} \|\boldsymbol{\delta}_i(t)\| &\leq \overline{\delta}_i
\end{aligned}$$

where state $\mathbf{z}_i$ is directly measurable as per assumption (2.1.1).

The constraint set $\mathcal{Z}_{i,t} \subset \mathbb{R}^9 \times \mathbb{T}^3$ is unchanged: it is the set that captures all the state constraints of the system's dynamics posed by the problem (2.4), at $t \in \mathbb{R}_{\geq 0}$. We include it again here for reference purposes.

$$\begin{aligned}
\mathcal{Z}_{i,t} = \big\{\mathbf{z}_i(t) \in \mathbb{R}^9 \times \mathbb{T}^3 : &\|\mathbf{p}_i(t) - \mathbf{p}_j(t)\| > \underline{d}_{ij,a}, \forall j \in \mathcal{R}_i(t),\\
&\|\mathbf{p}_i(t) - \mathbf{p}_j(t)\| < d_i, \forall j \in \mathcal{N}_i,\\
&\|\mathbf{p}_i(t) - \mathbf{p}_\ell\| > \underline{d}_{i\ell,o}, \forall \ell \in \mathcal{L},\\
&\|\mathbf{p}_W - \mathbf{p}_i(t)\| < \overline{d}_{i,W},\\
&-\frac{\pi}{2} < \theta_i(t) < \frac{\pi}{2}\big\}
\end{aligned}$$

4.2 The error model

A feasible desired configuration $\mathbf{z}_{i,des} \in \mathbb{R}^9 \times \mathbb{T}^3$ is assigned to each agent $i \in \mathcal{V}$, with the aim of agent i achieving it in steady-state: $\lim_{t\to\infty} \|\mathbf{z}_i(t) - \mathbf{z}_{i,des}\| = 0$. The interior of the norm of this expression denotes the state error of agent i:

$$\mathbf{e}_i(t) = \mathbf{z}_i(t) - \mathbf{z}_{i,des},\ \mathbf{e}_i(t) : \mathbb{R}_{\geq 0} \to \mathbb{R}^9 \times \mathbb{T}^3$$

The error dynamics are equally affected by the additive uncertainty; they are denoted by $g_i^R(\mathbf{e}_i, \mathbf{u}_i)$:

$$\begin{aligned}\dot{\mathbf{e}}_i(t) = \dot{\mathbf{z}}_i(t) - \dot{\mathbf{z}}_{i,des} = \dot{\mathbf{z}}_i(t) &= f_i^R\big(\mathbf{z}_i(t), \mathbf{u}_i(t)\big) = f_i\big(\mathbf{z}_i(t), \mathbf{u}_i(t)\big) + \boldsymbol{\delta}_i(t) \\ &= g_i\big(\mathbf{e}_i(t), \mathbf{u}_i(t)\big) + \boldsymbol{\delta}_i(t) \\ &= g_i^R(\mathbf{e}_i(t), \mathbf{u}_i(t)\big) \end{aligned} \tag{4.2}$$

with $\mathbf{e}_i(0) = \mathbf{z}_i(0) - \mathbf{z}_{i,des}$. The error-wise translated constraints that are required on the state $\mathbf{z}_i(t)$ are unchanged:

$$\mathcal{E}_{i,t} = \big\{\mathbf{e}_i(t) \in \mathbb{R}^9 \times \mathbb{T}^3 : \mathbf{e}_i(t) \in \mathcal{Z}_{i,t} \ominus \mathbf{z}_{i,des}\big\}$$

Again, $\mathcal{E}_{i,t}$ is the set that captures all constraints for the error dynamics (4.2) dictated by the problem (2.4) at time $t > \mathbb{R}_{\geq 0}$.
On functions g_i, g_i^R we make the following assumption:

Assumption 4.2.1. Functions g_i, g_i^R are Lipschitz continuous in $\mathcal{E}_{i,t}$ with Lipschitz constants L_{g_i}.

If we design control laws $\mathbf{u}_i \in \mathcal{U}_i$, $\forall i \in \mathcal{V}$ such that the error signal $\mathbf{e}_i(t)$ with dynamics given in (4.2), constrained under $\mathbf{e}_i(t) \in \mathcal{E}_{i,t}$, satisfies $\lim_{t\to\infty} \|\mathbf{e}_i(t)\| = 0$, while all system related signals remain bounded in their respective regions,– if all of the above are achieved, then problem (2.4) has been solved.

In order to achieve this task, we employ a Nonlinear Receding Horizon scheme.

4.3 The optimization problem

Consider a sequence of sampling times $\{t_k\}_{k\geq 0}$, with a constant sampling time h, $0 < h < T_p$, where T_p is the finite time-horizon, such that $t_{k+1} = t_k + h$. In sampling data NMPC, a finite-horizon open-loop optimal control problem (FHOCP) is solved at discrete sampling time instants t_k based on the then-current state error measurement $\mathbf{e}_i(t_k)$. The solution is an optimal control signal $\overline{\mathbf{u}}_i^\star(t)$, computed over $t \in [t_k, t_k + T_p]$. This signal is applied to the open-loop system in between sampling times t_k and $t_k + h$.

At a generic time t_k then, agent i solves the following optimization problem:

Problem 4.3.1.

Find

$$\overline{\mathbf{u}}_i^\star(\cdot;\ \mathbf{e}_i(t_k)) \triangleq \underset{\overline{\mathbf{u}}_i(\cdot)}{\operatorname{argmin}} \quad J_i\big(\mathbf{e}_i(t_k), \overline{\mathbf{u}}_i(\cdot)\big) \tag{4.3}$$

where

$$J_i\big(\mathbf{e}_i(t_k), \overline{\mathbf{u}}_i(\cdot)\big) \triangleq \int_{t_k}^{t_k+T_p} F_i\big(\overline{\mathbf{e}}_i(s), \overline{\mathbf{u}}_i(s)\big)ds + V_i\big(\overline{\mathbf{e}}_i(t_k + T_p)\big)$$

subject to:

$$\dot{\overline{\mathbf{e}}}_i(s) = g_i\big(\overline{\mathbf{e}}_i(s), \overline{\mathbf{u}}_i(s)\big), \quad \overline{\mathbf{e}}_i(t_k) = \mathbf{e}_i(t_k) \tag{4.4}$$

$$\overline{\mathbf{u}}_i(s) \in \mathcal{U}_i, \quad \overline{\mathbf{e}}_i(s) \in \mathcal{E}_{i,s-t_k}, \quad s \in [t_k, t_k + T_p]$$

$$\overline{\mathbf{e}}_i(t_k + T_p) \in \Omega_i$$

The notation $\bar{\cdot}$ is used to distinguish predicted states which are internal to the controller, as opposed to their actual values, because, even in the nominal case, the predicted values will not be equal to the actual closed-loop values. This means that $\overline{\mathbf{e}}_i(\cdot)$ is the solution to (4.4) driven by the control input $\overline{\mathbf{u}}_i(\cdot) : [t_k, t_k + T_p] \to \mathcal{U}_i$ with initial condition $\mathbf{e}_i(t_k)$.

The applied input signal is a portion of the optimal solution to an optimization problem where information on the states of the neighbouring agents of agent i are taken into account only in the constraints considered in the optimization problem. These constraints pertain to the set of its neighbours $\mathcal{N}_i$ and, in total, to the set of all agents within its sensing range $\mathcal{R}_i$. Regarding these, we assume assumption (3.3.1), i.e. at time t_k when agent i solves the optimization problem, he has access to the measurements of the states and the values of the predicted states for all agents within its sensing range. Naturally, the inter-agent and intra-horizon constraint regime adopted is identical[1] to the one used in the case without disturbances acting on the system (see figure (3.1) and the discussion preceding it).

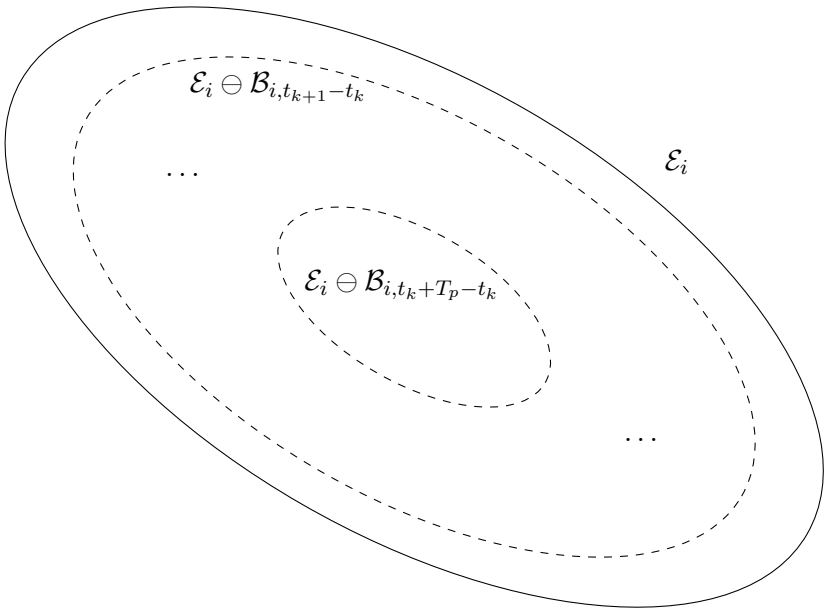

Figure 4.1: The nominal constraint set $\mathcal{E}_i$ in bold and the consecutive restricted constraint sets $\mathcal{E}_i \ominus \mathcal{B}_{i,s-t_k}$, $s \in [t_k, t_k + T_p]$, dashed.

While in the disturbance-free case the constraint set is $\mathcal{E}_i$, due to the existence of disturbances here, the constraint set is replaced in problem (4.3.1) by

$$\mathcal{E}_{i,s-t_k} \equiv \mathcal{E}_i \ominus \mathcal{B}_{i,s-t_k} \tag{4.5}$$

[1]In what follows, we will drop the subscript t from $\mathcal{E}_{i,t}$ to avoid confusion with the restricted constraint set notation and for notational economy. The reader should be able to discern that the set $\mathcal{E}_i$ is time-varying without it being explicitly expressed as such. The form of the set is deduced from context.

where

$$\mathcal{B}_{i,s-t} \equiv \left\{ \mathbf{e}_i \in \mathbb{R}^9 \times \mathbb{T}^3 : \|\mathbf{e}_i(s)\| \leq \frac{\overline{\delta}_i}{L_{g_i}} \left(e^{L_{g_i}(s-t)} - 1 \right),\ \forall s \in [t, t+T_p] \right\} \tag{4.6}$$

The reason for this substitution lies in the following. Consider that there are no disturbances affecting the states of the plant; the state evolution of the plant and its model considered in the solution to the optimization problem both abide by the state constraints since the two models are identical. Consider now that there are disturbances affecting the states of the plant − disturbances that are unknown to the model considered in the solution to the optimization problem. If the state constraint set was left unchanged during the solution of the optimization problem, the applied input to the plant, coupled with the uncertainty affecting the states of the plant could, without loss of generality[2], force the states of the plant to escape their intended bounds.

If the state constraint set considered in the solution of the optimization problem (4.3.1) is equal to (4.5), then the state of the real system, the plant, is guaranteed to abide by the original state constraint set $\mathcal{E}_i$. We formalize this statement in property (4.3.1).

Property 4.3.1. For every $s \in [t, t+T_p]$

$$\overline{\mathbf{e}}_i\big(s;\ \mathbf{u}_i(\cdot,\ \mathbf{e}_i(t)), \mathbf{e}_i(t)\big) \in \mathcal{E}_i \ominus \mathcal{B}_{i,s-t} \Rightarrow \mathbf{e}_i(s) \in \mathcal{E}_i$$

where $\mathcal{B}_{i,s-t}$ is given by (4.6).

Assumption 4.3.1. The terminal set $\Omega_i \subseteq \Psi_i$ is a subset of an admissible and positively invariant set Ψ_i as per definition (1.2.5), where Ψ_i is defined as

$$\Psi_i \triangleq \left\{ \mathbf{e}_i \in \mathcal{E}_i : V_i(\mathbf{e}_i) \leq \varepsilon_{\Psi_i} \right\},\ \varepsilon_{\Psi_i} > 0$$

[2]Receding Horizon Control is inherently robust under certain considerations, see [18] for more.

Assumption 4.3.2. The set Ψ_i belongs to the set Φ_i, $\Psi_i \subseteq \Phi_i$, which is the set of states within $\mathcal{E}_{i,T_p}$ for which there is an admissible control input whose form is of linear feedback with regard to the state[a]:

$$\exists \Phi_i \triangleq \left\{ \overline{\mathbf{e}}_i \in \mathcal{E}_{i,T_p} : h_i(\overline{\mathbf{e}}_i) \in \mathcal{U}_i \right\}$$

[a] This is equivalent to requiring that $\rangle, \mathcal{T}_{\surd} \neq \varnothing$

Remark 4.3.1. The existence of the linear state-feedback control law h_i is ensured if the linearisation of system (4.2) is stabilizable [9][8].

Assumption 4.3.3. The admissible and positively invariant set Ψ_i is such that

$$\forall \mathbf{e}_i(t) \in \Psi_i \Rightarrow \overline{\mathbf{e}}_i\big(t+\tau;\ h_i(\mathbf{e}_i(t)), \mathbf{e}_i(t)\big) \in \Omega_i \subseteq \Psi_i$$

for some $\tau \in [0, h]$

Assumption 4.3.4. The terminal set Ω_i is closed, includes the origin, and is defined by

$$\Omega_i \triangleq \left\{ \mathbf{e}_i \in \mathcal{E}_i : V_i(\mathbf{e}_i) \leq \varepsilon_{\Omega_i} \right\} \text{ , where } \varepsilon_{\Omega_i} \in (0, \varepsilon_{\Psi_i})$$

Remark 4.3.2. It may be the case that the length of the time-horizon T_p is large enough that $\mathcal{E}_{i,T_p} \subset \Phi_i$ instead of the desired opposite. The length of the time-horizon should hence be designed so that the above violation does not occur.

Functions $F_i : \mathcal{E}_i \times \mathcal{U}_i \to \mathbb{R}_{\geq 0}$ and $V_i : \Psi_i \to \mathbb{R}_{\geq 0}$ are defined by (3.8) and (3.9) respectively, as in the disturbance-free case. Matrices $\boldsymbol{R}_i \in \mathbb{R}^{6\times 6}$, $\boldsymbol{Q}_i, \boldsymbol{P}_i \in \mathbb{R}^{12\times 12}$ are positive definite. Consequently, lemmas (3.3.1), (3.3.2), (3.3.3) and (3.3.4) hold true here, as in the disturbance-free case: the running costs F_i are Lipschitz continuous in $\mathcal{E}_i \times \mathcal{U}_i$ with Lipschitz

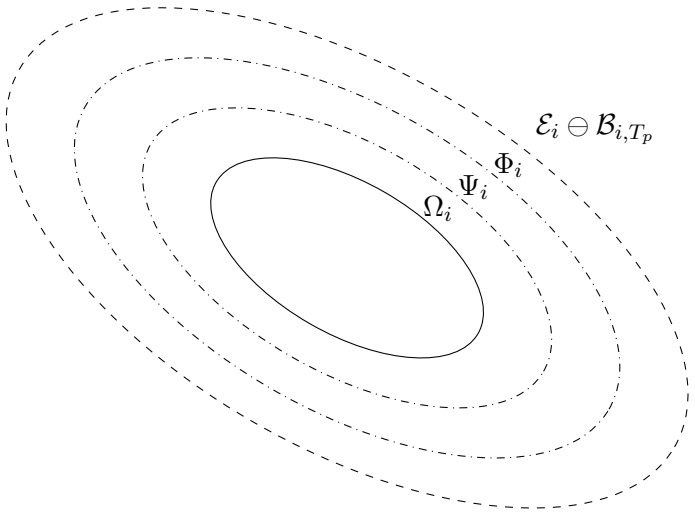

Figure 4.2: The hierarchy of sets $\Omega_i \subseteq \Psi_i \subseteq \Phi_i \subseteq \mathcal{E}_{i,T_p}$, in bold, dash-dotted, dash-dotted, and dashed, respectively. For every state in Φ_i there is a linear state feedback control $h_i(\mathbf{e}_i)$ which, when applied to a state $\mathbf{e}_i \in \Psi_i$, causes the trajectory of the state of the system to fall into the terminal set Ω_i.

constant L_{F_i} and they are lower- and upper-bounded by class $\mathcal{K}_\infty$ functions; the terminal penalty functions V_i are Lipschitz continuous in Ψ_i with Lipschitz constant L_{V_i}, and they are lower- and upper-bounded by class $\mathcal{K}_\infty$ functions.

The solution to the optimal control problem (4.3) at time t_k is an optimal control input, denoted by $\overline{\mathbf{u}}_i^\star(\cdot;\ \mathbf{e}_i(t_k))$, which is applied to the open-loop system until the next sampling instant $t_k + h$, with $h \in (0, T_p)$.

$$\mathbf{u}_i(t) = \overline{\mathbf{u}}_i^\star\big(t;\ \mathbf{e}_i(t_k)\big),\ t \in [t_k, t_k + h] \tag{4.7}$$

At time t_{k+1} a new finite horizon optimal control problem is solved in the same manner, leading to a receding horizon approach.

The control input $\mathbf{u}_i(\cdot)$ is of feedback form, since it is recalculated at each sampling instant based on the then-current state. The solution to equation (4.2), starting at time t_1, from an initial condition $\mathbf{e}_i(t_1) = \overline{\mathbf{e}}_i(t_1)$, by application of the control input $\mathbf{u}_i : [t_1, t_2] \to \mathcal{U}_i$ is denoted by

$$\mathbf{e}_i\big(t;\ \mathbf{u}_i(\cdot), \mathbf{e}_i(t_1)\big),\ t \in [t_1, t_2]$$

As before, the *predicted* state of the system (4.2) at time $t_k + \tau$, based on the measurement of the state at time t_k, $\mathbf{e}_i(t_k)$, by application of the control input $\mathbf{u}_i\big(t;\ \mathbf{e}_i(t_k)\big)$, for the time period $t \in [t_k, t_k + \tau]$ is denoted by

$$\overline{\mathbf{e}}_i\big(t_k + \tau;\ \mathbf{u}_i(\cdot), \mathbf{e}_i(t_k)\big)$$

On the existence of solutions to (4.2) we assume the following:

Assumption 4.3.5. The system (4.2) has a *continuous solution* for any $\mathbf{e}_i(0) \in \mathcal{E}_i$, any *piecewise continuous* input $\mathbf{u}_i(\cdot) : [0, T_p] \to \mathcal{U}_i$, and any *exogenous disturbance* $\boldsymbol{\delta}_i(\cdot) : [0, T_p] \to \Delta_i$.

In contrast to the disturbance-free case where the predicted state coincided with the state of the actual system, due to the existence of disturbances this equality is void.

Remark 4.3.3. The following holds true here because *there are* disturbances acting on the system.

$$\overline{\mathbf{e}}_i\big(\tau_1;\ \mathbf{u}_i(\cdot), \mathbf{e}_i(\tau_0)\big) \neq \mathbf{e}_i\big(\tau_1;\ \mathbf{u}_i(\cdot), \mathbf{e}_i(\tau_0)\big)$$

The closed-loop system for which stability is to be guaranteed is

$$\mathbf{e}_i(\tau) = g_i^R\big(\mathbf{e}_i(\tau), \overline{\mathbf{u}}_i^\star(\tau)\big),\ \tau \geq t_0 = 0 \tag{4.8}$$

where $\overline{\mathbf{u}}_i^\star(\tau) = \overline{\mathbf{u}}_i^\star(\tau;\ \mathbf{e}_i(t_k))$, $\tau \in [t_k, t_k + h)$.

We can now give the definition of an *admissible input* for the FHOCP (4.3.1):

Definition 4.3.1. (*Admissible input for the FHOCP* (4.3.1))

A control input $\mathbf{u}_i : [t_k, t_k + T_p] \to \mathbb{R}^6$ for a state $\mathbf{e}_i(t_k)$ is called *admissible* for the problem (4.3.1) if all the following hold:

1. $\mathbf{u}_i(\cdot)$ is piecewise continuous

2. $\mathbf{u}_i(\tau) \in \mathcal{U}_i,\ \forall \tau \in [t_k, t_k + T_p]$

3. $\overline{\mathbf{e}}_i\big(t_k + \tau;\ \mathbf{u}_i(\cdot), \mathbf{e}_i(t_k)\big) \in \mathcal{E}_i \ominus \mathcal{B}_{i,\tau},\ \forall \tau \in [0, T_p]$

4. $\overline{\mathbf{e}}_i\big(t_k + T_p;\ \mathbf{u}_i(\cdot), \mathbf{e}_i(t_k)\big) \in \Omega_i$

In other words, $\mathbf{u}_i$ is admissible if it conforms to the constraints on the input and its application yields states that conform to the prescribed state constraints of problem (4.3.1) along the entire horizon $[t_k, t_k + T_p]$, and the terminal predicted state conforms to the terminal constraint.

4.4 Stabilization: Feasibility and Convergence

Under these considerations, we can now state the theorem that relates to the guaranteeing of the stability of the compound system of agents $i \in \mathcal{V}$, when each of them is assigned a desired position which results in feasible displacements:

Theorem 4.4.1. Suppose that

1. a solution to the optimal control problem (4.3) is feasible at time $t = 0$, that is, assumptions (2.1.1), (2.2.1), and (2.3.1) hold at time $t = 0$

2. assumptions (3.3.1), (4.2.1) $-$(4.3.5) hold true

3. there exists an admissible control input of linear feedback form $h_i(\mathbf{e}_i) : [t_k + T_p, t_{k+1} + T_p] \to \mathcal{U}_i$ such that for all $\mathbf{e}_i \in \Psi_i$ and $\forall \tau \in [t_k + T_p, t_{k+1} + T_p]$:

$$\frac{\partial V_i}{\partial \mathbf{e}_i} g_i\big(\mathbf{e}_i(\tau), h_i(\mathbf{e}_i(\tau))\big) + F_i\big(\mathbf{e}_i(\tau), h_i(\mathbf{e}_i(\tau))\big) \leq 0$$

4. the upper bound $\overline{\delta}_i$ of the disturbance $\boldsymbol{\delta}_i(t)$, $\overline{\delta}_i = \sup_{t\geq 0} \|\boldsymbol{\delta}_i(t)\| = \|\boldsymbol{\delta}_i\|_\infty$ is in turn bounded by

$$\overline{\delta}_i \leq \frac{\varepsilon_{\Psi_i} - \varepsilon_{\Omega_i}}{\frac{L_{V_i}}{L_{g_i}}(e^{L_{g_i}h} - 1)e^{L_{g_i}(T_p - h)}}$$

for all $t \in \mathbb{R}_{\geq 0}$

then the closed loop system (4.8) under the control input (4.7) converges to the set Ω_i and is ultimately bounded there.

Proof. The proof of the above theorem consists of two parts: in the first, recursive feasibility is established, that is, initial feasibility is shown to imply subsequent feasibility; in the second, and based on the first part, it is shown that the error state $\mathbf{e}_i(t)$ reaches the terminal set Ω_i and is trapped there.

Remark 4.4.1. Given that disturbances *are* present, for the predicted and actual states at time $\tau_1 \geq \tau_0 \in \mathbb{R}_{\geq 0}$ it holds that:

$$\mathbf{e}_i\big(\tau_1;\ \mathbf{u}_i(\cdot), \mathbf{e}_i(\tau_0)\big) = \mathbf{e}_i(\tau_0) + \int_{\tau_0}^{\tau_1} g_i^R\big(\mathbf{e}_i(s;\ \mathbf{e}_i(\tau_0)), \mathbf{u}_i(s)\big)ds$$

$$\overline{\mathbf{e}}_i\big(\tau_1;\ \mathbf{u}_i(\cdot), \mathbf{e}_i(\tau_0)\big) = \mathbf{e}_i(\tau_0) + \int_{\tau_0}^{\tau_1} g_i\big(\overline{\mathbf{e}}_i(s;\ \mathbf{e}_i(\tau_0)), \mathbf{u}_i(s)\big)ds$$

Lemma 4.4.1. Suppose that the real system, which is under the existence of bounded additive disturbances, and the model are both at time t at state $\mathbf{e}_i(t)$. Applying at time t a control law $\mathbf{u}(\cdot)$ to the system model deemed "real" and its model will cause at time $t + \tau$, $\tau \geq 0$ a divergence between the states of the real system and its model. The norm of the difference between the state of the real system and the state of the

model system is bounded by

$$\left\| \mathbf{e}_i\big(t+\tau;\ \mathbf{u}(\cdot), \mathbf{e}_i(t)\big) - \overline{\mathbf{e}}_i\big(t+\tau;\ \mathbf{u}(\cdot), \mathbf{e}_i(t)\big) \right\| \leq \frac{\overline{\delta}_i}{\mathbf{L}_{g_i}} (e^{L_{g_i}\tau} - 1)$$

where $\overline{\delta}_i$ is the upper bound of the disturbance, and L_{g_i} the Lipschitz constant of both models.

Feasibility analysis In this section we will show that there can be constructed an admissible but not necessarily optimal control input according to definition (4.3.1).

Consider a sampling instant t_k for which a solution $\overline{\mathbf{u}}_i^\star\big(\cdot;\ \mathbf{e}_i(t_k)\big)$ to problem (4.3.1) exists. Suppose now a time instant t_{k+1} such that[3] $t_k < t_{k+1} < t_k + T_p$, and consider that the optimal control signal calculated at t_k is comprised by the following two portions:

$$\overline{\mathbf{u}}_i^\star\big(\cdot;\ \mathbf{e}_i(t_k)\big) = \begin{cases} \overline{\mathbf{u}}_i^\star\big(\tau_1;\ \mathbf{e}_i(t_k)\big), & \tau_1 \in [t_k, t_{k+1}] \\ \\ \overline{\mathbf{u}}_i^\star\big(\tau_2;\ \mathbf{e}_i(t_k)\big), & \tau_2 \in [t_{k+1}, t_k + T_p] \end{cases} \tag{4.9}$$

Both portions are admissible since the calculated optimal control input is admissible, and hence they both conform to the input constraints. As for the resulting predicted states, they satisfy the state constraints, and, crucially:

$$\overline{\mathbf{e}}_i\big(t_k + T_p;\ \overline{\mathbf{u}}_i^\star(\cdot), \mathbf{e}_i(t_k)\big) \in \Omega_i \tag{4.10}$$

Furthermore, according to assumption (3) of the theorem, there exists an admissible (and certainly not guaranteed optimal) input $h_i \in \mathcal{U}_i$ that renders Ψ_i (and consequently Ω_i) invariant over $[t_k + T_p, t_k + T_p + h]$.

Given the above facts, we can construct an admissible input $\widetilde{\mathbf{u}}_i(\cdot)$ for time t_{k+1} by sewing together the second portion of (4.9) and the admissible input $h_i(\cdot)$:

$$\widetilde{\mathbf{u}}_i(\tau) = \begin{cases} \overline{\mathbf{u}}_i^\star\big(\tau;\ \mathbf{e}_i(t_k)\big), & \tau \in [t_{k+1}, t_k + T_p] \\ \\ h_i\big(\overline{\mathbf{e}}_i\big(\tau;\ \overline{\mathbf{u}}_i^\star(\cdot), \mathbf{e}_i(t_{k+1})\big)\big), & \tau \in (t_k + T_p, t_{k+1} + T_p] \end{cases} \tag{4.11}$$

[3] It is not strictly necessary that $t_{k+1} = t_k + h$ here, however it is necessary for the following that $t_{k+1} - t_k \leq h$

Applied at time t_{k+1}, $\widetilde{\mathbf{u}}_i(\tau)$ is an admissible control input with regard to the input constraints as a composition of admissible control inputs, for all $\tau \in [t_{k+1}, t_{k+1} + T_p]$.

Furthermore, $\overline{\mathbf{e}}_i\big(t_{k+1} + s;\ \widetilde{\mathbf{u}}_i(\cdot), \mathbf{e}_i(t_{k+1})\big) \in \mathcal{E}_i \ominus \mathcal{B}_s$, for all $s \in [0, T_p]$.

By applying lemma (4.4.1) for $t = t_{k+1} + s$ and $\tau = t_k$ we get

$$\left\| \mathbf{e}_i\big(t_{k+1} + s;\ \overline{\mathbf{u}}_i^\star(\cdot), \mathbf{e}_i(t_k)\big) - \overline{\mathbf{e}}_i\big(t_{k+1} + s;\ \overline{\mathbf{u}}_i^\star(\cdot), \mathbf{e}_i(t_k)\big) \right\| \leq \frac{\overline{\delta}_i}{L_{g_i}} \big(e^{L_{g_i}(h+s)} - 1\big)$$

or, in set language

$$\mathbf{e}_i\big(t_{k+1} + s;\ \overline{\mathbf{u}}_i^\star(\cdot), \mathbf{e}_i(t_k)\big) - \overline{\mathbf{e}}_i\big(t_{k+1} + s;\ \overline{\mathbf{u}}_i^\star(\cdot), \mathbf{e}_i(t_k)\big) \in \mathcal{B}_{i,h+s}$$

By applying a reasoning identical to the proof (see (A.6)) of lemma (4.4.1) for $t = t_{k+1}$ (in the model equation) and $t = t_k$ (in the real model equation), and $\tau = s$ we get

$$\left\| \mathbf{e}_i\big(t_{k+1} + s;\ \overline{\mathbf{u}}_i^\star(\cdot), \mathbf{e}_i(t_k)\big) - \overline{\mathbf{e}}_i\big(t_{k+1} + s;\ \overline{\mathbf{u}}_i^\star(\cdot), \mathbf{e}_i(t_{k+1})\big) \right\| \leq \frac{\overline{\delta}_i}{L_{g_i}} \big(e^{L_{g_i} s} - 1\big)$$

which translates to

$$\mathbf{e}_i\big(t_{k+1} + s;\ \overline{\mathbf{u}}_i^\star(\cdot), \mathbf{e}_i(t_k)\big) - \overline{\mathbf{e}}_i\big(t_{k+1} + s;\ \overline{\mathbf{u}}_i^\star(\cdot), \mathbf{e}_i(t_{k+1})\big) \in \mathcal{B}_{i,s}$$

Furthermore, we know that the solution to the optimization problem is feasible at time t_k, which means that

$$\overline{\mathbf{e}}_i\big(t_{k+1} + s;\ \overline{\mathbf{u}}_i^\star(\cdot), \mathbf{e}_i(t_k)\big) \in \mathcal{E}_i \ominus \mathcal{B}_{i,h+s}$$

Let us for sake of readability set

$$\mathbf{e}_0 = \mathbf{e}_i\big(t_{k+1} + s;\ \overline{\mathbf{u}}_i^\star(\cdot), \mathbf{e}_i(t_k)\big)$$

$$\overline{\mathbf{e}}_0 = \overline{\mathbf{e}}_i\big(t_{k+1} + s;\ \overline{\mathbf{u}}_i^\star(\cdot), \mathbf{e}_i(t_k)\big)$$

$$\overline{\mathbf{e}}_1 = \overline{\mathbf{e}}_i\big(t_{k+1} + s;\ \overline{\mathbf{u}}_i^\star(\cdot), \mathbf{e}_i(t_{k+1})\big)$$

and translate the above system of include statements to:

$$\mathbf{e}_{i,0} - \overline{\mathbf{e}}_{i,0} \in \mathcal{B}_{i,h+s}$$

$$\mathbf{e}_{i,0} - \overline{\mathbf{e}}_{i,1} \in \mathcal{B}_{i,s}$$

$$\overline{\mathbf{e}}_{i,0} \in \mathcal{E}_i \ominus \mathcal{B}_{i,h+s}$$

First we will focus on the two first statements, and we will derive a result that will combine with the third statement so as to prove that the predicted state will be feasible from t_{k+1} to $t_{k+1} + T_p$. Subtracting the second from the first yields

$$\overline{\mathbf{e}}_{i,1} - \overline{\mathbf{e}}_{i,0} \in \mathcal{B}_{i,h+s} \ominus \mathcal{B}_{i,s}$$

Now we introduce the third statement

$$\overline{\mathbf{e}}_{i,0} \in \mathcal{E}_i \ominus \mathcal{B}_{i,h+s}$$

$$\overline{\mathbf{e}}_{i,1} - \overline{\mathbf{e}}_{i,0} \in \mathcal{B}_{i,h+s} \ominus \mathcal{B}_{i,s}$$

Adding the latter to the former yields

$$\overline{\mathbf{e}}_{i,1} \in \big(\mathcal{E}_i \ominus \mathcal{B}_{i,h+s}\big) \oplus \big(\mathcal{B}_{i,h+s} \ominus \mathcal{B}_{i,s}\big)$$

But[a] $(A \ominus B) \oplus (B \ominus C) = (A \oplus B) \ominus (B \oplus C)$ for arbitrary sets A, B, C. Hence

$$\overline{\mathbf{e}}_{i,1} \in \big(\mathcal{E}_i \oplus \mathcal{B}_{i,h+s}\big) \ominus \big(\mathcal{B}_{i,h+s} \oplus \mathcal{B}_{i,s}\big)$$

Using implication[b] (v) of theorem 2.1 from [21] yields

$$\overline{\mathbf{e}}_{i,1} \in \Big(\big(\mathcal{E}_i \oplus \mathcal{B}_{i,h+s} \big) \ominus \mathcal{B}_{i,h+s} \Big) \ominus \mathcal{B}_{i,s}$$

Using implication[c] (3.1.11) from [22] yields

$$\overline{\mathbf{e}}_{i,1} \in \mathcal{E}_i \ominus \mathcal{B}_{i,s}$$

Translating back to our native language

$$\overline{\mathbf{e}}_i\big(t_{k+1}+s;\ \overline{\mathbf{u}}_i^\star(\cdot), \mathbf{e}_i(t_{k+1})\big) \in \mathcal{E}_i \ominus \mathcal{B}_{i,s},\ \forall s \in [0, T_p] \tag{4.12}$$

Remark 4.4.2. Consulting with property (4.3.1), this means that the state of the "true" system does not violate the constraints $\mathcal{E}_i$ over the horizon $[t_{k+1}, t_{k+1}+T_p]$:

$$\overline{\mathbf{e}}_i\big(t_{k+1}+s;\ \overline{\mathbf{u}}_i^\star(\cdot), \mathbf{e}_i(t_{k+1})\big) \in \mathcal{E}_i \ominus \mathcal{B}_{i,s} \ \Rightarrow\ \mathbf{e}_i\big(t_{k+1}+s;\ \overline{\mathbf{u}}_i^\star(\cdot), \mathbf{e}_i(t_{k+1})\big) \in \mathcal{E}_i,\ \forall s \in [0, T_p]$$

■

---

[a] Suppose sets A, B, C and vectors $\mathbf{a} \in A, \mathbf{b} \in B, \mathbf{c} \in C$, where $\mathbf{a}, \mathbf{b}, \mathbf{c} \in \mathbb{R}^n$. Then

$$A \ominus B = \{\mathbf{a} - \mathbf{b},\ \mathbf{a} \in A, \mathbf{b} \in B\}$$

$$B \ominus C = \{\mathbf{b} - \mathbf{c},\ \mathbf{b} \in B, \mathbf{c} \in C\}$$

Adding the latter to the former yields

$$(A \ominus B) \oplus (B \ominus C) = \{\mathbf{a} - \mathbf{b} + \mathbf{b} - \mathbf{c},\ \mathbf{a} \in A, \mathbf{b} \in B, \mathbf{c} \in C\}$$

$$= \{\mathbf{a} - \mathbf{c},\ \mathbf{a} \in A, \mathbf{c} \in C\}$$

On the other hand

$$A \oplus B = \{\mathbf{a} + \mathbf{b},\ \mathbf{a} \in A, \mathbf{b} \in B\}$$

$$B \oplus C = \{\mathbf{b} + \mathbf{c},\ \mathbf{b} \in B, \mathbf{c} \in C\}$$

Subtracting the latter from the former yields

$$(A \oplus B) \ominus (B \oplus C) = \{\mathbf{a} + \mathbf{b} - \mathbf{b} - \mathbf{c},\ \mathbf{a} \in A, \mathbf{b} \in B, \mathbf{c} \in C\}$$

$$= \{\mathbf{a} - \mathbf{c},\ \mathbf{a} \in A, \mathbf{c} \in C\}$$

Therefore

$$(A \ominus B) \oplus (B \ominus C) = (A \oplus B) \ominus (B \oplus C)$$

[b] $A = B_1 \oplus B_2 \Rightarrow A \ominus B = (A \ominus B_1) \ominus B_2$
[c] $(A \oplus B) \ominus B \subset A$

Finally, $\overline{\mathbf{e}}_i\big(t_{k+1}+T_p;\ \widetilde{\mathbf{u}}_i(\cdot), \mathbf{e}_i(t_{k+1})\big) \in \Omega_i$.

To prove this statement we begin with

$$
\begin{aligned}
&V_i\big(\overline{\mathbf{e}}_i\big(t_k+T_p;\ \overline{\mathbf{u}}_i^{\star}(\cdot), \mathbf{e}_i(t_{k+1})\big)\big) - V_i\big(\overline{\mathbf{e}}_i\big(t_k+T_p;\ \overline{\mathbf{u}}_i^{\star}(\cdot), \mathbf{e}_i(t_k)\big)\big) \\
&\qquad \leq \Big| V_i\big(\overline{\mathbf{e}}_i\big(t_k+T_p;\ \overline{\mathbf{u}}_i^{\star}(\cdot), \mathbf{e}_i(t_{k+1})\big)\big) - V_i\big(\overline{\mathbf{e}}_i\big(t_k+T_p;\ \overline{\mathbf{u}}_i^{\star}(\cdot), \mathbf{e}_i(t_k)\big)\big) \Big| \\
&\qquad \leq L_{V_i} \Big\| \overline{\mathbf{e}}_i\big(t_k+T_p;\ \overline{\mathbf{u}}_i^{\star}(\cdot), \mathbf{e}_i(t_{k+1})\big) - \overline{\mathbf{e}}_i\big(t_k+T_p;\ \overline{\mathbf{u}}_i^{\star}(\cdot), \mathbf{e}_i(t_k)\big) \Big\| \\
&\qquad = L_{V_i} \Big\| \overline{\mathbf{e}}_i\big(t_k+T_p;\ \overline{\mathbf{u}}_i^{\star}(\cdot), \mathbf{e}_i(t_{k+1})\big) - \overline{\mathbf{e}}_i\big(t_k+T_p;\ \overline{\mathbf{u}}_i^{\star}(\cdot), \mathbf{e}_i(t_k)\big) \Big\| \qquad (4.13)
\end{aligned}
$$

Consulting with remark (4.4.1) we get that the two terms interior to the norm are respectively equal to

$$
\overline{\mathbf{e}}_i\big(t_k+T_p;\ \overline{\mathbf{u}}_i^{\star}(\cdot), \mathbf{e}_i(t_{k+1})\big) = \mathbf{e}_i(t_{k+1}) + \int_{t_{k+1}}^{t_k+T_p} g_i\big(\overline{\mathbf{e}}_i(s;\ \mathbf{e}_i(t_{k+1})), \overline{\mathbf{u}}_i^{\star}(s)\big) ds
$$

and

$$
\begin{aligned}
\overline{\mathbf{e}}_i\big(t_k+T_p;\ \overline{\mathbf{u}}_i^{\star}(\cdot), \mathbf{e}_i(t_k)\big) &= \mathbf{e}_i(t_k) \quad + \int_{t_k}^{t_k+T_p} g_i\big(\overline{\mathbf{e}}_i(s;\ \mathbf{e}_i(t_k)), \overline{\mathbf{u}}_i^{\star}(s)\big) ds \\
&= \mathbf{e}_i(t_k) \quad + \int_{t_k}^{t_{k+1}} g_i\big(\overline{\mathbf{e}}_i(s;\ \mathbf{e}_i(t_k)), \overline{\mathbf{u}}_i^{\star}(s)\big) ds \\
&\qquad\quad + \int_{t_{k+1}}^{t_k+T_p} g_i\big(\overline{\mathbf{e}}_i(s;\ \mathbf{e}_i(t_k)), \overline{\mathbf{u}}_i^{\star}(s)\big) ds \\
&= \overline{\mathbf{e}}_i(t_{k+1}) + \int_{t_{k+1}}^{t_k+T_p} g_i\big(\overline{\mathbf{e}}_i(s;\ \mathbf{e}_i(t_k)), \overline{\mathbf{u}}_i^{\star}(s)\big) ds
\end{aligned}
$$

Subtracting the latter from the former and taking norms on either side we get

$$
\begin{aligned}
&\left\|\overline{\mathbf{e}}_i\big(t_k+T_p;\ \overline{\mathbf{u}}_i^\star(\cdot),\mathbf{e}_i(t_{k+1})\big)-\overline{\mathbf{e}}_i\big(t_k+T_p;\ \overline{\mathbf{u}}_i^\star(\cdot),\mathbf{e}_i(t_k)\big)\right\| \\
&\quad=\Big\|\mathbf{e}_i(t_{k+1})-\overline{\mathbf{e}}_i(t_{k+1}) \\
&\quad+\int_{t_{k+1}}^{t_k+T_p} g_i\big(\overline{\mathbf{e}}_i(s;\ \mathbf{e}_i(t_{k+1})),\overline{\mathbf{u}}_i^\star(s)\big)ds-\int_{t_{k+1}}^{t_k+T_p} g_i\big(\overline{\mathbf{e}}_i(s;\ \mathbf{e}_i(t_k)),\overline{\mathbf{u}}_i^\star(s)\big)ds\Big\| \\
&\quad\le\Big\|\mathbf{e}_i(t_{k+1})-\overline{\mathbf{e}}_i(t_{k+1})\Big\| \\
&\quad+\Big\|\int_{t_{k+1}}^{t_k+T_p} g_i\big(\overline{\mathbf{e}}_i(s;\ \mathbf{e}_i(t_{k+1})),\overline{\mathbf{u}}_i^\star(s)\big)ds-\int_{t_{k+1}}^{t_k+T_p} g_i\big(\overline{\mathbf{e}}_i(s;\ \mathbf{e}_i(t_k)),\overline{\mathbf{u}}_i^\star(s)\big)ds\Big\| \\
&\quad=\Big\|\mathbf{e}_i(t_{k+1})-\overline{\mathbf{e}}_i(t_{k+1})\Big\| \\
&\quad+\Big\|\int_{t_{k+1}}^{t_k+T_p}\Big(g_i\big(\overline{\mathbf{e}}_i(s;\ \mathbf{e}_i(t_{k+1})),\overline{\mathbf{u}}_i^\star(s)\big)-g_i\big(\overline{\mathbf{e}}_i(s;\ \mathbf{e}_i(t_k)),\overline{\mathbf{u}}_i^\star(s)\big)\Big)ds\Big\| \\
&\quad\le\Big\|\mathbf{e}_i(t_{k+1})-\overline{\mathbf{e}}_i(t_{k+1})\Big\| \\
&\quad+\int_{t_{k+1}}^{t_k+T_p}\Big\|g_i\big(\overline{\mathbf{e}}_i(s;\ \mathbf{e}_i(t_{k+1})),\overline{\mathbf{u}}_i^\star(s)\big)-g_i\big(\overline{\mathbf{e}}_i(s;\ \mathbf{e}_i(t_k)),\overline{\mathbf{u}}_i^\star(s)\big)\Big\|ds \\
&\quad\le\Big\|\mathbf{e}_i(t_{k+1})-\overline{\mathbf{e}}_i(t_{k+1})\Big\| \\
&\quad+L_{g_i}\int_{t_{k+1}}^{t_k+T_p}\Big\|\overline{\mathbf{e}}_i\big(s;\ \overline{\mathbf{u}}_i^\star(\cdot),\mathbf{e}_i(t_{k+1})\big)-\overline{\mathbf{e}}_i\big(s;\ \overline{\mathbf{u}}_i^\star(\cdot),\mathbf{e}_i(t_k)\big)\Big\|ds \\
&\quad=\Big\|\mathbf{e}_i(t_{k+1})-\overline{\mathbf{e}}_i(t_{k+1})\Big\| \\
&+L_{g_i}\int_h^{T_p}\Big\|\overline{\mathbf{e}}_i\big(t_k+s;\ \overline{\mathbf{u}}_i^\star(\cdot),\mathbf{e}_i(t_{k+1})\big)-\overline{\mathbf{e}}_i\big(t_k+s;\ \overline{\mathbf{u}}_i^\star(\cdot),\mathbf{e}_i(t_k)\big)\Big\|ds
\end{aligned}
$$

By applying the Grönwall-Bellman inequality we get

$$\left\|\overline{\mathbf{e}}_i\big(t_k+T_p;\ \overline{\mathbf{u}}_i^\star(\cdot),\mathbf{e}_i(t_{k+1})\big)-\overline{\mathbf{e}}_i\big(t_k+T_p;\ \overline{\mathbf{u}}_i^\star(\cdot),\mathbf{e}_i(t_k)\big)\right\| \leq \left\|\mathbf{e}_i(t_{k+1})-\overline{\mathbf{e}}_i(t_{k+1})\right\| e^{L_{g_i}(T_p-h)}$$

By applying lemma (4.4.1) for $t=t_k$ and $\tau=h$ we get

$$\left\|\overline{\mathbf{e}}_i\big(t_k+T_p;\ \overline{\mathbf{u}}_i^\star(\cdot),\mathbf{e}_i(t_{k+1})\big)-\overline{\mathbf{e}}_i\big(t_k+T_p;\ \overline{\mathbf{u}}_i^\star(\cdot),\mathbf{e}_i(t_k)\big)\right\| \leq \frac{\overline{\delta}_i}{L_{g_i}}(e^{L_{g_i}h}-1)e^{L_{g_i}(T_p-h)}$$

Hence (4.13) becomes

$$\begin{aligned} &V_i\big(\overline{\mathbf{e}}_i\big(t_k+T_p;\ \overline{\mathbf{u}}_i^\star(\cdot),\mathbf{e}_i(t_{k+1})\big)\big)-V_i\big(\overline{\mathbf{e}}_i\big(t_k+T_p;\ \overline{\mathbf{u}}_i^\star(\cdot),\mathbf{e}_i(t_k)\big)\big)\\ &\quad\leq L_{V_i}\left\|\overline{\mathbf{e}}_i\big(t_k+T_p;\ \overline{\mathbf{u}}_i^\star(\cdot),\mathbf{e}_i(t_{k+1})\big)-\overline{\mathbf{e}}_i\big(t_k+T_p;\ \overline{\mathbf{u}}_i^\star(\cdot),\mathbf{e}_i(t_k)\big)\right\|\\ &\quad= L_{V_i}\frac{\overline{\delta}_i}{L_{g_i}}(e^{L_{g_i}h}-1)e^{L_{g_i}(T_p-h)} \end{aligned} \tag{4.14}$$

Since the solution to the optimization problem is assumed to be feasible at time t_k, all states abide by their respective constraints, and in particular, from (4.10), the predicted state $\overline{\mathbf{e}}_i\big(t_k+T_p;\ \overline{\mathbf{u}}_i^\star(\cdot),\mathbf{e}_i(t_k)\big)\in\Omega_i$. This means that $V_i\big(\overline{\mathbf{e}}_i\big(t_k+T_p;\ \overline{\mathbf{u}}_i^\star(\cdot),\mathbf{e}_i(t_k)\big)\leq\varepsilon_{\Omega_i}$. Hence (4.14) becomes

$$\begin{aligned} &V_i\big(\overline{\mathbf{e}}_i\big(t_k+T_p;\ \overline{\mathbf{u}}_i^\star(\cdot),\mathbf{e}_i(t_{k+1})\big)\big)\\ &\quad\leq V_i\big(\overline{\mathbf{e}}_i\big(t_k+T_p;\ \overline{\mathbf{u}}_i^\star(\cdot),\mathbf{e}_i(t_k)\big)+L_{V_i}\frac{\overline{\delta}_i}{L_{g_i}}(e^{L_{g_i}h}-1)e^{L_{g_i}(T_p-h)}\\ &\quad\leq \varepsilon_{\Omega_i}+L_{V_i}\frac{\overline{\delta}_i}{L_{g_i}}(e^{L_{g_i}h}-1)e^{L_{g_i}(T_p-h)} \end{aligned}$$

From assumption 4 of theorem (4.4.1), the upper bound of the disturbance is in turn bounded by

$$\overline{\delta}_i \leq \frac{\varepsilon_{\Psi_i} - \varepsilon_{\Omega_i}}{\frac{L_{V_i}}{L_{g_i}}(e^{L_{g_i}h} - 1)e^{L_{g_i}(T_p - h)}} \tag{4.15}$$

Therefore

$$V_i\big(\overline{\mathbf{e}}_i\big(t_k + T_p;\ \overline{\mathbf{u}}_i^{\star}(\cdot), \mathbf{e}_i(t_{k+1})\big)\big) \leq \varepsilon_{\Omega_i} - \varepsilon_{\Omega_i} + \varepsilon_{\Psi_i} = \varepsilon_{\Psi_i}$$

or, expressing the above in terms of t_{k+1} instead of t_k

$$V_i\big(\overline{\mathbf{e}}_i\big(t_{k+1} + T_p - h;\ \overline{\mathbf{u}}_i^{\star}(\cdot), \mathbf{e}_i(t_{k+1})\big)\big) \leq \varepsilon_{\Psi_i}$$

This means that the state $\overline{\mathbf{e}}_i\big(t_{k+1} + T_p - h;\ \overline{\mathbf{u}}_i^{\star}(\cdot), \mathbf{e}_i(t_{k+1})\big) \in \Psi_i$. From assumption (4.3.3), and since $\Psi_i \subseteq \Phi_i$, there is an admissible control signal $h_i\big(\overline{\mathbf{e}}_i\big(t_{k+1} + T_p - h;\ \overline{\mathbf{u}}_i^{\star}(\cdot), \mathbf{e}_i(t_{k+1})\big)\big)$ such that

$$\overline{\mathbf{e}}_i\big(t_{k+1} + T_p;\ h_i(\cdot), \overline{\mathbf{e}}_i\big(t_{k+1} + T_p - h;\ \overline{\mathbf{u}}_i^{\star}(\cdot), \mathbf{e}_i(t_{k+1})\big)\big) \in \Omega_i$$

Therefore, overall

$$\overline{\mathbf{e}}_i\big(t_{k+1} + T_p;\ \widetilde{\mathbf{u}}_i(\cdot), \mathbf{e}_i(t_{k+1})\big) \in \Omega_i \tag{4.16}$$

■

Piecing the admissibility of $\widetilde{\mathbf{u}}_i(\cdot)$ from (4.11) together with conclusions (4.12) and (4.16), we conclude that the application of the control input $\widetilde{\mathbf{u}}_i(\cdot)$ at time t_{k+1} results in the states of the real system abiding by their intended constraints across the entire horizon $[t_{k+1}, t_{k+1} + T_p]$. Therefore, overall, the (sub-optimal) control input $\widetilde{\mathbf{u}}_i(\cdot)$ is admissible at time t_{k+1} according to definition (4.3.1), which means that feasibility of a solution to the optimization problem at time t_k implies feasibility at time $t_{k+1} > t_k$. Thus, since at time $t = 0$ a solution is assumed to be feasible, a solution to the optimal control problem is feasible for all $t \geq 0$.

Remark 4.4.3. In consistence with remark (4.3.2), the length of the time horizon T_p should be designed in such a way that, given the bound of the disturbance and the size ε_{Ω_i} of the desired terminal set Ω_i, the size ε_{Ψ_i} of set Ψ_i is smaller than that of set Φ_i[a]. In general, T_p should have such a value that the hierarchy of sets $\mathcal{E}_{i,T_p}$, Φ_i, Ψ_i and Ω_i abides by the intended one (see fig.(4.2)). Furthermore, T_p should be such that there is a successful trade-off between feasibility and disturbance attenuation: the lower the value of T_p, the larger the disturbances that can be accommodated; however a low enough value can make the problem infeasible.

[a]Consider for instance the case where T_p is large: the denominator of inequality (4.15) may become large enough to limit the size of accommodated disturbances.

Convergence analysis The second part of the proof involves demonstrating that the state $\mathbf{e}_i$ is ultimately bounded in Ω_i. We will show that the *optimal* cost $J_i^\star\big(\mathbf{e}_i(t)\big)$ is an ISS Lyapunov function for the closed loop system (4.8) according to definition (1.2.4), with

$$J_i^\star\big(\mathbf{e}_i(t)\big) \triangleq J_i\Big(\mathbf{e}_i(t), \overline{\mathbf{u}}_i^\star\big(\cdot;\ \mathbf{e}_i(t)\big)\Big)$$

by way of remark (1.2.2).

In order not to wreak notational havoc, let us as before define the following terms:

- $\mathbf{u}_{0,i}(\tau) \triangleq \overline{\mathbf{u}}_i^\star\big(\tau;\ \mathbf{e}_i(t_k)\big)$ as the *optimal* input that results from the solution to problem (3.3.1) based on the measurement of state $\mathbf{e}_i(t_k)$, applied at time $\tau \geq t_k$
- $\mathbf{e}_{0,i}(\tau) \triangleq \overline{\mathbf{e}}_i\big(\tau;\ \overline{\mathbf{u}}_i^\star\big(\cdot;\ \mathbf{e}_i(t_k)\big), \mathbf{e}_i(t_k)\big)$ as the *predicted* state at time $\tau \geq t_k$, that is, the state that results from the application of the above input $\overline{\mathbf{u}}_i^\star\big(\cdot;\ \mathbf{e}_i(t_k)\big)$ to the state $\mathbf{e}_i(t_k)$, at time τ
- $\mathbf{u}_{1,i}(\tau) \triangleq \widetilde{\mathbf{u}}_i(\tau)$ as the *admissible* input at $\tau \geq t_{k+1}$ (see eq. (4.11))

- $\mathbf{e}_{1,i}(\tau) \triangleq \overline{\mathbf{e}}_i\big(\tau;\ \widetilde{\mathbf{u}}_i(\cdot), \mathbf{e}_i(t_{k+1})\big)$ as the *predicted* state at time $\tau \geq t_{k+1}$, that is, the state that results from the application of the above input $\widetilde{\mathbf{u}}_i(\cdot)$ to the state $\mathbf{e}_i\big(t_{k+1};\ \overline{\mathbf{u}}_i^\star\big(\cdot;\ \mathbf{e}_i(t_k)\big), \mathbf{e}_i(t_k)\big)$, at time τ

Before beginning to prove convergence, it is worth noting that while the cost

$$J_i\Big(\mathbf{e}_i(t), \overline{\mathbf{u}}_i^\star\big(\cdot;\ \mathbf{e}_i(t)\big)\Big)$$

is optimal (in the sense that it is based on the optimal input, which provides its minimum realization), a cost that is based on a plainly admissible (and thus, without loss of generality, sub-optimal) input $\mathbf{u}_i \neq \overline{\mathbf{u}}_i^\star$ will result in a configuration where

$$J_i\Big(\mathbf{e}_i(t), \mathbf{u}_i\big(\cdot;\ \mathbf{e}_i(t)\big)\Big) \geq J_i\Big(\mathbf{e}_i(t), \overline{\mathbf{u}}_i^\star\big(\cdot;\ \mathbf{e}_i(t)\big)\Big)$$

Let us now begin our investigation on the sign of the difference between the cost that results from the application of the feasible input $\mathbf{u}_{1,i}$, which we shall denote by $\overline{J}_i\big(\mathbf{e}_i(t_{k+1})\big)$, and the optimal cost $J_i^\star\big(\mathbf{e}_i(t_k)\big)$, while reminding ourselves that $J_i\big(\mathbf{e}_i(t), \overline{\mathbf{u}}_i(\cdot)\big) = \int_t^{t+T_p} F_i\big(\overline{\mathbf{e}}_i(s), \overline{\mathbf{u}}_i(s)\big)ds$ $+\ V_i\big(\overline{\mathbf{e}}_i(t+T_p)\big)$:

$$\overline{J}_i\big(\mathbf{e}_i(t_{k+1})\big) - J_i^\star\big(\mathbf{e}_i(t_k)\big) = V_i\big(\mathbf{e}_{1,i}(t_{k+1}+T_p)\big) + \int_{t_{k+1}}^{t_{k+1}+T_p} F_i\big(\mathbf{e}_{1,i}(s), \mathbf{u}_{1,i}(s)\big)ds$$

$$-V_i\big(\mathbf{e}_{0,i}(t_k+T_p)\big) - \int_{t_k}^{t_k+T_p} F_i\big(\mathbf{e}_{0,i}(s), \mathbf{u}_{0,i}(s)\big)ds$$

Considering that $t_k < t_{k+1} < t_k + T_p < t_{k+1} + T_p$, we break down the two integrals above in between these intervals:

$$\overline{J}_i\big(\mathbf{e}_i(t_{k+1})\big) - J_i^\star\big(\mathbf{e}_i(t_k)\big) =$$

$$V_i\big(\mathbf{e}_{1,i}(t_{k+1}+T_p)\big) + \int_{t_{k+1}}^{t_k+T_p} F_i\big(\mathbf{e}_{1,i}(s), \mathbf{u}_{1,i}(s)\big)ds + \int_{t_k+T_p}^{t_{k+1}+T_p} F_i\big(\mathbf{e}_{1,i}(s), \mathbf{u}_{1,i}(s)\big)ds$$

$$-V_i\big(\mathbf{e}_{0,i}(t_k+T_p)\big) - \int_{t_k}^{t_{k+1}} F_i\big(\mathbf{e}_{0,i}(s), \mathbf{u}_{0,i}(s)\big)ds - \int_{t_{k+1}}^{t_k+T_p} F_i\big(\mathbf{e}_{0,i}(s), \mathbf{u}_{0,i}(s)\big)ds \tag{4.17}$$

We begin working on (4.17) focusing first on the difference between the two intervals over $[t_{k+1}, t_{k+1}+T_p]$:

$$\begin{aligned}
&\int_{t_{k+1}}^{t_k+T_p} F_i\big(\mathbf{e}_{1,i}(s), \mathbf{u}_{1,i}(s)\big)ds - \int_{t_{k+1}}^{t_k+T_p} F_i\big(\mathbf{e}_{0,i}(s), \mathbf{u}_{0,i}(s)\big)ds \\
&\qquad = \int_{t_k+h}^{t_k+T_p} F_i\big(\mathbf{e}_{1,i}(s), \mathbf{u}_{1,i}(s)\big)ds - \int_{t_k+h}^{t_k+T_p} F_i\big(\mathbf{e}_{0,i}(s), \mathbf{u}_{0,i}(s)\big)ds \\
&\qquad \leq \left| \int_{t_k+h}^{t_k+T_p} F_i\big(\mathbf{e}_{1,i}(s), \mathbf{u}_{1,i}(s)\big)ds - \int_{t_k+h}^{t_k+T_p} F_i\big(\mathbf{e}_{0,i}(s), \mathbf{u}_{0,i}(s)\big)ds \right| \\
&\qquad = \left| \int_{t_k+h}^{t_k+T_p} \Big(F_i\big(\mathbf{e}_{1,i}(s), \mathbf{u}_{1,i}(s)\big) - F_i\big(\mathbf{e}_{0,i}(s), \mathbf{u}_{0,i}(s)\big) \Big) ds \right| \\
&\qquad = \int_{t_k+h}^{t_k+T_p} \left| F_i\big(\mathbf{e}_{1,i}(s), \mathbf{u}_{1,i}(s)\big) - F_i\big(\mathbf{e}_{0,i}(s), \mathbf{u}_{0,i}(s)\big) \right| ds \\
&\qquad \leq L_{F_i} \int_{t_k+h}^{t_k+T_p} \left\| \overline{\mathbf{e}}_i\big(s;\ \mathbf{u}_{1,i}(\cdot), \mathbf{e}_i(t_k+h)\big) - \overline{\mathbf{e}}_i\big(s;\ \mathbf{u}_{0,i}(\cdot), \mathbf{e}_i(t_k)\big) \right\| ds \\
&\qquad = L_{F_i} \int_{h}^{T_p} \left\| \overline{\mathbf{e}}_i\big(t_k+s;\ \overline{\mathbf{u}}_i^\star(\cdot), \mathbf{e}_i(t_k+h)\big) - \overline{\mathbf{e}}_i\big(t_k+s;\ \overline{\mathbf{u}}_i^\star(\cdot), \mathbf{e}_i(t_k)\big) \right\| ds \qquad (4.18)
\end{aligned}$$

Consulting with remark (4.4.1) for the two different initial conditions we get

$$\overline{\mathbf{e}}_i\big(t_k+s;\ \overline{\mathbf{u}}_i^\star(\cdot), \mathbf{e}_i(t_k+h)\big) = \mathbf{e}_i(t_k+h) + \int_{t_k+h}^{t_k+s} g_i\big(\overline{\mathbf{e}}_i(\tau;\ \mathbf{e}_i(t_k+h)), \overline{\mathbf{u}}_i^\star(\tau)\big)d\tau$$

and

$$\begin{aligned}
\overline{\mathbf{e}}_i\big(t_k+s;\ \overline{\mathbf{u}}_i^\star(\cdot), \mathbf{e}_i(t_k)\big) &= \mathbf{e}_i(t_k) + \int_{t_k}^{t_k+s} g_i\big(\overline{\mathbf{e}}_i(\tau;\ \mathbf{e}_i(t_k)), \overline{\mathbf{u}}_i^\star(\tau)\big)d\tau \\
&= \mathbf{e}_i(t_k) + \int_{t_k}^{t_k+h} g_i\big(\overline{\mathbf{e}}_i(\tau;\ \mathbf{e}_i(t_k)), \overline{\mathbf{u}}_i^\star(\tau)\big)d\tau \\
&\quad + \int_{t_k+h}^{t_k+s} g_i\big(\overline{\mathbf{e}}_i(\tau;\ \mathbf{e}_i(t_k)), \overline{\mathbf{u}}_i^\star(\tau)\big)d\tau
\end{aligned}$$

Subtracting the latter from the former and taking norms on either side yields

$$
\begin{aligned}
&\left\|\overline{\mathbf{e}}_i\big(t_k+s;\ \overline{\mathbf{u}}_i^\star(\cdot),\mathbf{e}_i(t_k+h)\big)-\overline{\mathbf{e}}_i\big(t_k+s;\ \overline{\mathbf{u}}_i^\star(\cdot),\mathbf{e}_i(t_k)\big)\right\| \\
&=\left\|\mathbf{e}_i(t_k+h)-\left(\mathbf{e}_i(t_k)+\int_{t_k}^{t_k+h} g_i\big(\overline{\mathbf{e}}_i(\tau;\ \mathbf{e}_i(t_k)),\overline{\mathbf{u}}_i^\star(\tau)\big)d\tau\right)\right. \\
&\left.+\int_{t_k+h}^{t_k+s} g_i\big(\overline{\mathbf{e}}_i(\tau;\ \mathbf{e}_i(t_k+h)),\overline{\mathbf{u}}_i^\star(\tau)\big)d\tau-\int_{t_k+h}^{t_k+s} g_i\big(\overline{\mathbf{e}}_i(\tau;\ \mathbf{e}_i(t_k)),\overline{\mathbf{u}}_i^\star(\tau)\big)d\tau\right\| \\
&=\left\|\mathbf{e}_i(t_k+h)-\overline{\mathbf{e}}_i(t_k+h)\right. \\
&\left.+\int_{t_k+h}^{t_k+s}\left(g_i\big(\overline{\mathbf{e}}_i(\tau;\ \mathbf{e}_i(t_k+h)),\overline{\mathbf{u}}_i^\star(\tau)\big)-g_i\big(\overline{\mathbf{e}}_i(\tau;\ \mathbf{e}_i(t_k)),\overline{\mathbf{u}}_i^\star(\tau)\big)\right)d\tau\right\| \\
&\le\left\|\mathbf{e}_i(t_k+h)-\overline{\mathbf{e}}_i(t_k+h)\right\| \\
&+\left\|\int_{t_k+h}^{t_k+s}\left(g_i\big(\overline{\mathbf{e}}_i(\tau;\ \mathbf{e}_i(t_k+h)),\overline{\mathbf{u}}_i^\star(\tau)\big)-g_i\big(\overline{\mathbf{e}}_i(\tau;\ \mathbf{e}_i(t_k)),\overline{\mathbf{u}}_i^\star(\tau)\big)\right)d\tau\right\| \\
&\le\left\|\mathbf{e}_i(t_k+h)-\overline{\mathbf{e}}_i(t_k+h)\right\| \\
&+\int_{t_k+h}^{t_k+s}\left\|g_i\big(\overline{\mathbf{e}}_i(\tau;\ \mathbf{e}_i(t_k+h)),\overline{\mathbf{u}}_i^\star(\tau)\big)-g_i\big(\overline{\mathbf{e}}_i(\tau;\ \mathbf{e}_i(t_k)),\overline{\mathbf{u}}_i^\star(\tau)\big)\right\|d\tau \\
&\le\left\|\mathbf{e}_i(t_k+h)-\overline{\mathbf{e}}_i(t_k+h)\right\| \\
&+L_{g_i}\int_{t_k+h}^{t_k+s}\left\|\overline{\mathbf{e}}_i\big(\tau;\ \overline{\mathbf{u}}_i^\star(\cdot),\mathbf{e}_i(t_k+h)\big)-\overline{\mathbf{e}}_i\big(\tau;\ \overline{\mathbf{u}}_i^\star(\cdot),\mathbf{e}_i(t_k)\big)\right\|d\tau \\
&=\left\|\mathbf{e}_i(t_k+h)-\overline{\mathbf{e}}_i(t_k+h)\right\| \\
&+L_{g_i}\int_{h}^{s}\left\|\overline{\mathbf{e}}_i\big(t_k+\tau;\ \overline{\mathbf{u}}_i^\star(\cdot),\mathbf{e}_i(t_k+h)\big)-\overline{\mathbf{e}}_i\big(t_k+\tau;\ \overline{\mathbf{u}}_i^\star(\cdot),\mathbf{e}_i(t_k)\big)\right\|d\tau
\end{aligned}
\tag{4.19}
$$

Given that from lemma (4.4.1) the first term of the sum featured in (4.19) is a constant, by application of the the Grönwall-Bellman inequality, (4.19) becomes:

$$\begin{aligned}
&\left\|\overline{\mathbf{e}}_i\big(t_k+s;\ \overline{\mathbf{u}}_i^{\star}(\cdot),\mathbf{e}_i(t_k+h)\big)-\overline{\mathbf{e}}_i\big(t_k+s;\ \overline{\mathbf{u}}_i^{\star}(\cdot),\mathbf{e}_i(t_k)\big)\right\| \\
&\qquad\qquad \leq \left\|\mathbf{e}_i(t_k+h)-\overline{\mathbf{e}}_i(t_k+h)\right\| e^{L_{g_i}(s-h)} \\
&\qquad\qquad \leq \frac{\overline{\delta}_i}{Ł_{g_i}}(e^{L_{g_i}h}-1)e^{L_{g_i}(s-h)}
\end{aligned}$$

Given the above result, (4.18) becomes

$$\begin{aligned}
&\int_{t_{k+1}}^{t_k+T_p} F_i\big(\mathbf{e}_{1,i}(s),\mathbf{u}_{1,i}(s)\big)ds-\int_{t_{k+1}}^{t_k+T_p} F_i\big(\mathbf{e}_{0,i}(s),\mathbf{u}_{0,i}(s)\big)ds \\
&\qquad \leq L_{F_i}\int_h^{T_p}\frac{\overline{\delta}_i}{Ł_{g_i}}(e^{L_{g_i}h}-1)e^{L_{g_i}(s-h)}ds \\
&\qquad = L_{F_i}\frac{\overline{\delta}_i}{Ł_{g_i}}(e^{L_{g_i}h}-1)\int_h^{T_p} e^{L_{g_i}(s-h)}ds \\
&\qquad = L_{F_i}\frac{\overline{\delta}_i}{Ł_{g_i}}(e^{L_{g_i}h}-1)\frac{1}{L_{g_i}}(e^{L_{g_i}(T_p-h)}-1) \\
&\qquad = L_{F_i}\frac{\overline{\delta}_i}{Ł_{g_i}^2}(e^{L_{g_i}h}-1)(e^{L_{g_i}(T_p-h)}-1)
\end{aligned}$$

Hence, we discovered that

$$\begin{aligned}
&\int_{t_{k+1}}^{t_k+T_p} F_i\big(\mathbf{e}_{1,i}(s),\mathbf{u}_{1,i}(s)\big)ds-\int_{t_{k+1}}^{t_k+T_p} F_i\big(\mathbf{e}_{0,i}(s),\mathbf{u}_{0,i}(s)\big)ds \\
&\qquad\qquad \leq L_{F_i}\frac{\overline{\delta}_i}{Ł_{g_i}^2}(e^{L_{g_i}h}-1)(e^{L_{g_i}(T_p-h)}-1) \qquad (4.20)
\end{aligned}$$

With this partial result established, we turn back to the remaining terms found in (4.17) and, in particular, we focus on the integral

$$\int_{t_k+T_p}^{t_{k+1}+T_p} F_i\big(\mathbf{e}_{1,i}(s), \mathbf{u}_{1,i}(s)\big)ds$$

We discern that the range of the above integral has a length[a] equal to the length of the interval where assumption 2 of theorem (4.4.1) holds. Integrating the expression found in the assumption over the interval $[t_k+T_p, t_{k+1}+T_p]$, for the controls and states applicable in it we get

$$\int_{t_k+T_p}^{t_{k+1}+T_p} \left(\frac{\partial V_i}{\partial \mathbf{e}_{1,i}} g_i\big(\mathbf{e}_{1,i}(s), \mathbf{u}_{1,i}(s)\big) + F_i\big(\mathbf{e}_{1,i}(s), \mathbf{u}_{1,i}(s)\big) \right) ds \leq 0$$

$$\int_{t_k+T_p}^{t_{k+1}+T_p} \frac{d}{ds} V_i\big(\mathbf{e}_{1,i}(s)\big)ds + \int_{t_k+T_p}^{t_{k+1}+T_p} F_i\big(\mathbf{e}_{1,i}(s), \mathbf{u}_{1,i}(s)\big)ds \leq 0$$

$$V_i\big(\mathbf{e}_{1,i}(t_{k+1}+T_p)\big) - V_i\big(\mathbf{e}_{1,i}(t_k+T_p)\big) + \int_{t_k+T_p}^{t_{k+1}+T_p} F_i\big(\mathbf{e}_{1,i}(s), \mathbf{u}_{1,i}(s)\big)ds \leq 0$$

$$V_i\big(\mathbf{e}_{1,i}(t_{k+1}+T_p)\big) + \int_{t_k+T_p}^{t_{k+1}+T_p} F_i\big(\mathbf{e}_{1,i}(s), \mathbf{u}_{1,i}(s)\big)ds \leq V_i\big(\mathbf{e}_{1,i}(t_k+T_p)\big)$$

The left-hand side expression is the same as the first two terms in the right-hand side of equality (4.17). We can introduce the third one by subtracting it from both sides:

$$\begin{aligned}
&V_i\big(\mathbf{e}_{1,i}(t_{k+1}+T_p)\big) + \int_{t_k+T_p}^{t_{k+1}+T_p} F_i\big(\mathbf{e}_{1,i}(s), \mathbf{u}_{1,i}(s)\big)ds - V_i\big(\mathbf{e}_{0,i}(t_k+T_p)\big) \\
&\qquad \leq V_i\big(\mathbf{e}_{1,i}(t_k+T_p)\big) - V_i\big(\mathbf{e}_{0,i}(t_k+T_p)\big) \\
&\qquad \leq \Big| V_i\big(\mathbf{e}_{1,i}(t_k+T_p)\big) - V_i\big(\mathbf{e}_{0,i}(t_k+T_p)\big) \Big| \\
&\qquad \leq L_{V_i} \Big\| \overline{\mathbf{e}}_i\big(t_k+T_p;\ \overline{\mathbf{u}}_i^{\star}(\cdot), \mathbf{e}_i(t_{k+1})\big) - \overline{\mathbf{e}}_i\big(t_k+T_p;\ \overline{\mathbf{u}}_i^{\star}(\cdot), \mathbf{e}_i(t_k)\big) \Big\| \\
&\qquad \leq L_{V_i} \frac{\overline{\delta}_i}{L_{g_i}} (e^{L_{g_i}h} - 1) e^{L_{g_i}(T_p - h)} \text{ (from (4.14))}
\end{aligned}$$

[a] $(t_{k+1}+T_p) - (t_k+T_p) = t_{k+1} - t_k = h$

Hence, we discovered that

$$V_i\big(\mathbf{e}_{1,i}(t_{k+1}+T_p)\big)+\int_{t_k+T_p}^{t_{k+1}+T_p}F_i\big(\mathbf{e}_{1,i}(s),\mathbf{u}_{1,i}(s)\big)ds-V_i\big(\mathbf{e}_{0,i}(t_k+T_p)\big)\\ \leq L_{V_i}\frac{\overline{\delta}_i}{L_{g_i}}(e^{L_{g_i}h}-1)e^{L_{g_i}(T_p-h)} \tag{4.21}$$

Adding the milestone inequalities (4.20) and (4.21) yields

$$\int_{t_{k+1}}^{t_k+T_p}F_i\big(\mathbf{e}_{1,i}(s),\mathbf{u}_{1,i}(s)\big)ds-\int_{t_{k+1}}^{t_k+T_p}F_i\big(\mathbf{e}_{0,i}(s),\mathbf{u}_{0,i}(s)\big)ds\\ +V_i\big(\mathbf{e}_{1,i}(t_{k+1}+T_p)\big)+\int_{t_k+T_p}^{t_{k+1}+T_p}F_i\big(\mathbf{e}_{1,i}(s),\mathbf{u}_{1,i}(s)\big)ds-V_i\big(\mathbf{e}_{0,i}(t_k+T_p)\big)\\ \leq L_{F_i}\frac{\overline{\delta}_i}{\mathrm{L}_{g_i}^2}(e^{L_{g_i}h}-1)(e^{L_{g_i}(T_p-h)}-1)+L_{V_i}\frac{\overline{\delta}_i}{L_{g_i}}(e^{L_{g_i}h}-1)e^{L_{g_i}(T_p-h)}$$

and therefore (4.17), by bringing the integral ranging from t_k to t_{k+1} to the left-hand side, becomes

$$\overline{J}_i\big(\mathbf{e}_i(t_{k+1})\big)-J_i^\star\big(\mathbf{e}_i(t_k)\big)+\int_{t_k}^{t_{k+1}}F_i\big(\mathbf{e}_{0,i}(s),\mathbf{u}_{0,i}(s)\big)ds\\ \leq L_{F_i}\frac{\overline{\delta}_i}{\mathrm{L}_{g_i}^2}(e^{L_{g_i}h}-1)(e^{L_{g_i}(T_p-h)}-1)+L_{V_i}\frac{\overline{\delta}_i}{L_{g_i}}(e^{L_{g_i}h}-1)e^{L_{g_i}(T_p-h)}$$

By rearranging terms, the cost difference becomes bounded by

$$\overline{J}_i\big(\mathbf{e}_i(t_{k+1})\big)-J_i^\star\big(\mathbf{e}_i(t_k)\big)=\xi_i\overline{\delta}_i-\int_{t_k}^{t_{k+1}}F_i\big(\mathbf{e}_{0,i}(s),\mathbf{u}_{0,i}(s)\big)ds$$

where

$$\xi_i = \frac{1}{L_{g_i}}\Big(e^{L_{g_i}h} - 1\Big)\Big(\big(L_{V_i} + \frac{L_{F_i}}{\text{Ł}_{g_i}}\big)\big(e^{L_{g_i}(T_p-h)} - 1\big) + L_{V_i}\Big) > 0$$

and $\xi_i\overline{\delta}_i$ is the contribution of the bounded additive disturbance $\boldsymbol{\delta}_i(t)$ to the nominal cost difference (i.e. the case without disturbances).

F_i is a positive-definite function as a sum of a positive-definite $\|\mathbf{u}_i\|^2_{\boldsymbol{R}_i}$ and a positive semi-definite function $\|\mathbf{e}_i\|^2_{\boldsymbol{Q}_i}$. If we denote by $m_i = \lambda_{min}(\boldsymbol{Q}_i, \boldsymbol{R}_i) \geq 0$ the minimum eigenvalue between those of matrices $\boldsymbol{R}_i$, $\boldsymbol{Q}_i$, this means that

$$F_i\big(\mathbf{e}_{0,i}(s), \mathbf{u}_{0,i}(s)\big) \geq m_i\|\mathbf{e}_{0,i}(s)\|^2$$

By integrating the above between our interval of interest $[t_k, t_{k+1}]$ we get

$$\int_{t_k}^{t_{k+1}} F_i\big(\mathbf{e}_{0,i}(s), \mathbf{u}_{0,i}(s)\big) \geq \int_{t_k}^{t_{k+1}} m_i\|\mathbf{e}_{0,i}(s)\|^2 ds$$

or

$$-\int_{t_k}^{t_{k+1}} F_i\big(\mathbf{e}_{0,i}(s), \mathbf{u}_{0,i}(s)\big) \leq -m_i\int_{t_k}^{t_{k+1}} \|\overline{\mathbf{e}}_i(s;\ \overline{\mathbf{u}}_i^\star, \mathbf{e}_i(t_k))\|^2 ds$$

This means that the cost difference is upper-bounded by

$$\overline{J}_i\big(\mathbf{e}_i(t_{k+1})\big) - J_i^\star\big(\mathbf{e}_i(t_k)\big) \leq \xi_i\overline{\delta}_i - m_i\int_{t_k}^{t_{k+1}} \|\overline{\mathbf{e}}_i(s;\ \overline{\mathbf{u}}_i^\star(\cdot), \mathbf{e}_i(t_k))\|^2 ds$$

and since the cost $\overline{J}_i\big(\mathbf{e}_i(t_{k+1})\big)$ is, in general, sub-optimal: $J_i^\star\big(\mathbf{e}_i(t_{k+1})\big) - \overline{J}_i\big(\mathbf{e}_i(t_{k+1})\big) \leq 0$:

$$J_i^\star\big(\mathbf{e}_i(t_{k+1})\big) - J_i^\star\big(\mathbf{e}_i(t_k)\big) \leq \xi_i\overline{\delta}_i - m_i\int_{t_k}^{t_{k+1}} \|\overline{\mathbf{e}}_i(s;\ \overline{\mathbf{u}}_i^\star(\cdot), \mathbf{e}_i(t_k))\|^2 ds$$

Let $\Xi_i(\mathbf{e}_i) \triangleq J_i^\star(\mathbf{e}_i)$. Then, between consecutive times t_k and t_{k+1} when the FHOCP is solved, the above inequality reforms into

$$\begin{aligned}\Xi_i\big(\mathbf{e}_i(t_{k+1})\big) - \Xi_i\big(\mathbf{e}_i(t_k)\big) &\leq \xi_i\overline{\delta}_i - m_i\int_{t_k}^{t_{k+1}} \|\overline{\mathbf{e}}_i(s;\ \overline{\mathbf{u}}_i^\star(\cdot), \mathbf{e}_i(t_k))\|^2 ds \\ &= \xi_i\|\boldsymbol{\delta}_i\|_\infty - \int_{t_k}^{t_{k+1}} m_i\|\overline{\mathbf{e}}_i(s;\ \overline{\mathbf{u}}_i^\star(\cdot), \mathbf{e}_i(t_k))\|^2 ds \\ &\leq \int_{t_k}^{t_{k+1}} \left(\frac{\xi_i}{h}\|\boldsymbol{\delta}_i(s)\| - m_i\|\overline{\mathbf{e}}_i(s;\ \overline{\mathbf{u}}_i^\star(\cdot), \mathbf{e}_i(t_k))\|^2\right) ds \qquad (4.22)\end{aligned}$$

The functions $\sigma\big(\|\boldsymbol{\delta}_i\|\big) = \dfrac{\xi_i}{h}\|\boldsymbol{\delta}_i\|$ and $\alpha_3\big(\|\mathbf{e}_i\|\big) = m_i\|\mathbf{e}_i\|^2$ are class $\mathcal{K}$ functions according to definition (1.2.1), and therefore, according to lemma (3.3.4), remark (1.2.2) and definition (1.2.4), $\Xi_i\big(\mathbf{e}_i\big)$ is an ISS Lyapunov function in $\mathcal{E}_i$.

Given this fact, theorem (1.2.1), implies that the closed-loop system is input-to-state stable in $\mathcal{E}_i$. Inevitably then, given assumptions (4.3.2) and (4.3.3), and assumption 4 of theorem (4.4.1), the closed-loop trajectories for the error state of agent $i \in \mathcal{V}$ reach the terminal set Ω_i regardless of all $\boldsymbol{\delta}_i(t) : \|\boldsymbol{\delta}_i(t)\| \leq \overline{\delta}_i$, at some point[4] $t = t^\star \geq 0$. Once inside Ω_i, the trajectory is trapped there because of the implications[5] of (4.22) and assumption (4.3.3).

In turn, this means that the system (4.1) converges to $\mathbf{z}_{i,des}$ and is trapped in a vicinity of it − smaller than that in which it would have been trapped (if actively trapped at all) in the case of unattenuated disturbances −, while simultaneously conforming to all constraints $\mathcal{Z}_{i,t}$. This conclusion holds for all $i \in \mathcal{V}$, and hence, the compound system of agents $\mathcal{V}$ is stable. ■

[4] The difference with the scheme designed in [20] is that in sections III, IV, the equivalent of assumption (4.3.3) does not exist.

[5] For more details, refer to the discussion after the declaration of theorem 7.6 in [19].

Part III

Simulations

5

Introduction

The present part illustrates the efficacy of the advocated solutions, as described in chapters 3 and 4, with regard to stabilization of multiple inter-constrained agents, under the absence or presence of additive disturbances, in chapters 6 and 7 respectively.

The benefit of solving the problem this thesis addresses, as was formulated in chapter 2 and approached in chapters 3 and 4, is that the procured solutions can be applied to a general class of likewise problems − the similarity relation relates to/the terms, the dynamic nature of the actors, and the structure of their habitat, but not the spirit of the problem itself.

All simulations were performed with the MATLAB NMPC routine provided with [10]. The source code of the simulations can be found on github[1].

[1] `https://github.com/li9i/KTH_thesis_simulations`

5.1 The operational model

The simulacrum used for all agents in the following chapters shall be the three-dimensional model of the unicycle; its motion shall be expressed by the nonlinear continuous-time kinematic equations

$$\begin{aligned} \dot{x}(t) &= v(t)\cos\theta(t) \\ \dot{y}(t) &= v(t)\sin\theta(t) \\ \dot{\theta}(t) &= \omega(t) \end{aligned} \tag{5.1}$$

with $\mathbf{z} = [x, y, \theta]^\top$ the vector of states, $\mathbf{u} = [v, \omega]^\top$ the vector of inputs, and $\dot{\mathbf{z}} = f(\mathbf{z}, \mathbf{u})$ the (model) system's equation. We consider that $\mathbf{x} \in X$, $\mathbf{y} \in Y$ where $X \equiv Y \equiv \mathbb{R}$, $\theta \in \Theta \equiv (-\pi, \pi]$ and $\mathbf{u} \in \mathcal{U}$. In this 2D spatial environment, the obstacles of the workspace along with the workspace boundary itself assume an appropriately reformed form: that of a circle. The labeled space in which an arbitrary agent i moves, along with the spherical-obstacles-transformed-to-circles, is depicted in figure (5.1).

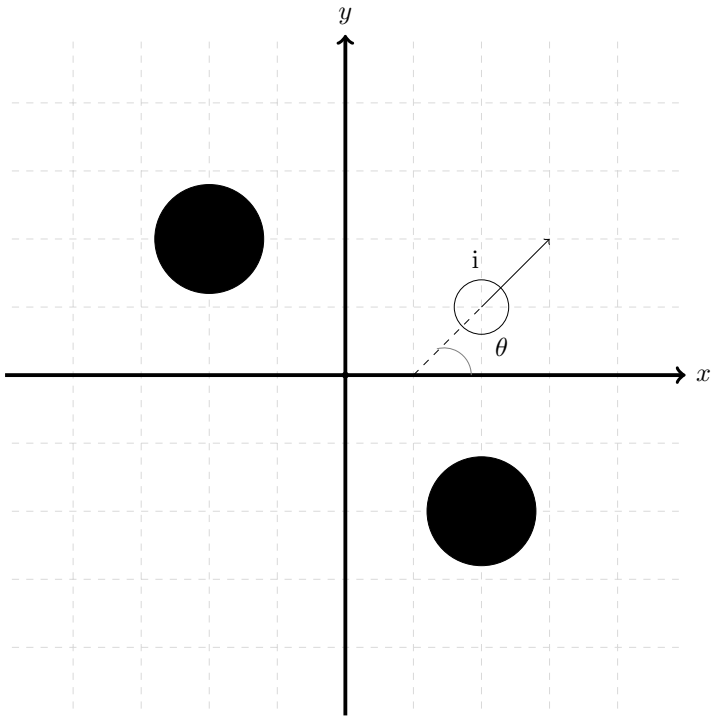

Figure 5.1: The 2D plane, agent i, whose orientation relative to the x axis is θ, and two obstacles.

The desired configuration shall be denoted by $\mathbf{z}_{des}$, the error dynamics by $\dot{\mathbf{e}} = g(\mathbf{e}, \mathbf{u})$, where $\mathbf{e}(t) = \mathbf{z}(t) - \mathbf{z}_{des}$ and $\mathbf{e} \in \mathcal{E} \equiv X \times Y \times \Theta \ominus \mathbf{z}_{des}$.

In the case where additive disturbances are considered, system (5.1) is expressed by

$$\begin{aligned} \dot{x}(t) &= v(t)\cos\theta(t) + \delta(t) \\ \dot{y}(t) &= v(t)\sin\theta(t) + \delta(t) \\ \dot{\theta}(t) &= \omega(t) + \delta(t) \end{aligned} \tag{5.2}$$

and its error dynamics are noted $\dot{\mathbf{e}} = g^R(\mathbf{e}, \mathbf{u})$ where $\mathbf{e}(t) = \mathbf{z}(t) - \mathbf{z}_{des}$ and $\mathbf{e} \in \mathcal{E} \equiv X \times Y \times \Theta \ominus \mathbf{z}_{des}$.

Lemma 5.1.1. Function g is Lipschitz continuous in $\mathcal{E} \times \mathcal{U}$ with a Lipschitz constant

$$L_g = v_{max}\sqrt{Q_{1,1} + Q_{1,2} + Q_{2,1} + Q_{2,2}}$$

where $\boldsymbol{Q} = Q_{\mu\nu}$ is the 3×3 matrix used to weigh the norms involved.

5.2 The problem reformed

Considering the conditions of the motivational problem as stated by problem (2.4), the reformed problem assumes the following form:

Problem 5.2.1. Assuming that

- all agents $i \in \mathcal{V}$ have access to their own and their neighbours' state and input vectors
- all agents $i \in \mathcal{V}$ have a (upper-bounded) sensing range d_i such that

$$d_i > \max\{r_i + r_j : \forall i, j \in \mathcal{V}, i \neq j\}$$

- at time $t = 0$ the sets $\mathcal{N}_i$ are known for all $i \in \mathcal{V}$ and $\sum_i |\mathcal{N}_i| > 0$
- at time $t = 0$ all agents are in a collision-free configuration with each other and the obstacles $\ell \in \mathcal{L}$
- All obstacles $\ell \in \mathcal{L}$ are situated in such a way that the distance between the two least distant obstacles is larger than the diameter of the agent with the largest diameter

the problem lies in procuring feasible controls for each agent $i \in \mathcal{V}$ such that for all agents and for all obstacles $\ell \in \mathcal{L}$ the following hold

1. Position and orientation configuration is achieved in steady-state $\mathbf{z}_{i,des}$

$$\lim_{t\to\infty} \|\mathbf{z}_i(t) - \mathbf{z}_{i,des}\| = 0$$

2. Inter-agent collision is avoided

$$\|\mathbf{p}_i(t) - \mathbf{p}_j(t)\| = d_{ij,a}(t) > \underline{d}_{ij,a}, \forall j \in \mathcal{V}\backslash\{i\}$$

   where $\mathbf{p}(t) = [x(t), y(t)]^\top$

3. Inter-agent connectivity loss between neighbouring agents is avoided

$$\|\mathbf{p}_i(t) - \mathbf{p}_j(t)\| = d_{ij,a}(t) < d_i, \forall j \in \mathcal{N}_i, \forall i : |\mathcal{N}_i| \neq 0$$

4. Agent-with-obstacle collision is avoided

$$\|\mathbf{p}_i(t) - \mathbf{p}_\ell(t)\| = d_{i\ell,o}(t) > \underline{d}_{i\ell,o}, \forall \ell \in \mathcal{L}$$

5. The control laws $\mathbf{u}_i(t)$ abide by their respective input constraints

$$\mathbf{u}_i(t) \in \mathcal{U}_i$$

for appropriate choice of constants $r_i, \mathbf{z}_{i,des}, \underline{d}_{ij,a}, d_i, \underline{d}_{i\ell,o}$ and neighbour sets $\mathcal{N}_i$, where $i \in \mathcal{V}$.

From the above we conclude that the constraint set $\mathcal{Z}_i$ for agent $i \in \mathcal{V}$ is

$$\mathcal{Z}_{i,t} = \big\{\mathbf{z}_i(t) \in X \times Y \times \Theta : \|\mathbf{p}_i(t) - \mathbf{p}_j(t)\| > \underline{d}_{ij,a}, \forall j \in \mathcal{R}_i(t),$$

$$\|\mathbf{p}_i(t) - \mathbf{p}_j(t)\| < d_i, \forall j \in \mathcal{N}_i,$$

$$\|\mathbf{p}_i(t) - \mathbf{p}_\ell\| > \underline{d}_{i\ell,o}, \forall \ell \in \mathcal{L},$$

$$-\pi < \theta_i(t) \leq \pi\Big\}$$

and the constraint set that corresponds to each agent for all $i \in \mathcal{V}$ is given by the Minkowski difference

$$\mathcal{E}_{i,t} = \mathcal{Z}_{i,t} \ominus \mathbf{z}_{i,des} \tag{5.3}$$

In the case of additive disturbances being considered, when each agent solves its own FHOCP, its constraint set $\mathcal{E}_i$ is replaced by a restricted constraint set that follows the same structure as (4.5). Furthermore, through the fact that remark (4.3.1) holds for the unicycle's error model, i.e. the model is stabilizable − the existence of the local linear feedback control law h that steers the trajectory of the states of the system into Ω is ensured[2].
The content of chapters 6 and 7 will demonstrate that agents $i \in \mathcal{V}$ can be stabilized when disturbances are absent, as demonstrated in chapter 3, and, in the case where disturbances are present, that the $\boldsymbol{P}-$weighted quadratic error measure about the equilibrium does not exceed a certain ceiling, as demonstrated in chapter 4.

5.3 Simulation scenarios

The simulations were carried out under four different agents-obstacles configurations:

1. Two agents avoid one obstacle on their way to their steady-state configurations, without colliding with each other and without being separated by the obstacle (we demand that their distance is always smaller than the obstacle's diameter for the aim of cooperation).

2. Two agents pass through the space between two obstacles on their way to their steady-state configurations − again, the maximum allowed distance between the two agents is smaller than the diameter of the obstacle with the smallest radius.

[2]The proof can be found in appendix (A.8)

3. Three agents avoid one obstacle on their way to their steady-state configurations, without colliding with each other and without being separated by the obstacle. In this case, two agents are (independently) neighbours of the third, that is, the third agent should maintain connectivity and avoid collision with both of the other two, but the latter will only have to avoid colliding with each other.

4. Three agents pass through the space between two obstacles on their way to their steady-state configurations. The conditions of this scenario assume those of points 2 and 3.

The four configurations are depicted in figures (5.2), (5.3), (5.4) and (5.5). Agent 1 is depicted in blue, agent 2 in red and agent 3 in yellow. The obstacles are depicted in black. Mark X denotes the desired position of an agent and its colour signifies the agent to be stabilized in that position.

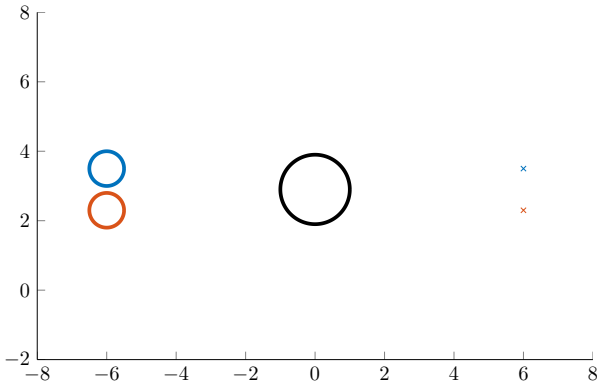

Figure 5.2: Test case one: two agents and one obstacle.

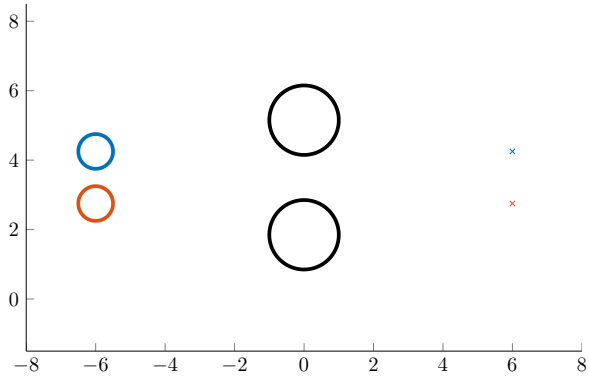

Figure 5.3: Test case two: two agents and two obstacles.

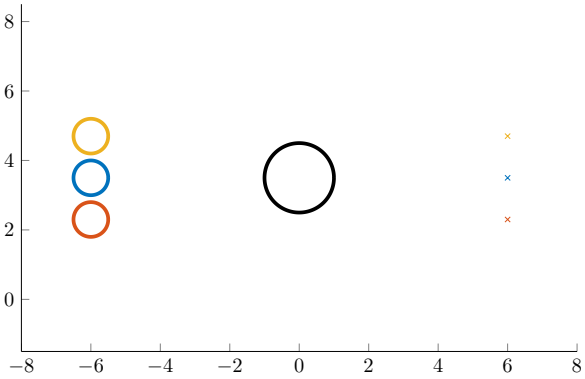

Figure 5.4: Test case three: three agents and one obstacle.

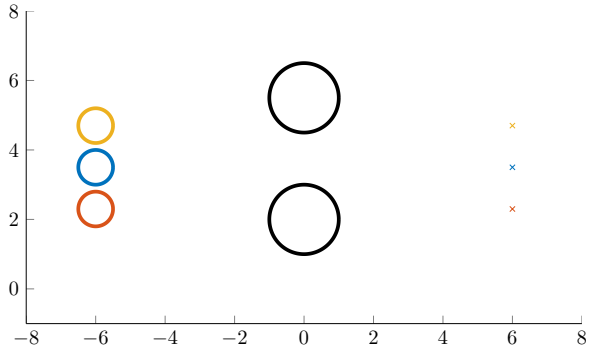

Figure 5.5: Test case four: three agents and two obstacles.

All configurations are as follows: the radius of all agents $i, j \in \mathcal{V}$ is $r_i = 0.5$; the radius of all obstacles is $r_\ell = 1.0$; the sensing range of all agents has a radius of $d_i = 4r_i + \epsilon = 2.0 + \epsilon$; the minimum distance between agents is $\underline{d}_{ij,a} = 2r_i + \epsilon = 1.0 + \epsilon$, and the minimum distance between agents and obstacles is $\underline{d}_{i\ell,o} = r_i + r_\ell + \epsilon = 1.5 + \epsilon$. ϵ was set to $\epsilon = 0.1$ in the disturbance-free cases and $\epsilon = 0.01$ in the cases where disturbances are present.
In the case of two agents, $\mathcal{V} = \{1, 2\}$, the neighbouring sets are $\mathcal{N}_1 = \{2\}$ and $\mathcal{N}_2 = \{1\}$, while in the case of three agents, $\mathcal{V} = \{1, 2, 3\}$, $\mathcal{N}_1 = \{2, 3\}$, $\mathcal{N}_2 = \{1\}$ and $\mathcal{N}_3 = \{1\}$.
Under the above configuration regime, all agents are constrained in bypassing the obstacle(s) from the same side, as they are prohibited from overtaking it (them) from different sides by the requirement that their sensing range be lower than the sum of the diameter of one obstacle and the radii of any two agents.

All simulations exhibit the translation of the visited theory into practice: in all test scenarios, all agents are successfully stabilized at, or about their desired configurations, without their constraints being violated. Therefore, the next two chapters, instead of featuring all simulation results, will feature an anthology of the results pertaining to the most challenging task of those among the ones considered − that of three agents having to negotiate bypassing two obstacles while maintaining appropriate connectivity and avoiding collisions. A comprehensive collection of all simulation results is featured in appendices B and C. The individual initial and terminal configurations of each agent, the positions of the obstacles and various other parameters are reported in the appropriate sections.

5.4 Process & information flow

The designed procedure flow can be either concurrent or sequential, meaning that agents can solve their individual FHOCP's and apply the control inputs either at the same time as everyone else, or one by one. The conceptual design itself is procedure-flow agnostic, and hence it can accommodate both without loss of feasibility or successful stabilization. For lack of a stable and usable multi-threaded `MATLAB` framework, the simulations where carried out under the latter approach: each agent solves its own FHOCP and applies the corresponding admissible control input in a round robin way, considering the current and planned (open-loop

state predictions) configurations of all agents within its sensing range. Figures (5.6) and (5.7) depict the sequential procedural and informational regimes.

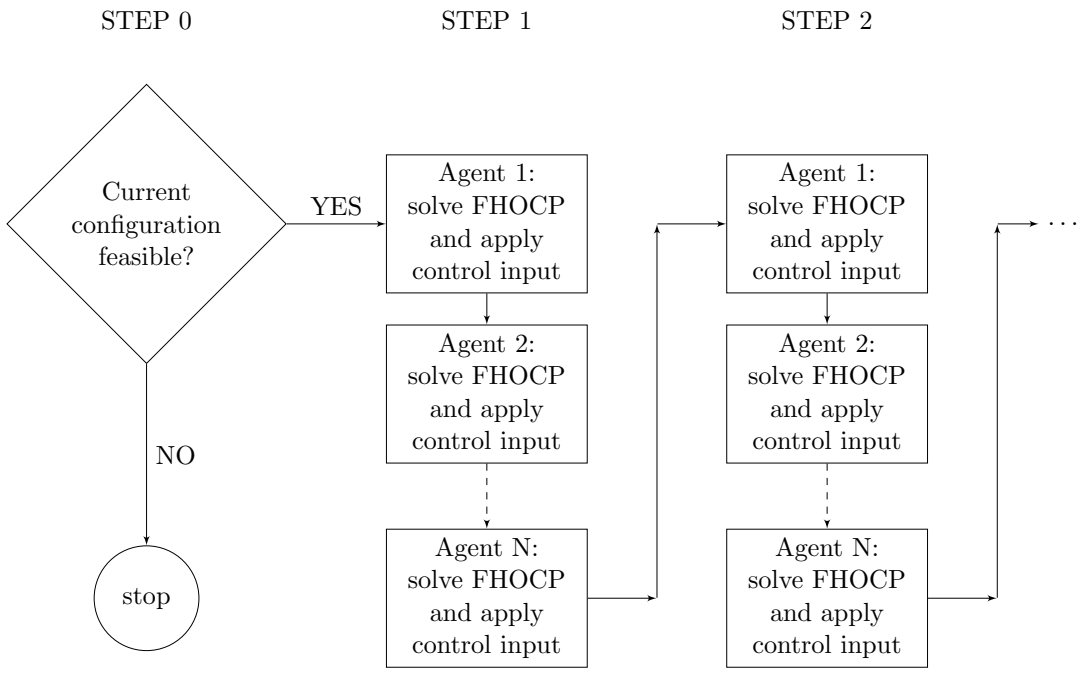

Figure 5.6: The procedure is approached sequentially. Notice that the figure implies that recursive feasibility is established if the initial configuration is itself feasible.

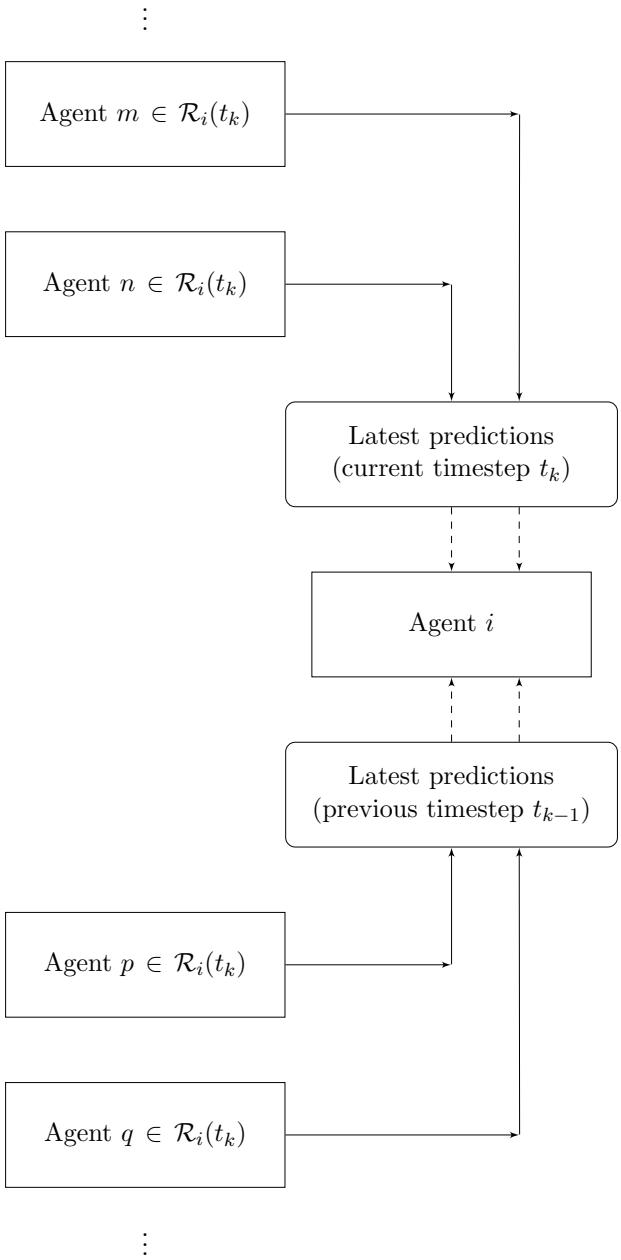

Figure 5.7: The flow of information to agent i regarding his perception of agents within its sensing range $\mathcal{R}_i$ at arbitrary FHOCP solution time t_k. Agents $m, n \in \mathcal{R}_i(t_k)$ have solved their FHOCP; agent i is next; agents $p, q \in \mathcal{R}_i(t_k)$ have not solved their FHOCP yet.

6

Simulations of Disturbance-free Stabililization

The present chapter illustrates the stabilization of a group of agents whose motion dynamics are expressed by equations (5.1), and whose errors with respect to their respective steady-state configurations are constrained by the set found in equation (5.3). The control laws are designed as in chapter 3.

In this setting, we consider the stabilization of three agents. Agent 1 is constrained in maintaining connectivity with agents 2 and 3 (and homologously vice-versa). All agents have to avoid colliding with each other and with the obstacles in the workspace, and reach their desired configurations. The number of obstacles is two. The gap between them suffices for one agent to pass between them, but not for two or more.

6.1 Simulation results

The initial configurations of the three agents are $\mathbf{z}_1 = [-6, 3.5, 0]^\top$, $\mathbf{z}_2 = [-6, 2.3, 0]^\top$ and $\mathbf{z}_3 = [-6, 4.7, 0]^\top$. Their desired configurations in steady-state are $\mathbf{z}_{1,des} = [6, 3.5, 0]^\top$, $\mathbf{z}_{2,des} = [6, 2.3, 0]^\top$ and $\mathbf{z}_{3,des} = [6, 4.7, 0]^\top$. Obstacles o_1 and o_2 are placed between the two at $[0, 2.0]^\top$ and $[0, 5.5]^\top$ respectively. The penalty matrices $\boldsymbol{Q}$, $\boldsymbol{R}$, $\boldsymbol{P}$ were set to $\boldsymbol{Q} = 0.5(I_3 + 0.05\dagger_3)$, $\boldsymbol{R} = 0.005I_2$ and $\boldsymbol{P} = 0.5(I_3 + 0.05\dagger_3)$, where $\dagger_N$ is a $N \times N$ matrix whose elements are chosen at random between the values 0.0 and 1.0. The sampling time is $h = 0.1$ sec, the time-horizon is $T_p = 0.5$ sec, and the total execution time given was 3 sec.

Frames of the evolution of the trajectories of the three agents in the $x - y$ plane are depicted in figure (6.1). Here, the compound system avoids the pitfall of coming to a dead-end by having agent 1 act as a kind of mediator between the agents at the extremes as regards their trajectories: a too strict terminal penalty matrix $\boldsymbol{P}$, or an insufficient time-horizon length in relation to the maximum allowed input values, or a strongly diagonal structure for the penalty matrix $\boldsymbol{Q}$ could result in a situation where agent 1 is trapped between the two obstacles, with agents 2 and 3 following behind him, halted by the insufficient space between the two obstacles, and the geometry of the compound system resembling an isosceles triangle.

Once agent 3 clears the narrow, it is held up by agent 1, since their maximum allowed distance is tightly constrained. Agent 1 in turn has to make sure that its distance to agent 2 is within the allowed bounds as well. Figure (6.3) shows the evolution of the distance between agents 1 and 3 through time, and their abiding by the maximum-allowed-distance-between-agents constraint. The minimum and maximum allowed distances between the two agents are portrayed in the colour cyan.

Figure (6.4) shows the evolution of the distance between all agents and obstacle o_2 respectively, and, most crucially, it illustrates the fact that all agents avoid colliding with it. Figure (6.5) shows the input signals directing agent 1 through time. The minimum allowed distance between the agents and the obstacle, as well as the minimum and maximum allowed input sizes are portrayed in the colour cyan.

Figure (6.2) depicts the evolution of the error states of agent 1 through time. As the three error states converge to zero, the agent is stabilized at its desired 3D configuration.

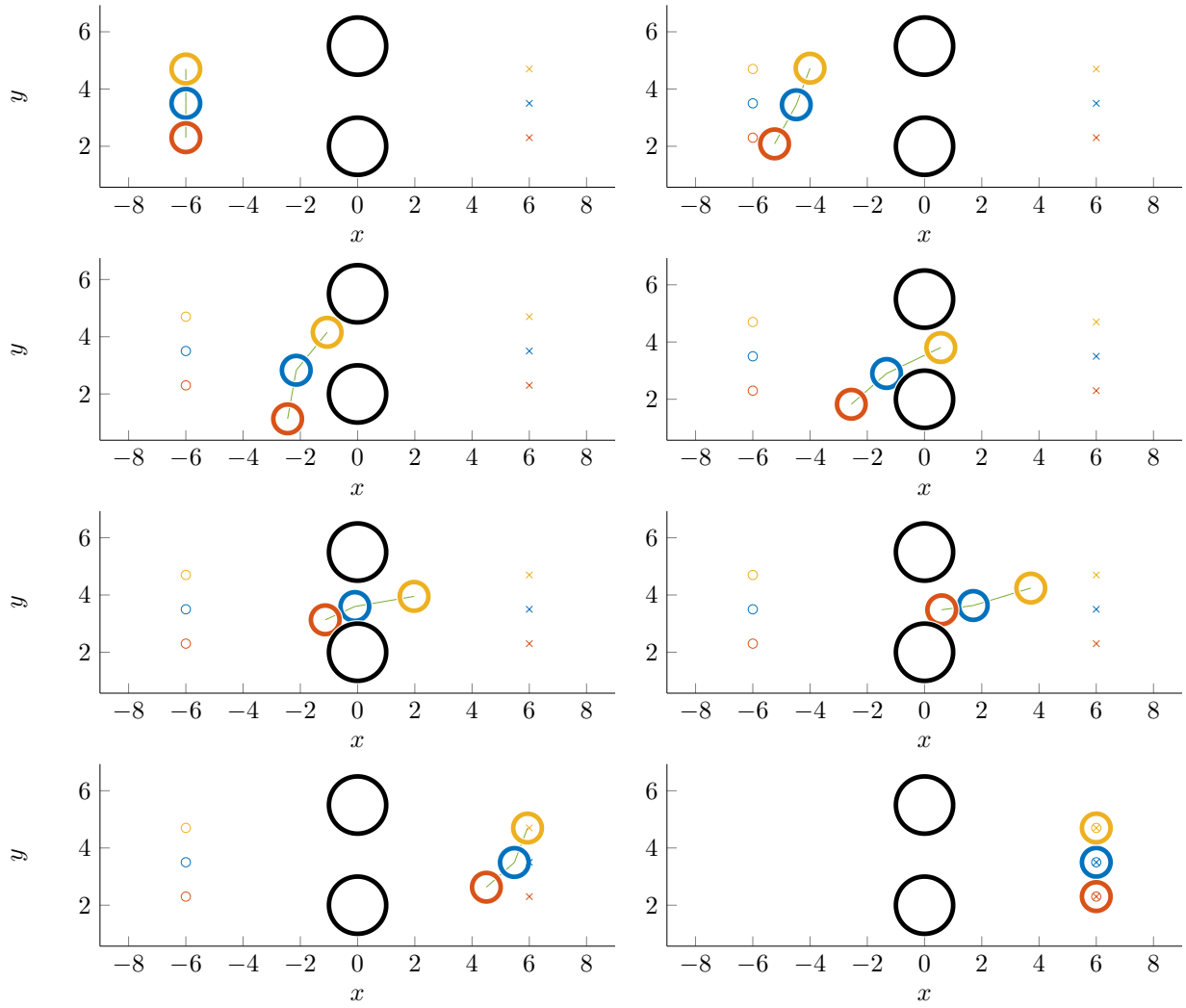

Figure 6.1: The trajectories of the three agents in the $x-y$ plane. Agent 1 is with blue, agent 2 with red and agent 3 with yellow. A faint green line connects agents deemed neighbours. The obstacles are black. Mark O denotes equilibrium configurations. Mark X marks desired configurations.

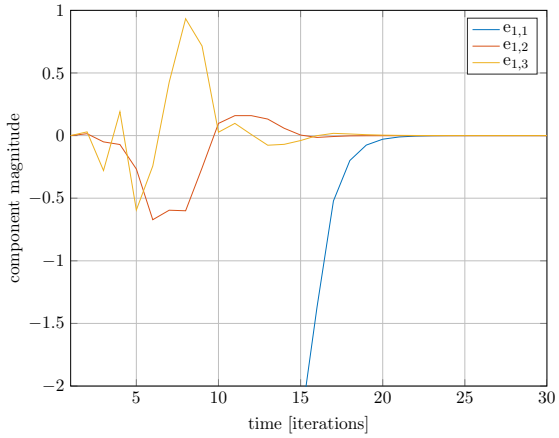

Figure 6.2: The evolution of the error states of agent 1 over time.

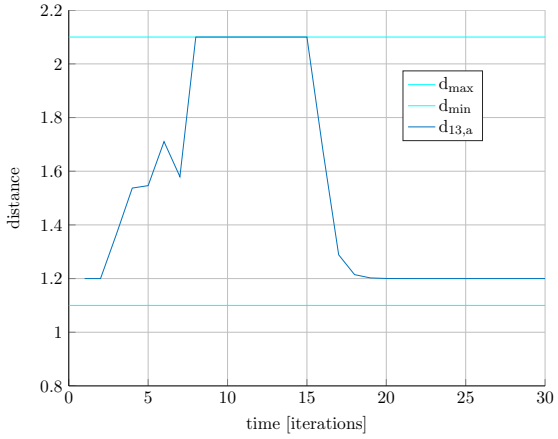

Figure 6.3: The distance between agents 1 and 3 over time. The maximum allowed distance has a value of 2.1 and the minimum allowed distance a value of 1.1.

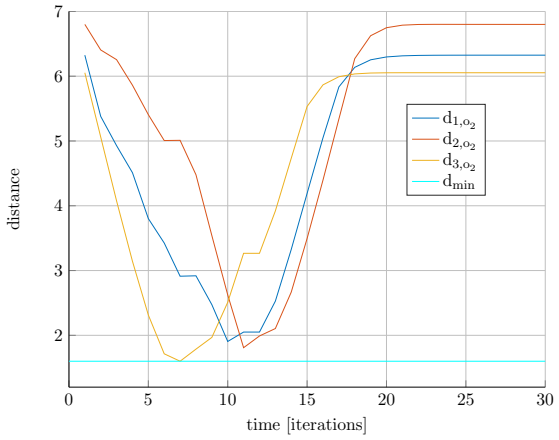

Figure 6.4: The distance between each agent and obstacle 2 over time. The minimum allowed distance has a value of 1.6.

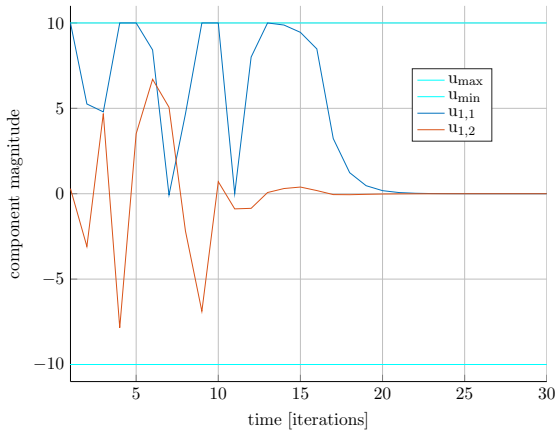

Figure 6.5: The inputs signals directing agent 1 over time. Their value is constrained between -10 and 10.

7

Simulations of Stabilization in the face of Disturbances

The present chapter illustrates the stabilization of a group of agents whose motion dynamics are expressed by equations (5.2), and whose errors with respect to their respective steady-state configurations are constrained by a restricted (compared to the unadulterated $\mathcal{E}_i$) constraint set, aiming at attenuating disturbances. The control laws are designed as in chapter 4.

In this setting, we consider the stabilization of three agents. Agent 1 is constrained in maintaining connectivity with agents 2 and 3 (and homologously vice-versa). All have to avoid colliding with each other and the obstacles in the workspace, and reach their desired configurations under the pressure of being disturbed. The number of obstacles is two. The gap between them suffices for one agent to pass between them, but not for two or more.

7.1 Simulation results

In this case the initial configurations of the three agents are $\mathbf{z}_1 = [-6, 3.5, 0]^\top$, $\mathbf{z}_2 = [-6, 2.3, 0]^\top$ and $\mathbf{z}_3 = [-6, 4.7, 0]^\top$. Their desired configurations in steady-state are $\mathbf{z}_{1,des} = [6, 3.5, 0]^\top$, $\mathbf{z}_{2,des} = [6, 2.3, 0]^\top$ and $\mathbf{z}_{3,des} = [6, 4.7, 0]^\top$. Obstacles o_1 and o_2 are placed between the two at $[0, 2.0]^\top$ and $[0, 5.5]^\top$ respectively. The penalty matrices $\boldsymbol{Q}$, $\boldsymbol{R}$, $\boldsymbol{P}$ were set to $\boldsymbol{Q} = 0.7(I_3 + 0.5\dagger_3)$, $\boldsymbol{R} = 0.005I_2$ and $\boldsymbol{P} = 0.5(I_3 + 0.5\dagger_3)$, where $\dagger_N$ is a $N \times N$ matrix whose elements are chosen at random between the values 0.0 and 1.0. The sampling time is $h = 0.1$ sec, the time-horizon is $T_p = 0.5$ sec, and the total execution time given was 10 sec.

For compatibility with real situations, we assume that the disturbance signals affecting the agents are of the same nature (consider for instance the case of UAV's affected by wind); the disturbance signal considered was $\delta_i(t) = 0.1 * \sin 2t$ for all $i \in \mathcal{V} = \{1, 2, 3\}$. Therefore, $\overline{\delta}_i = 0.1$.

The evolution of the trajectories of the agents in the $x - y$ plane is omitted; they are (with minor variations) equivalent to those in the case where disturbances are absent. Figures (7.2) and (7.3) show the evolution of the distance between agents 1 and 3 through time, and the evolution of the distance between all agents and obstacle o_1 respectively. Figure (7.4) shows the input signals directing agent 2 through time. Just as in the case of absent disturbances, the compound system manages to clear the narrow between the two obstacles without agents colliding with each other or the obstacles, and in general, without violating any constraint present.

Figure (7.1) depicts the evolution of the error states of agent 1 through time. In contrast to the disturbance-free case, the error states do not converge to 0 at steady-state; rather, they oscillate periodically in accordance with the periodic nature of the disturbance, and in this case, with different amplitudes. Component-wise, the $y-$component exhibits the largest amplitude (the compound system oscillates in the vertical direction), however the largest effect of the disturbance is still being attenuated by a factor of 2: the peak-to-peak values of the $y-$component are approximately 0.1, which is half of the peak-to-peak value of the disturbance signal. For the $x-$ and $\theta-$components, the disturbance is attenuated by a factor of approximately 4. Boundary values for the inputs and distances are portrayed in the colour cyan.

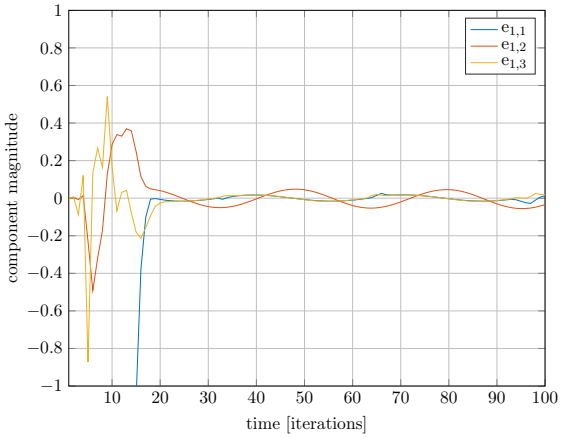

Figure 7.1: The evolution of the error states of agent 1 over time.

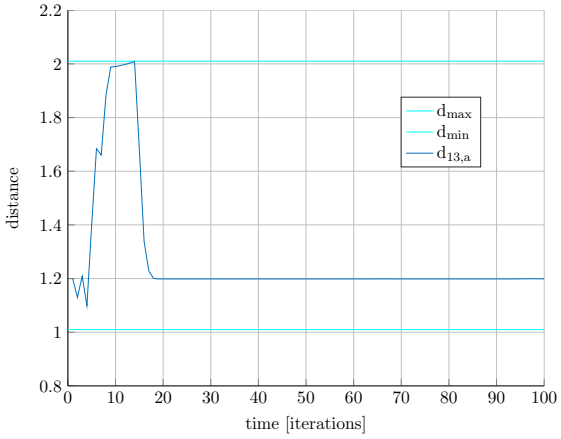

Figure 7.2: The distance between agents 1 and 3 over time. The maximum allowed distance has a value of 2.01 and the minimum allowed distance a value of 1.01.

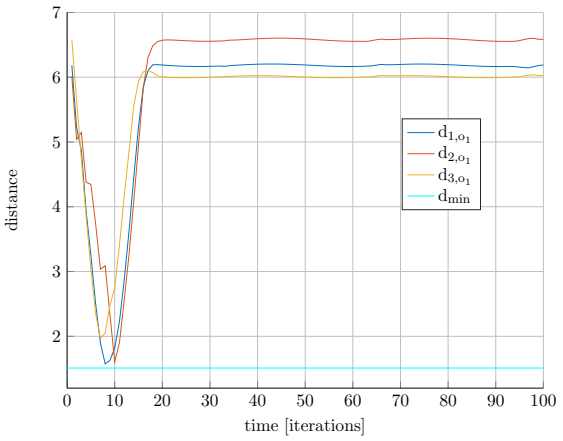

Figure 7.3: The distance between each agent and obstacle 1 over time. The minimum allowed distance has a value of 1.51.

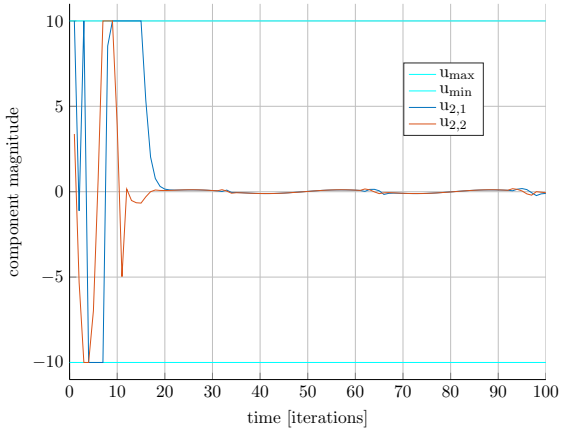

Figure 7.4: The inputs signals directing agent 2 over time. Their value is constrained between -10 and 10.

Last but not at all least, figures (7.5), (7.6) and (7.7) depict the evolution of the quadratic function $\mathbf{e}^\top \boldsymbol{P}\mathbf{e}$ through time for all three agents. The related constants concerned with the execution of this simulation are as follows: $L_{g_i} = 10.7354$, $L_{V_i} = 0.0471$, $\varepsilon_{\Psi_i} = 0.0654$ and $\varepsilon_{\Omega_i} = 0.0035$ for all $i \in \mathcal{V}$. Figures (7.6), and (7.7) illustrate that once the energy measure of each agent (as measured by the errors' $\boldsymbol{P}-$norm function $V = \mathbf{e}^\top \boldsymbol{P}\mathbf{e}$) becomes lower than ε_Ψ (alternatively $-$ when each system's trajectory enters set Ψ), it gets trapped below the value ε_Ω (and hence each system's trajectory is in turn trapped inside the terminal set Ω) in

finite time, and does not exit it. Figure (7.8) illustrates the effect of the disturbance on the quadratic measure $\mathbf{e}^\top \boldsymbol{P}\mathbf{e}$ *in the case where the disturbance is left unaddressed.* It is included for comparison purposes to figure (7.7).

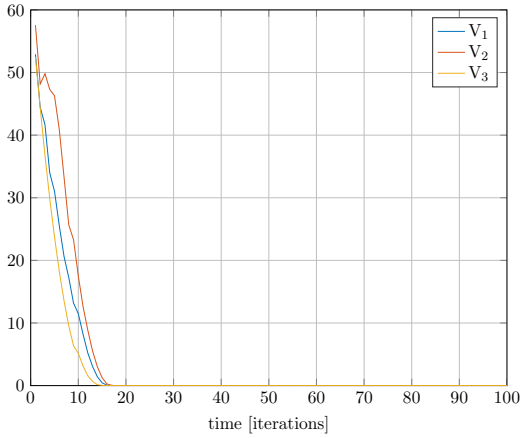

Figure 7.5: The $\boldsymbol{P}-$norms of the errors of the three agents through time.

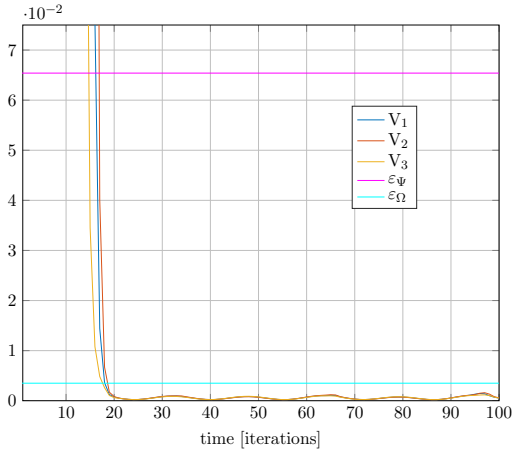

Figure 7.6: The $\boldsymbol{P}-$norms of the errors of the three agents through time, focused. The colour magenta is used to illustrate the threshold ε_Ψ, while cyan is used for ε_Ω.

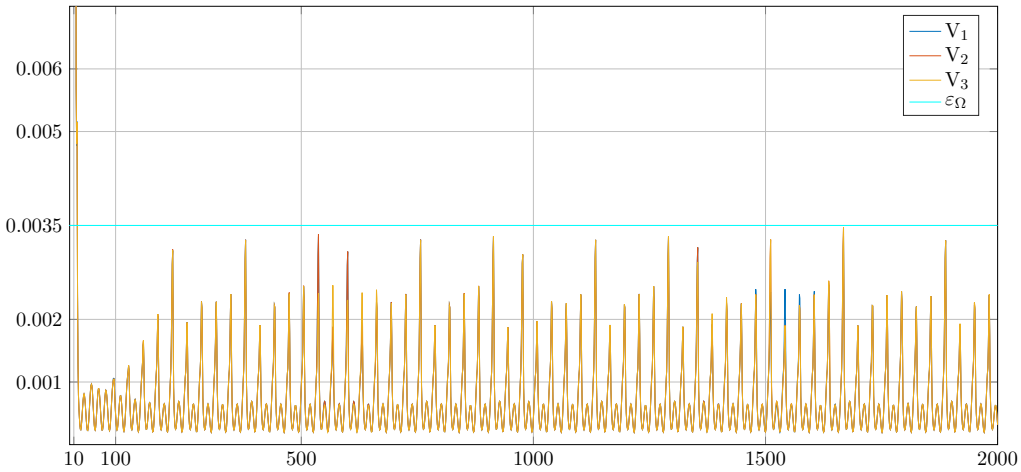

Figure 7.7: The $\boldsymbol{P}-$norms of the errors of the three agents through time, in greater detail and for a longer time-period of execution. The colour cyan is used to depict their ceiling ε_Ω.

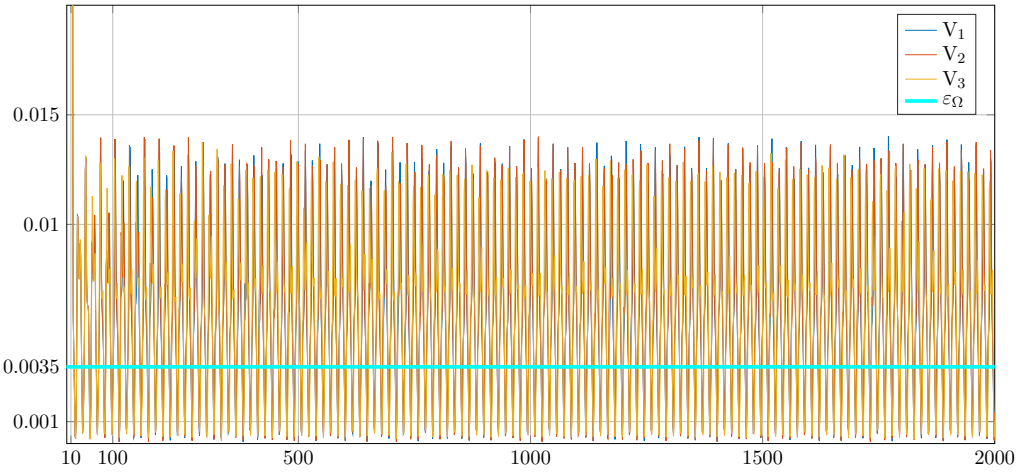

Figure 7.8: The $\boldsymbol{P}-$norms of the errors of the three agents through time, *if the disturbance is left unaddressed*. In direct comparison with figure (7.7), it is clear that the energy of the system, as measured by the $\boldsymbol{P}-$norms of the agents' errors, oscillates with a larger magnitude than that under the proposed control regime.

Due to the inter-constrained nature of the compound system, it is advisable that once the trajectories of *all* agents reach set Ψ – in other words, once they all reach the vicinity of their desired configurations as measured by ε_Ψ – it is advisable that they disable their interconnectedness: since they have all reached the intended feasible desired configurations it is already guaranteed that they will not collide with each other or violate the connectivity constraints. If their interconnectedness is not disabled, then the disturbance affecting each agent could propagate from one agent to the rest due the fact that the trajectory of each agent is regulated indirectly by the predicted states of its neighbours.

Part IV

Conclusions & future work

8

Future work

Future work as I understand it should begin by visiting these two independent (but not necessarily independent) topics: (A) Since simulations are not actual experiments, the designed control regimes appear to be less falsifiable than they could possibly be. Which alludes to implementing the two regimes in real life and testing it on real agents − the motivating problem in itself is posed under the consideration of robotic holonomic agents that operate in physical 3D space. Practice will measure the non-falsifiability of theory. (B) The equivalent of this problem − in relative nature − is instead of handing each agent a desired set point, a neighbour set, and constraints on their distances to their neighbours − instead of these, giving them a relative configuration they should hold (relative set points) with each other, and drive the compound system(s) of neighbours to a configuration where at most only one agents should receive a set point, and formation is achieved in terms of relative agent configurations. This I think may be a relevant problem and one that is more difficult in nature and implications to approach. Lastly, and as a side quest, the answer to the question of what

happens to the trajectory of the compound system if an agent breaks down mid-way would be beneficial to be given, as the current regime does not, and cannot, handle disturbances of this sort.

9

Conclusions

This thesis addressed the problem of stabilizing a non-point multi-agent system under constraints relating to the maintenance of connectivity between agents, the aversion of collision among agents and between agents and stationary obstacles within their working environment, and constraints regarding their states and control inputs. In this thesis, two non-linear model-predictive control schemes were designed, with the aim of stabilizing all agents of the multi-agent system to predetermined desired configurations while satisfying all pertinent constraints at all times. The first scheme considered that the model of the system is perfectly known and that disturbances affecting its states are absent; the second considered the presence of bounded additive uncertainties.

After formulating and positing the motivating problem of this work (chapter 2), the control regimes and sufficient or necessary conditions were documented (the conditions are mild in reality), leading to the proofs that the compound multi-agent system *can* be stabilized asymp-

totically in the disturbance-free case (chapter 3), and in the case where uncertainty is present (chapter 4), that the trajectory of each agent *can* be made to get trapped in a neighbourhood of its desired set point − a neighbourhood smaller than if disturbances were left unattenuated. The efficacy of the two designed control regimes was verified through computer simulations (chapters 6 and 7) on the equivalent problem to the posed $12 - D$ one, the problem of a multi-unicycle system having to avoid collisions altogether, while agents were obliged to keep within certain distance bounds between them, and the obstacles littered in their environment, − and state and input constraints.

In terms of pros over cons, the designed regime: (a) addresses in full the objective sought (as captured in sections (2.3) and (2.4)) in terms of solution to the problem of stabilization in the face of disturbances and in their absence; (b) is favored over the equivalent centralized regime due to its reduced complexity and the increased autonomy of the inner system; (c) is not difficult to be implemented in code; (d) does not require the transmission and reception of more than the current and predicted trajectories of each agent to others within its sensing range; (e) is system-agnostic in terms of dynamics. On the other hand, (x) it requires the continuous and unobstructed transmission and reception of such a volume of information that could potentially require much resources if the communication protocols cannot accommodate such a demand, or if frugality in resources is required to be made; (y) it requires the tuning of penalty matrices, which, in practice, requires carefulness, patience, and caution − intuition helps. (z) If, for any reason, an agent breaks down and becomes uncooperative, the control regime is not designed to recover such a failure.

This is the conclusion of this work.

Appendices

A

Proofs of lemmas

A.1 Proof of lemma 3.3.1

Let $\lambda_{min}(\boldsymbol{Q}_i, \boldsymbol{R}_i)$ denote the smallest eigenvalue between those of matrices $\boldsymbol{Q}_i$ and $\boldsymbol{R}_i$, and let $\lambda_{max}(\boldsymbol{Q}_i, \boldsymbol{R}_i)$ denote the largest. Then

$$\lambda_{min}(\boldsymbol{Q}_i, \boldsymbol{R}_i)\|\mathbf{e}_i(t)\|^2 \leq \lambda_{min}(\boldsymbol{Q}_i, \boldsymbol{R}_i)\left\| \begin{bmatrix} \mathbf{e}_i(t) \\ \mathbf{u}_i(t) \end{bmatrix} \right\|^2$$

$$\leq F_i\big(\mathbf{e}_i(t), \mathbf{u}_i(t)\big)$$

$$\leq \lambda_{max}(\boldsymbol{Q}_i, \boldsymbol{R}_i)\left\| \begin{bmatrix} \mathbf{e}_i(t) \\ \mathbf{u}_i(t) \end{bmatrix} \right\|^2 \leq \lambda_{max}(\boldsymbol{Q}_i, \boldsymbol{R}_i)\|\mathbf{e}_i(t)\|^2$$

Matrices $\boldsymbol{Q}_i, \boldsymbol{R}_i$ are positive definite, hence the functions $\alpha_1\big(\|\mathbf{e}_i\|\big) = \lambda_{min}(\boldsymbol{Q}_i, \boldsymbol{R}_i)\|\mathbf{e}_i\|^2$ and $\alpha_2\big(\|\mathbf{e}_i\|\big) = \lambda_{max}(\boldsymbol{Q}_i, \boldsymbol{R}_i)\|\mathbf{e}_i\|^2$ are class $\mathcal{K}_\infty$ functions according to definition (1.2.1). Therefore, F_i is lower- and upper-bounded by class $\mathcal{K}_\infty$ functions:

$$\alpha_1\big(\|\mathbf{e}_i\|\big) \leq F_i\big(\mathbf{e}_i, \mathbf{u}_i\big) \leq \alpha_2\big(\|\mathbf{e}_i\|\big)$$

A.2 Proof of lemma 3.3.2

For every $\mathbf{e}_1, \mathbf{e}_2 \in \mathcal{E}_i$, and $\mathbf{u}_i \in \mathcal{U}_i$ it holds that

$$\begin{aligned}
\big|F_i(\mathbf{e}_1, \mathbf{u}_i) - F_i(\mathbf{e}_2, \mathbf{u}_i)\big| &= \big|\mathbf{e}_1^\top \boldsymbol{Q}_i \mathbf{e}_1 + \mathbf{u}_i^\top \boldsymbol{R}_i \mathbf{u}_i - \mathbf{e}_2^\top \boldsymbol{Q}_i \mathbf{e}_2 - \mathbf{u}_i^\top \boldsymbol{R}_i \mathbf{u}_i\big| \\
&= \big|\mathbf{e}_1^\top \boldsymbol{Q}_i \mathbf{e}_1 - \mathbf{e}_2^\top \boldsymbol{Q}_i \mathbf{e}_2 \pm \mathbf{e}_1^\top \boldsymbol{Q}_i \mathbf{e}_2\big| \\
&= \big|\mathbf{e}_1^\top \boldsymbol{Q}_i (\mathbf{e}_1 - \mathbf{e}_2) - \mathbf{e}_2^\top \boldsymbol{Q}_i (\mathbf{e}_1 - \mathbf{e}_2)\big| \\
&\leq \big|\mathbf{e}_1^\top \boldsymbol{Q}_i (\mathbf{e}_1 - \mathbf{e}_2)\big| + \big|\mathbf{e}_2^\top \boldsymbol{Q}_i (\mathbf{e}_1 - \mathbf{e}_2)\big|
\end{aligned}$$

But for any $\mathbf{e}_1, \mathbf{e}_2 \in \mathcal{E}_i$

$$|\mathbf{e}_1^\top \boldsymbol{Q}_i \mathbf{e}_2| \leq \sigma_{max}(\boldsymbol{Q}_i)\|\mathbf{e}_1\|\|\mathbf{e}_2\|$$

where $\sigma_{max}(\boldsymbol{Q}_i)$ denotes the largest singular value of matrix $\boldsymbol{Q}_i$. Hence:

$$\begin{aligned}
\big|F_i(\mathbf{e}_1, \mathbf{u}_i) - F_i(\mathbf{e}_2, \mathbf{u}_i)\big| &\leq \sigma_{max}(\boldsymbol{Q}_i)\|\mathbf{e}_1\|\|\mathbf{e}_1 - \mathbf{e}_2\| + \sigma_{max}(\boldsymbol{Q}_i)\|\mathbf{e}_2\|\|\mathbf{e}_1 - \mathbf{e}_2\| \\
&= \sigma_{max}(\boldsymbol{Q}_i)(\|\mathbf{e}_1\| + \|\mathbf{e}_2\|)\|\mathbf{e}_1 - \mathbf{e}_2\| \\
&= \sigma_{max}(\boldsymbol{Q}_i) \sup_{\mathbf{e}_1, \mathbf{e}_2 \in \mathcal{E}_i} \big(\|\mathbf{e}_1\| + \|\mathbf{e}_2\|\big)\|\mathbf{e}_1 - \mathbf{e}_2\| \\
&= 2\sigma_{max}(\boldsymbol{Q}_i) \sup_{\mathbf{e}_i \in \mathcal{E}_i} \big(\|\mathbf{e}_i\|\big)\|\mathbf{e}_1 - \mathbf{e}_2\| \\
&= 2\sigma_{max}(\boldsymbol{Q}_i)\bar{\varepsilon}_i\|\mathbf{e}_1 - \mathbf{e}_2\|
\end{aligned}$$

A.3 Proof of lemma 3.3.3

For every $\mathbf{e}_1, \mathbf{e}_2 \in \Omega_i$, it holds that

$$\begin{aligned}
\big|V_i(\mathbf{e}_1) - V_i(\mathbf{e}_2)\big| &= \big|\mathbf{e}_1^\top \boldsymbol{P}_i \mathbf{e}_1 - \mathbf{e}_2^\top \boldsymbol{P}_i \mathbf{e}_2\big| \\
&= \big|\mathbf{e}_1^\top \boldsymbol{P}_i \mathbf{e}_1 - \mathbf{e}_2^\top \boldsymbol{P}_i \mathbf{e}_2 \pm \mathbf{e}_1^\top \boldsymbol{P}_i \mathbf{e}_2\big| \\
&= \big|\mathbf{e}_1^\top \boldsymbol{P}_i (\mathbf{e}_1 - \mathbf{e}_2) - \mathbf{e}_2^\top \boldsymbol{P}_i (\mathbf{e}_1 - \mathbf{e}_2)\big| \\
&\leq \big|\mathbf{e}_1^\top \boldsymbol{P}_i (\mathbf{e}_1 - \mathbf{e}_2)\big| + \big|\mathbf{e}_2^\top \boldsymbol{P}_i (\mathbf{e}_1 - \mathbf{e}_2)\big|
\end{aligned}$$

But for any $\mathbf{e}_1, \mathbf{e}_2 \in \mathbb{R}^n$

$$\big|\mathbf{e}_1^\top \boldsymbol{P}_i \mathbf{e}_2\big| \leq \sigma_{max}(\boldsymbol{P}_i)\|\mathbf{e}_1\|\|\mathbf{e}_2\|$$

where $\sigma_{max}(\boldsymbol{P}_i)$ denotes the largest singular value of matrix $\boldsymbol{P}_i$. Hence:

$$\begin{aligned}
\big|V_i(\mathbf{e}_1) - V_i(\mathbf{e}_2)\big| &\leq \sigma_{max}(\boldsymbol{P}_i)\|\mathbf{e}_1\|\|\mathbf{e}_1 - \mathbf{e}_2\| + \sigma_{max}(\boldsymbol{P}_i)\|\mathbf{e}_2\|\|\mathbf{e}_1 - \mathbf{e}_2\| \\
&= \sigma_{max}(\boldsymbol{P}_i)(\|\mathbf{e}_1\| + \|\mathbf{e}_2\|)\|\mathbf{e}_1 - \mathbf{e}_2\| \\
&\leq \sigma_{max}(\boldsymbol{P}_i)(\overline{\varepsilon}_{i,\Omega_i} + \overline{\varepsilon}_{i,\Omega_i})\|\mathbf{e}_1 - \mathbf{e}_2\| \\
&= 2\sigma_{max}(\boldsymbol{P}_i)\overline{\varepsilon}_{i,\Omega_i}\|\mathbf{e}_1 - \mathbf{e}_2\|
\end{aligned}$$

A.4 Proof of lemma 3.3.4

V_i is defined as $V_i\big(\mathbf{e}_i\big) = \mathbf{e}_i^\top \boldsymbol{P}_i \mathbf{e}_i$. Let us denote the minimum and maximum eigenvalues of matrix $\boldsymbol{P}_i$ by $\lambda_{min}(\boldsymbol{P}_i)$ and $\lambda_{max}(\boldsymbol{P}_i)$ respectively. Then, the following series of inequalities holds:

$$\lambda_{min}(\boldsymbol{P}_i)\|\mathbf{e}_i\|^2 \leq V_i(\mathbf{e}_i) \leq \lambda_{max}(\boldsymbol{P}_i)\|\mathbf{e}_i\|^2$$

Matrix $\boldsymbol{P}_i$ is positive definite, hence the functions $\alpha_1 = \lambda_{min}(\boldsymbol{P}_i)\|\mathbf{e}_i\|^2$ and $\alpha_2 = \lambda_{max}(\boldsymbol{P}_i)\|\mathbf{e}_i\|^2$ are class $\mathcal{K}_\infty$ functions according to definition (1.2.1). Therefore, V_i is lower- and upper-bounded by class $\mathcal{K}_\infty$ functions:

$$\alpha_1\big(\|\mathbf{e}_i\|\big) \leq V_i(\mathbf{e}_i) \leq \alpha_2\big(\|\mathbf{e}_i\|\big)$$

A.5 Proof of property 4.3.1

Let us define for convenience $\boldsymbol{\zeta}_i : \mathbb{R}_{\geq 0} \to \mathbb{R}^9 \times \mathbb{T}^3$: $\boldsymbol{\zeta}_i(s) \triangleq \mathbf{e}_i(s) - \overline{\mathbf{e}}_i(s;\ \mathbf{u}_i(s;\ \mathbf{e}_i(t)), \mathbf{e}_i(t))$, for $s \in [t, t+T_p]$.

According to lemma (4.4.1)

$$\|\mathbf{e}_i(s) - \overline{\mathbf{e}}_i\big(s;\ \mathbf{u}_i(s;\ \mathbf{e}_i(t)), \mathbf{e}_i(t)\big)\| \leq \frac{\overline{\delta}_i}{\mathrm{L}_{g_i}}(e^{L_{g_i}(s-t)} - 1)$$

$$\|\boldsymbol{\zeta}_i(s)\| \leq \frac{\overline{\delta}_i}{\mathrm{L}_{g_i}}(e^{L_{g_i}(s-t)} - 1)$$

which means that $\boldsymbol{\zeta}_i(s) \in \mathcal{B}_{i,s-t}$. Now let us assume that $\overline{\mathbf{e}}_i\big(s;\ \mathbf{u}_i(\cdot,\ \mathbf{e}_i(t)), \mathbf{e}_i(t)\big) \in \mathcal{E}_i \ominus \mathcal{B}_{i,s-t}$. Then, we add the two include statements:

$$\overline{\mathbf{e}}_i\big(s;\ \mathbf{u}_i(\cdot,\ \mathbf{e}_i(t)), \mathbf{e}_i(t)\big) \in \mathcal{E}_i \ominus \mathcal{B}_{i,s-t}$$

$$\boldsymbol{\zeta}_i(s) \in \mathcal{B}_{i,s-t}$$

which yields

$$\boldsymbol{\zeta}_i(s) + \overline{\mathbf{e}}_i\big(s;\ \mathbf{u}_i(s;\ \mathbf{e}_i(t)), \mathbf{e}_i(t)\big) \in \big(\mathcal{E}_i \ominus \mathcal{B}_{i,s-t}\big) \oplus \mathcal{B}_{i,s-t}$$

Utilizing Theorem 2.1 (ii) from [21] yields

$$\boldsymbol{\zeta}_i(s) + \overline{\mathbf{e}}_i\big(s;\ \mathbf{u}_i(s;\ \mathbf{e}_i(t)), \mathbf{e}_i(t)\big) \in \mathcal{E}_i$$

$$\mathbf{e}_i(s) \in \mathcal{E}_i$$

A.6 Proof of lemma 4.4.1

Since there are disturbances present, consulting remark (4.4.1) and substituting for $\tau_0 = t$ and $\tau_1 = t + \tau$ yields:

$$\mathbf{e}_i\big(t+\tau;\ \overline{\mathbf{u}}_i^\star\big(\cdot;\ \mathbf{e}_i(t)\big), \mathbf{e}_i(t)\big) = \mathbf{e}_i(t) + \int_t^{t+\tau} g_i\big(\mathbf{e}_i(s;\ \mathbf{e}_i(t)), \overline{\mathbf{u}}_i^\star(s)\big)ds + \int_t^{t+\tau} \delta_i(s)ds$$

$$\overline{\mathbf{e}}_i\big(t+\tau;\ \overline{\mathbf{u}}_i^\star\big(\cdot;\ \mathbf{e}_i(t)\big), \mathbf{e}_i(t)\big) = \mathbf{e}_i(t) + \int_t^{t+\tau} g_i\big(\overline{\mathbf{e}}_i(s;\ \mathbf{e}_i(t)), \overline{\mathbf{u}}_i^\star(s)\big)ds$$

Subtracting the latter from the former and taking norms on either side yields:

$$\begin{aligned}
&\left\|\mathbf{e}_i\big(t+\tau;\ \overline{\mathbf{u}}_i^\star\big(\cdot;\ \mathbf{e}_i(t)\big), \mathbf{e}_i(t)\big) - \overline{\mathbf{e}}_i\big(t+\tau;\ \overline{\mathbf{u}}_i^\star\big(\cdot;\ \mathbf{e}_i(t)\big), \mathbf{e}_i(t)\big)\right\| \\
&\quad = \left\| \int_t^{t+\tau} g_i\big(\mathbf{e}_i(s;\ \mathbf{e}_i(t)), \overline{\mathbf{u}}_i^\star(s)\big)ds - \int_t^{t+\tau} g_i\big(\overline{\mathbf{e}}_i(s;\ \mathbf{e}_i(t)), \overline{\mathbf{u}}_i^\star(s)\big)ds + \int_t^{t+\tau} \delta_i(s)ds \right\| \\
&\quad \leq \left\| \int_t^{t+\tau} g_i\big(\mathbf{e}_i(s;\ \mathbf{e}_i(t)), \overline{\mathbf{u}}_i^\star(s)\big)ds - \int_t^{t+\tau} g_i\big(\overline{\mathbf{e}}_i(s;\ \mathbf{e}_i(t)), \overline{\mathbf{u}}_i^\star(s)\big)ds \right\| + (t+\tau-t)\overline{\delta}_i \\
&\quad \leq \int_t^{t+\tau} \left\| g_i\big(\mathbf{e}_i(s;\ \mathbf{e}_i(t)), \overline{\mathbf{u}}_i^\star(s)\big)s - g_i\big(\overline{\mathbf{e}}_i(s;\ \mathbf{e}_i(t)), \overline{\mathbf{u}}_i^\star(s)\big) \right\| ds + \tau\overline{\delta}_i \\
&\quad \leq L_{g_i} \int_t^{t+\tau} \left\| \mathbf{e}_i\big(s;\ \overline{\mathbf{u}}_i^\star\big(\cdot;\ \mathbf{e}_i(t)\big), \mathbf{e}_i(t)\big) - \overline{\mathbf{e}}_i\big(s;\ \overline{\mathbf{u}}_i^\star\big(\cdot;\ \mathbf{e}_i(t)\big), \mathbf{e}_i(t)\big) \right\| ds + \tau\overline{\delta}_i
\end{aligned}$$

since g_i is Lipschitz continuous in $\mathcal{E}_i$ with Lipschitz constant L_{g_i}. Reformulation yields

$$\begin{aligned}
&\left\|\mathbf{e}_i\big(t+\tau;\ \overline{\mathbf{u}}_i^\star\big(\cdot;\ \mathbf{e}_i(t)\big), \mathbf{e}_i(t)\big) - \overline{\mathbf{e}}_i\big(t+\tau;\ \overline{\mathbf{u}}_i^\star\big(\cdot;\ \mathbf{e}_i(t)\big), \mathbf{e}_i(t)\big)\right\| \\
&\qquad \leq \tau\overline{\delta}_i + L_{g_i} \int_0^{\tau} \left\| \mathbf{e}_i\big(t+s;\ \overline{\mathbf{u}}_i^\star\big(\cdot;\ \mathbf{e}_i(t)\big), \mathbf{e}_i(t)\big) - \overline{\mathbf{e}}_i\big(t+s;\ \overline{\mathbf{u}}_i^\star\big(\cdot;\ \mathbf{e}_i(t)\big), \mathbf{e}_i(t)\big) \right\| ds
\end{aligned}$$

By applying the Grönwall-Bellman inequality we get:

$$\begin{aligned}
&\left\|\mathbf{e}_i\big(t+\tau;\ \overline{\mathbf{u}}_i^\star\big(\cdot;\ \mathbf{e}_i(t)\big),\mathbf{e}_i(t)\big) - \overline{\mathbf{e}}_i\big(t+\tau;\ \overline{\mathbf{u}}_i^\star\big(\cdot;\ \mathbf{e}_i(t)\big),\mathbf{e}_i(t)\big)\right\| \\
&\qquad \leq \tau\overline{\delta}_i + L_{g_i}\int_0^\tau s\overline{\delta}_i e^{L_{g_i}(\tau-s)}ds \\
&\qquad = \tau\overline{\delta}_i - \overline{\delta}_i\int_0^\tau s\big(e^{L_{g_i}(\tau-s)}\big)'ds \\
&\qquad = \tau\overline{\delta}_i - \overline{\delta}_i\left(\big[se^{L_{g_i}(\tau-s)}\big]_0^\tau - \int_0^\tau e^{L_{g_i}(\tau-s)}ds\right) \\
&\qquad = \tau\overline{\delta}_i - \overline{\delta}_i\left(\tau + \frac{1}{L_{g_i}}(1-e^{L_{g_i}\tau})\right) \\
&\qquad = \frac{\overline{\delta}_i}{L_{g_i}}(e^{L_{g_i}\tau}-1)
\end{aligned}$$

A.7 Proof of lemma 5.1.1

Let $g(\mathbf{e},\mathbf{u})$ be the differential equation describing the error of the motion of the unicycle with respect to a fixed desired configuration, and $\boldsymbol{Q} = Q_{\mu\nu}$ a 3×3 matrix. Then

$$\begin{aligned}
\|g(\mathbf{e}_1,\mathbf{u}) - g(\mathbf{e}_2,\mathbf{u})\|_Q &= \left\| \begin{bmatrix} v\cos\theta_1 - v\cos\theta_2 \\ v\sin\theta_1 - v\sin\theta_2 \\ \omega-\omega \end{bmatrix} \right\|_Q \\
&= \sqrt{v^2\begin{bmatrix}\cos\theta_1-\cos\theta_2 & \sin\theta_1-\sin\theta_2 & 0\end{bmatrix} Q \begin{bmatrix}\cos\theta_1-\cos\theta_2 \\ \sin\theta_1-\sin\theta_2 \\ 0\end{bmatrix}} \\
&= \sqrt{v^2(\cos\theta_1-\cos\theta_2)\Big((Q_{11}+Q_{12})(\cos\theta_1-\cos\theta_2)+(Q_{21}+Q_{22})(\sin\theta_1-\sin\theta_2)\Big)}
\end{aligned}$$

From the mean value theorem we derive the following

$$\cos\theta_1 - \cos\theta_2 = -\sin\gamma(\theta_1 - \theta_2) \leq |\theta_1 - \theta_2|$$

$$\sin\theta_1 - \sin\theta_2 = \cos\gamma(\theta_1 - \theta_2) \leq |\theta_1 - \theta_2|$$

where $\theta_1 \leq \gamma \leq \theta_2$. Hence

$$\begin{aligned}
\|g(\mathbf{e}_1, \mathbf{u}) - g(\mathbf{e}_2, \mathbf{u})\|_Q &\leq \sqrt{v^2|\theta_1 - \theta_2|\Big((Q_{11} + Q_{12})|\theta_1 - \theta_2| + (Q_{21} + Q_{22})|\theta_1 - \theta_2|\Big)} \\
&= \sqrt{v^2|\theta_1 - \theta_2|^2(Q_{1,1} + Q_{1,2} + Q_{2,1} + Q_{2,2})} \\
&= v\sqrt{Q_{1,1} + Q_{1,2} + Q_{2,1} + Q_{2,2}} \cdot |\theta_1 - \theta_2| \\
&\leq v_{max}\sqrt{Q_{1,1} + Q_{1,2} + Q_{2,1} + Q_{2,2}} \cdot |\theta_1 - \theta_2|
\end{aligned}$$

A.8 Stabilizability of the unicycle model

Suppose that $\mathbf{x} = [x_1, x_2, x_3]^\top \in X$. The equations that express the kinematic model of the unicycle are

$$\begin{aligned}
\dot{x}_1 &= u_1 \cos x_3 \\
\dot{x}_2 &= u_1 \sin x_3 \\
\dot{x}_3 &= u_2
\end{aligned}$$

Linearizing around $\mathbf{x}^0 = [x_1^0, x_2^0, x_3^0]^\top$ and $\mathbf{u}^0 = [u_1^0, u_2^0]$, the equivalent linear system becomes

$$\dot{\mathbf{x}} = A\mathbf{x} + B\mathbf{u} \tag{A.1}$$

where

$$A = \begin{bmatrix} 0 & 0 & -u_1^0 \sin x_3^0 \\ 0 & 0 & u_1^0 \cos x_3^0 \\ 0 & 0 & 0 \end{bmatrix}, \; B = \begin{bmatrix} \cos x_3^0 & 0 \\ \sin x_3^0 & 0 \\ 0 & 1 \end{bmatrix}$$

The controllability matrix of (A.1) is

$$C_3 = [B\ AB\ A^2B] = \begin{bmatrix} \cos x_3^0 & 0 & 0 & -u_1^0 \sin x_3^0 & 0 & 0 \\ \sin x_3^0 & 0 & 0 & u_1^0 \cos x_3^0 & 0 & 0 \\ 0 & 1 & 0 & 0 & 0 & 0 \end{bmatrix}$$

and its rank is 3 if $u_1 \neq 0$. Hence system (A.1) is controllable. Given that controllable systems are stabilizable, the kinematics model of the unicycle is found to be stabilizable in X if $u_1 \neq 0$.

B

Simulation figures – disturbances absent

Each of the following sections describes the initial and terminal configurations, and the penalty matrices $\boldsymbol{Q}$, $\boldsymbol{R}$ and $\boldsymbol{P}$ used in each setting. Furthermore, the errors of each agent with respect to its terminal configuration are portrayed, along with its input signals and the distances between all agents and obstacles. Boundary values for the aforementioned inputs and distances shall be portrayed in the colour cyan. All simulations were performed with a sampling time of $h = 0.1$ sec, and a time-horizon of $T_p = 0.5$ sec; the total execution time given was 3 sec.

B.1 Test case one: two agents − one obstacle

In this case the initial configurations of the two agents are $\mathbf{z}_1 = [-6, 3.5, 0]^\top$ and $\mathbf{z}_2 = [-6, 2.3, 0]^\top$. Their desired configurations in steady-state are $\mathbf{z}_{1,des} = [6, 3.5, 0]^\top$ and $\mathbf{z}_{2,des} = [6, 2.3, 0]^\top$. The obstacle is placed between the two, at $[0, 2.9]^\top$. The penalty matrices $\boldsymbol{Q}$, $\boldsymbol{R}$, $\boldsymbol{P}$ were set to $\boldsymbol{Q} = 0.5(I_3 + 0.1\dagger_3)$, $\boldsymbol{R} = 0.005I_2$ and $\boldsymbol{P} = 0.5I_3$, where $\dagger_N$ is a $N \times N$ matrix whose elements are chosen at random between the values 0.0 and 1.0.

In subsection B.1.1, frames of the evolution of the trajectories of the two agents are depicted. Subsections B.1.2 and B.1.4 illustrate the evolution of the error states and the input signals of the two agents respectively. Subsection B.1.3 features the figures relating to the evolution of the distance between the two agents along with that between them and the obstacle.

B.1.1 Trajectories in 2D

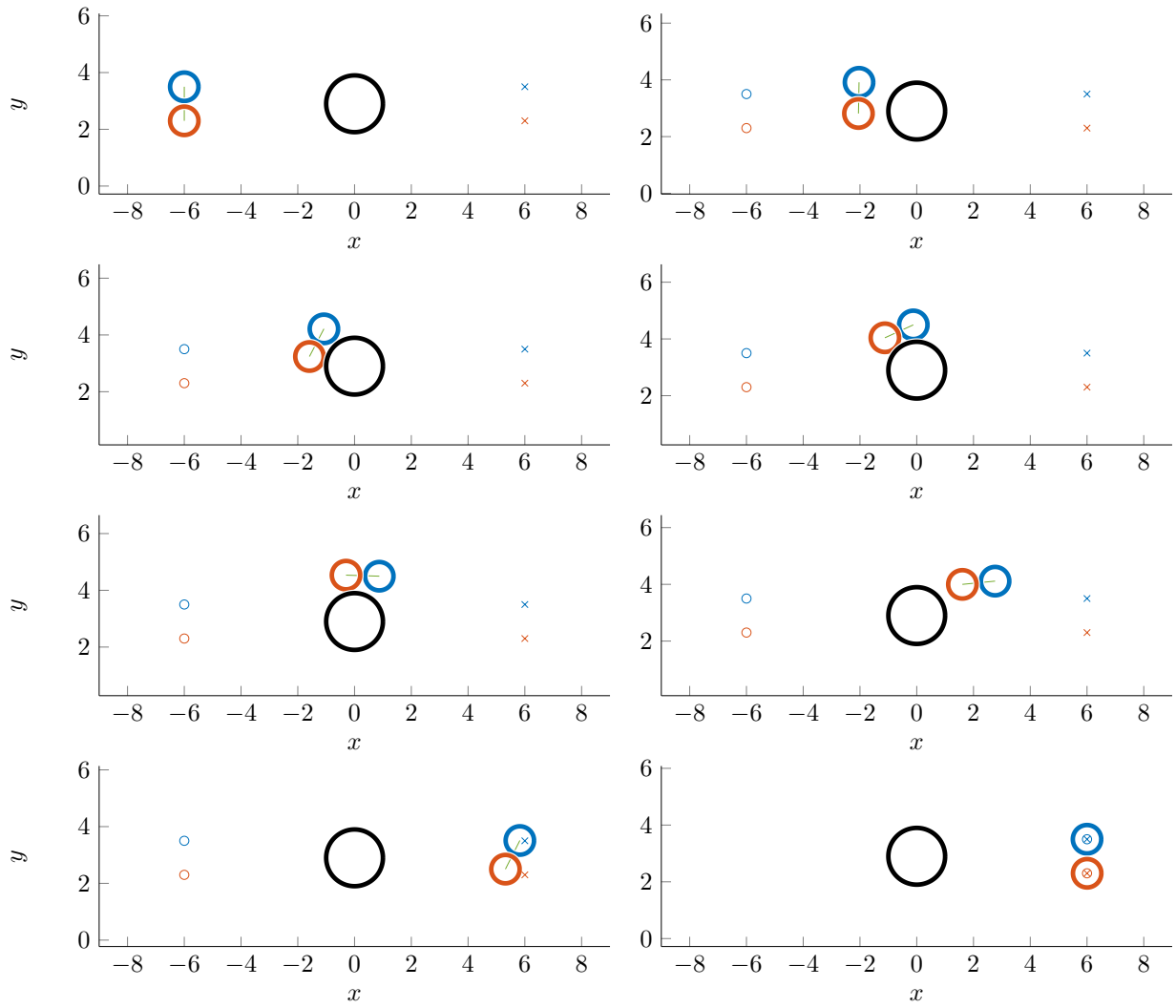

Figure B.1: The trajectories of the two agents in the $x - y$ plane. Agent 1 is with blue and agent 2 with red. The obstacle is black. Mark O denotes equilibrium configurations. Mark X marks desired configurations.

B.1.2 State errors

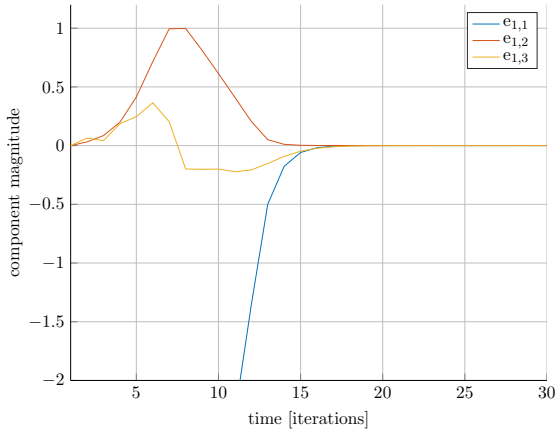

Figure B.2: The evolution of the error states of agent 1 over time.

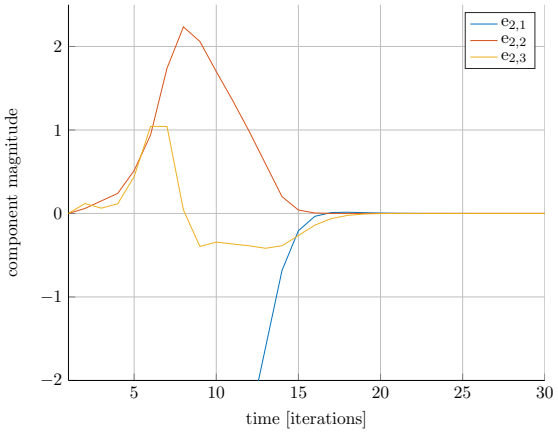

Figure B.3: The evolution of the error states of agent 2 over time.

B.1.3 Distances between actors

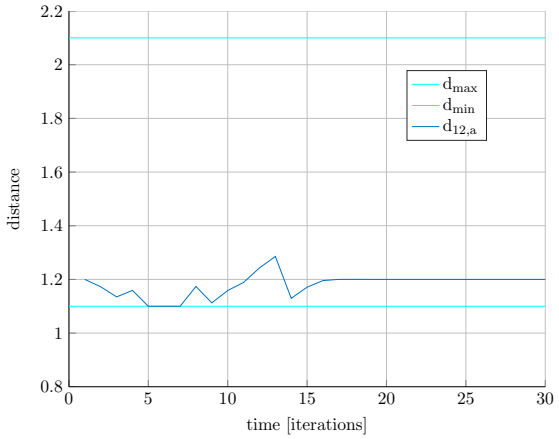

Figure B.4: The distance between the two agents over time. The maximum allowed distance has a value of 2.1 and the minimum allowed distance a value of 1.1.

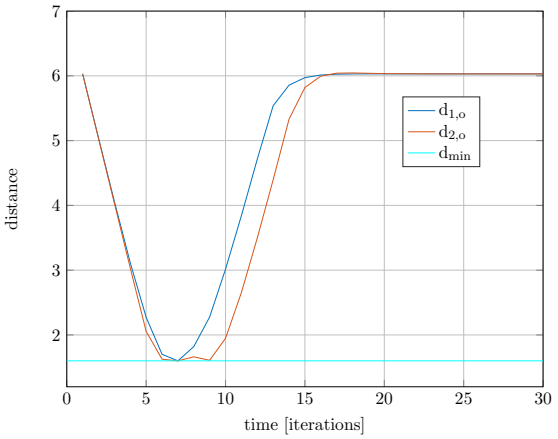

Figure B.5: The distance between each agent and the obstacle over time. The minimum allowed distance has a value of 1.6.

B.1.4 Input signals

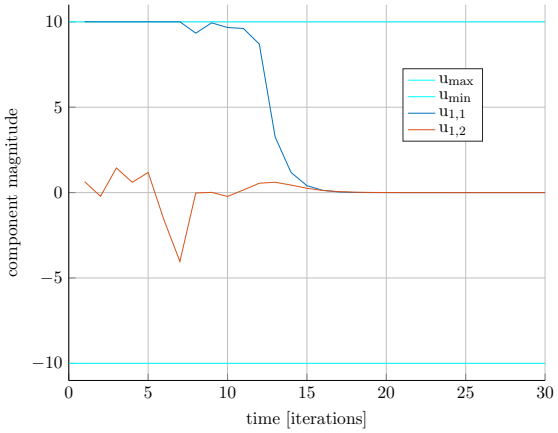

Figure B.6: The inputs signals directing agent 1 over time. Their value is constrained between −10 and 10.

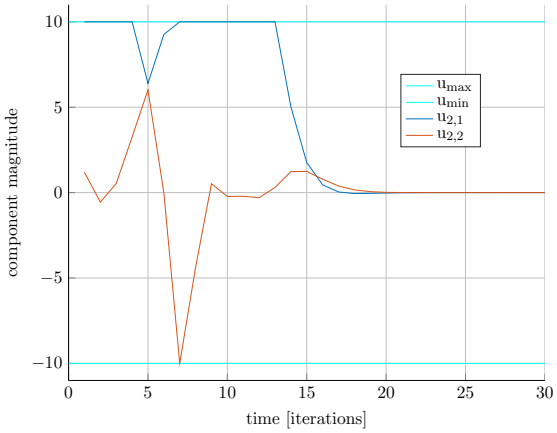

Figure B.7: The inputs signals directing agent 2 over time. Their value is constrained between −10 and 10.

B.2 Test case two: two agents − two obstacles

In this case the initial configurations of the two agents are $\mathbf{z}_1 = [-6, 2.75, 0]^\top$ and $\mathbf{z}_2 = [-6, 4.25, 0]^\top$. Their desired configurations in steady-state are $\mathbf{z}_{1,des} = [6, 2.75, 0]^\top$ and $\mathbf{z}_{2,des} = [6, 4.25, 0]^\top$. Obstacles o_1, 0_2 are placed between the two, at $[0, 1.85]^\top$ and $[0, 5.15]^\top$ respectively. The penalty matrices $\boldsymbol{Q}$, $\boldsymbol{R}$, $\boldsymbol{P}$ were set to $\boldsymbol{Q} = 0.5(I_3 + 0.1\dagger_3)$, $\boldsymbol{R} = 0.005I_2$ and $\boldsymbol{P} = 0.5I_3$, where $\dagger_N$ is a $N \times N$ matrix whose elements are chosen at random between the values 0.0 and 1.0.

In subsection B.2.1, frames of the evolution of the trajectories of the two agents are depicted. Subsections B.2.2 and B.2.4 illustrate the evolution of the error states and the input signals of the two agents respectively. Subsection B.2.3 features the figures relating to the evolution of the distance between the two agents along with that between them and the two obstacles.

B.2.1 Trajectories in 2D

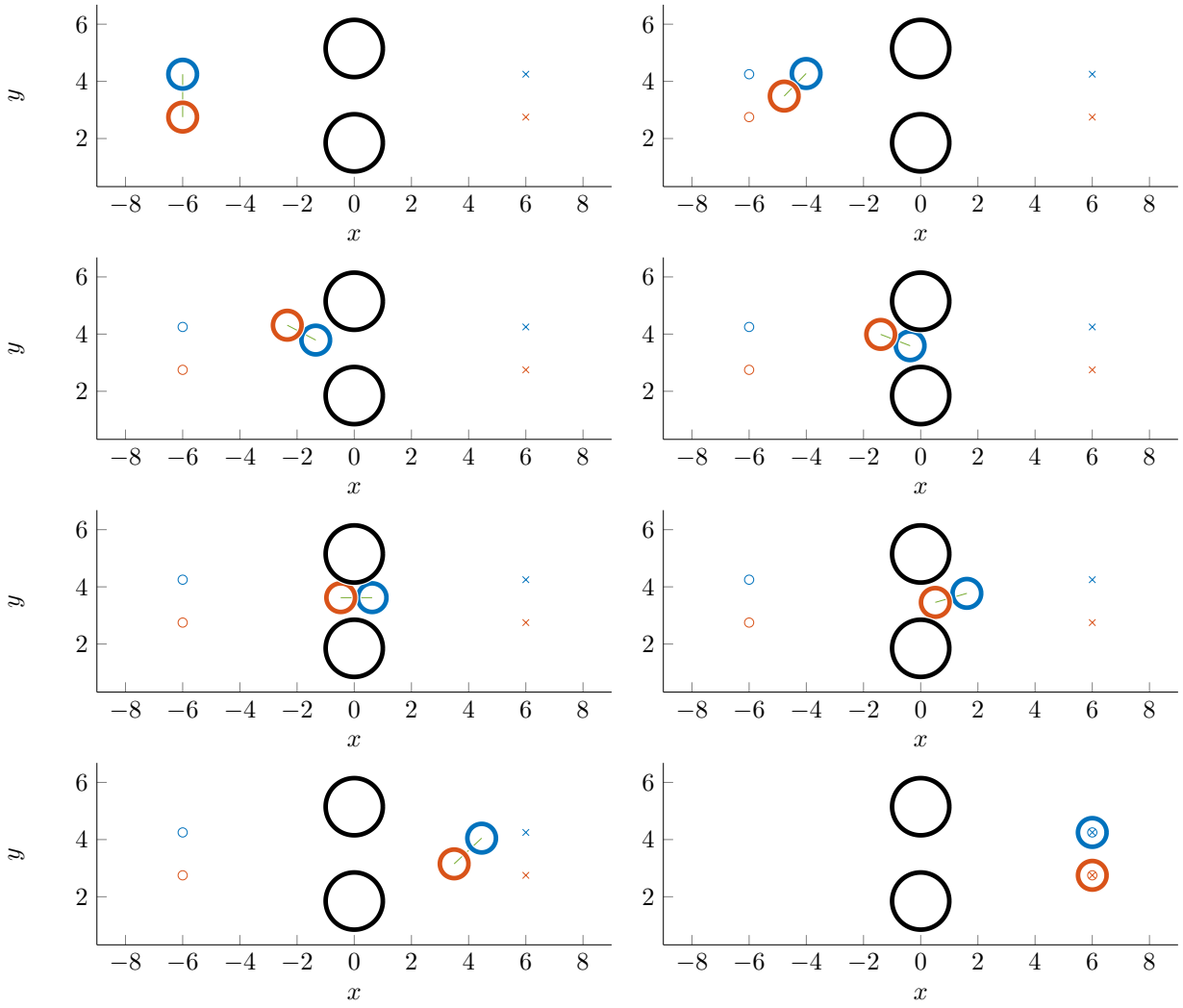

Figure B.8: The trajectories of the two agents in the $x - y$ plane. Agent 1 is with blue and agent 2 with red. The obstacles are black. Mark O denotes equilibrium configurations. Mark X marks desired configurations.

B.2.2 State errors

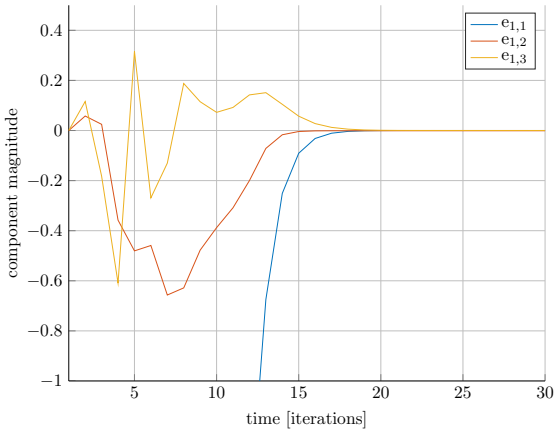

Figure B.9: The evolution of the error states of agent 1 over time.

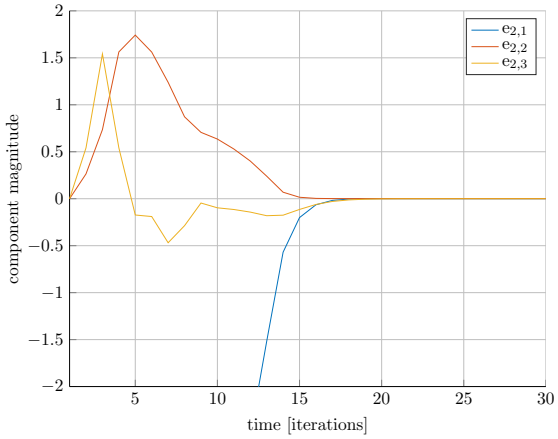

Figure B.10: The evolution of the error states of agent 2 over time.

B.2.3 Distances between actors

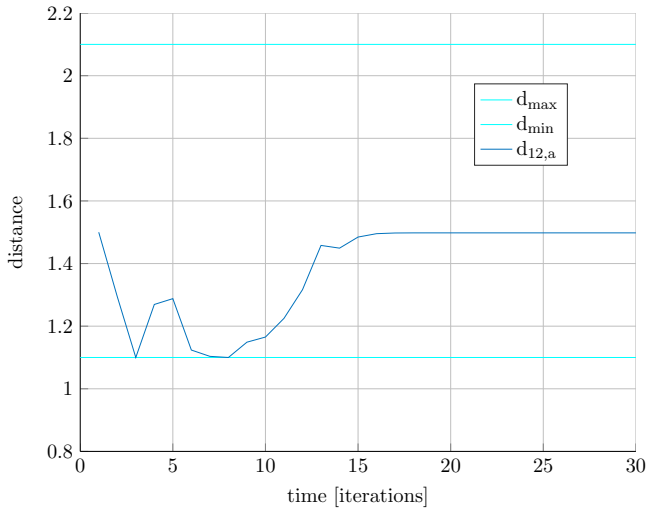

Figure B.11: The distance between the two agents over time. The maximum allowed distance has a value of 2.1 and the minimum allowed distance a value of 1.1.

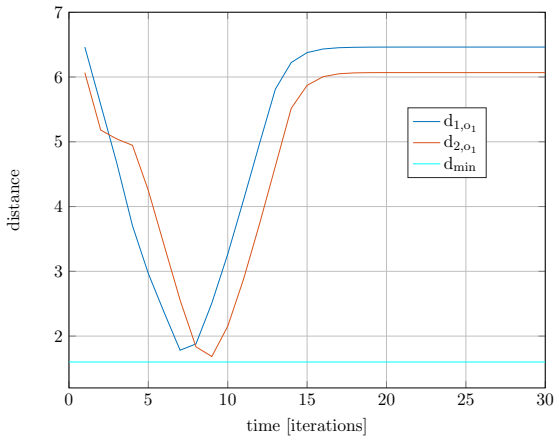

Figure B.12: The distance between each agent and obstacle 1 over time. The minimum allowed distance has a value of 1.6.

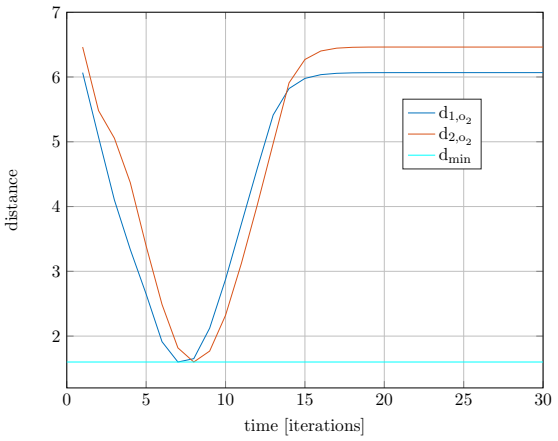

Figure B.13: The distance between each agent and obstacle 2 over time. The minimum allowed distance has a value of 1.6.

B.2.4 Input signals

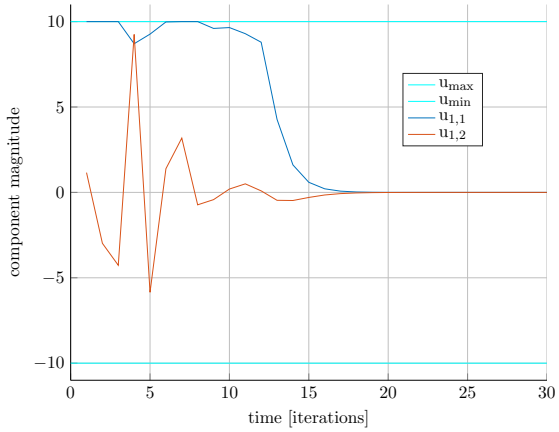

Figure B.14: The inputs signals directing agent 1 over time. Their value is constrained between -10 and 10.

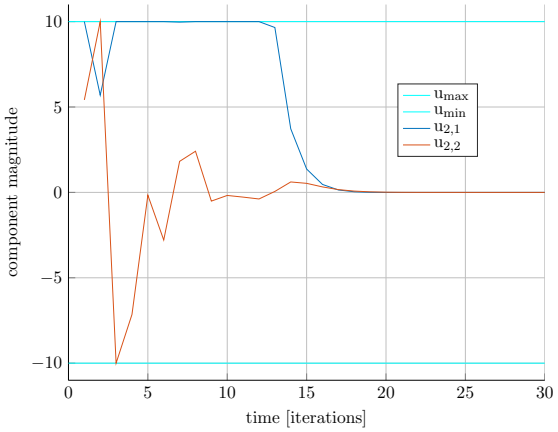

Figure B.15: The inputs signals directing agent 2 over time. Their value is constrained between -10 and 10.

B.3 Test case three: three agents – one obstacle

In this case the initial configurations of the three agents are $\mathbf{z}_1 = [-6, 3.5, 0]^\top$, $\mathbf{z}_2 = [-6, 2.3, 0]^\top$ and $\mathbf{z}_3 = [-6, 4.7, 0]^\top$. Their desired configurations in steady-state are $\mathbf{z}_{1,des} = [6, 3.5, 0]^\top$, $\mathbf{z}_{2,des} = [6, 2.3, 0]^\top$ and $\mathbf{z}_{3,des} = [6, 4.7, 0]^\top$. Obstacle o_1 is placed between the two at $[0, 3.5]^\top$.

The penalty matrices $\boldsymbol{Q}$, $\boldsymbol{R}$, $\boldsymbol{P}$ were set to $\boldsymbol{Q} = 0.5(I_3 + \dagger_3)$, $\boldsymbol{R} = 0.005I_2$ and $\boldsymbol{P} = 0.5I_3$, where $\dagger_N$ is a $N \times N$ matrix whose elements are chosen at random between the values 0.0 and 1.0.

In subsection B.3.1, frames of the evolution of the trajectories of the three agents are depicted. Subsections B.3.2 and B.3.4 illustrate the evolution of the error states and the input signals of the three agents respectively. Subsection B.3.3 features the figures relating to the evolution of the distance between the three agents along with that between them and the obstacle.

B.3.1 Trajectories in 2D

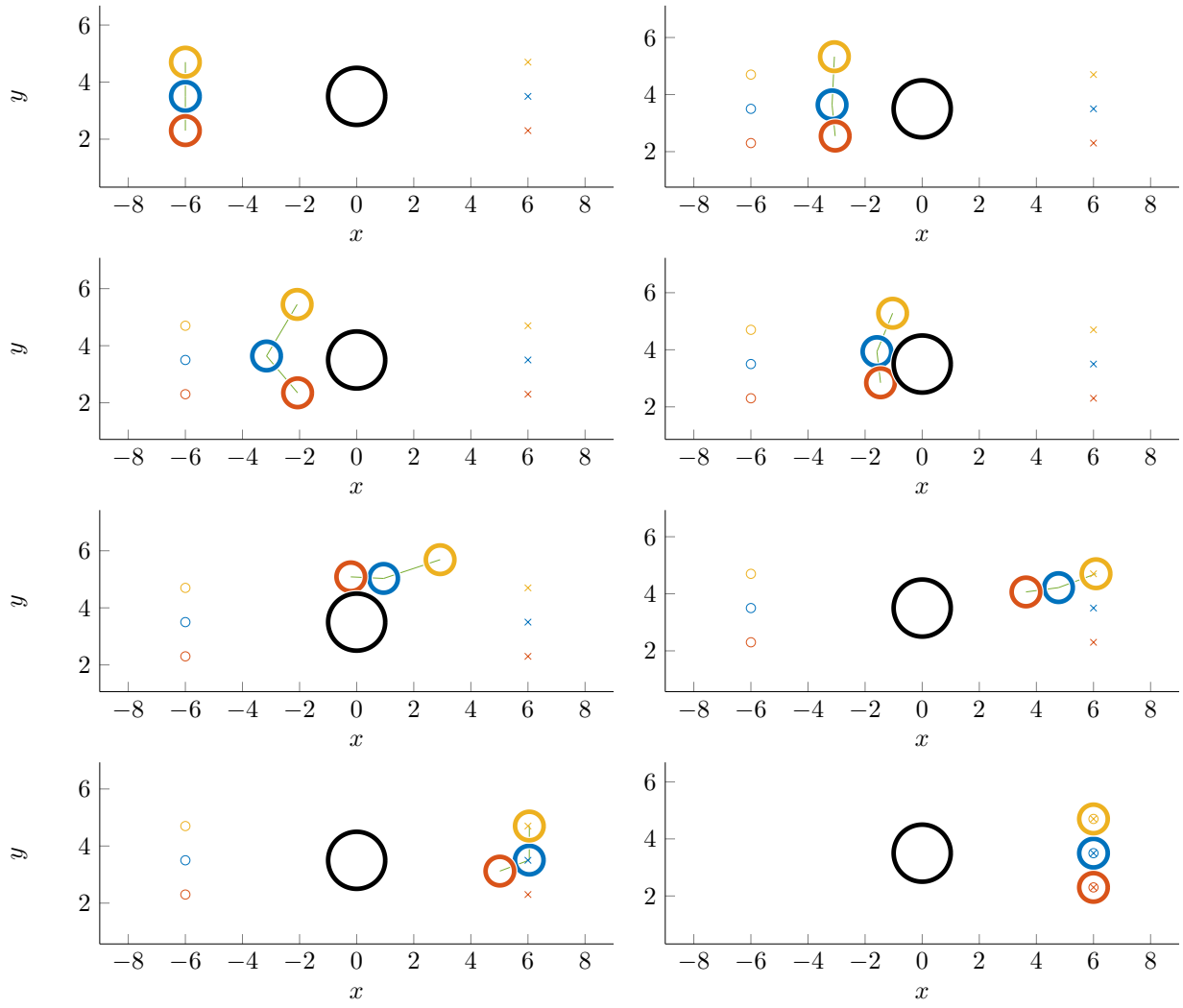

Figure B.16: The trajectories of the three agents in the $x - y$ plane. Agent 1 is with blue, agent 2 with red and agent 3 with yellow. The obstacle is black. Mark O denotes equilibrium configurations. Mark X marks desired configurations.

B.3.2 State errors

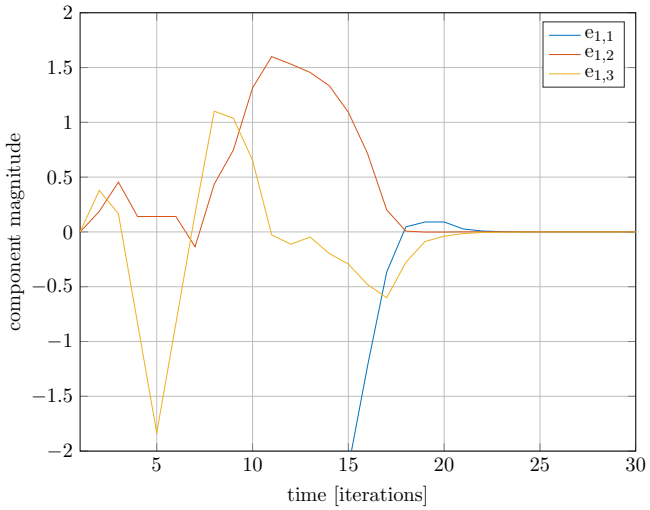

Figure B.17: The evolution of the error states of agent 1 over time.

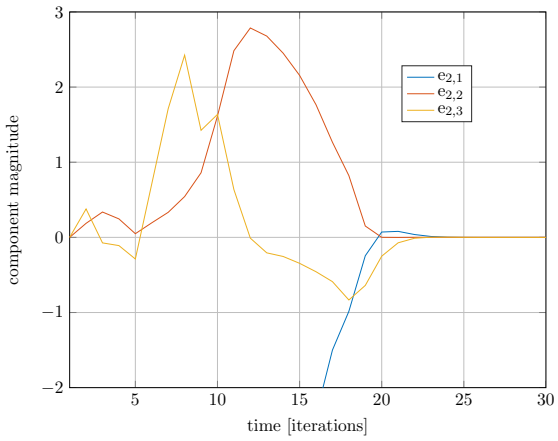

Figure B.18: The evolution of the error states of agent 2 over time.

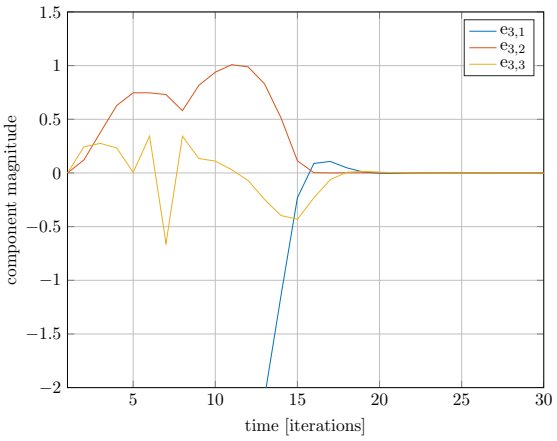

Figure B.19: The evolution of the error states of agent 3 over time.

B.3.3 Distances between actors

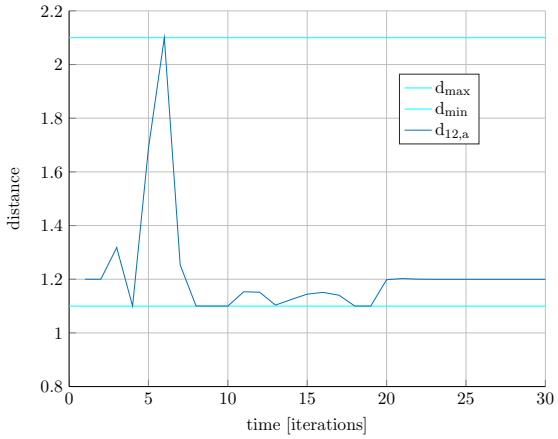

Figure B.20: The distance between agents 1 and 2 over time. The maximum allowed distance has a value of 2.1 and the minimum allowed distance a value of 1.1.

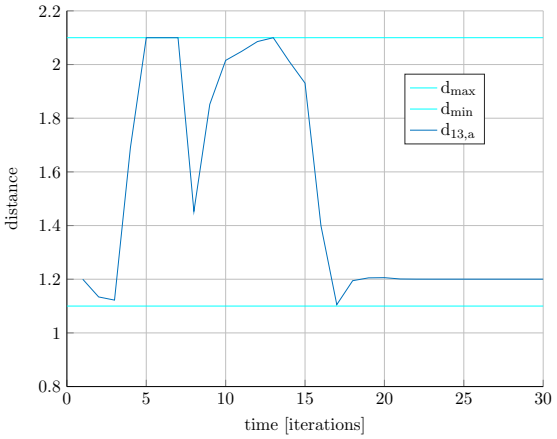

Figure B.21: The distance between agents 1 and 3 over time. The maximum allowed distance has a value of 2.1 and the minimum allowed distance a value of 1.1.

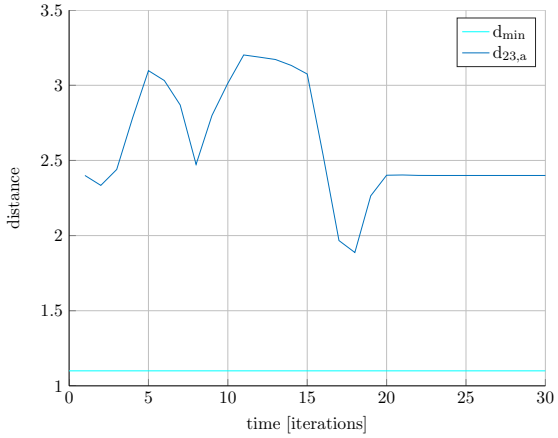

Figure B.22: The distance between agents 2 and 3 over time. The minimum allowed distance a value of 1.1.

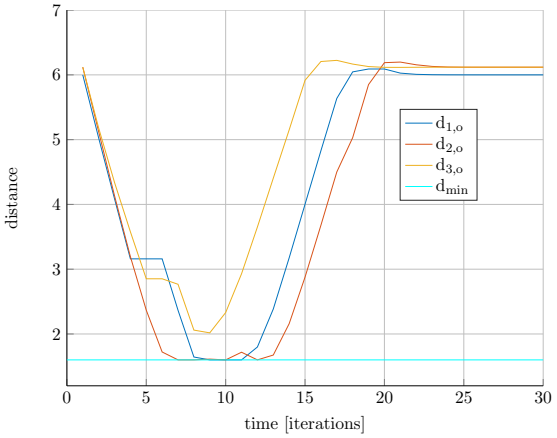

Figure B.23: The distance between each agent and the obstacle over time. The minimum allowed distance has a value of 1.6.

B.3.4 Input signals

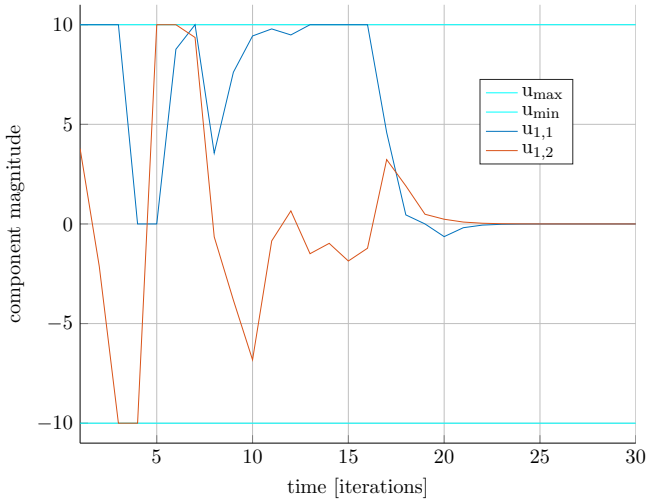

Figure B.24: The inputs signals directing agent 1 over time. Their value is constrained between −10 and 10.

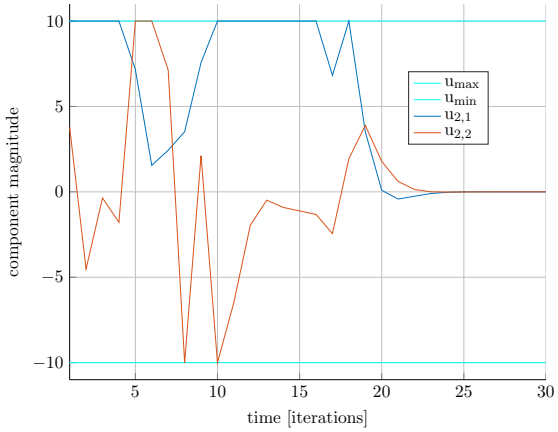

Figure B.25: The inputs signals directing agent 2 over time. Their value is constrained between −10 and 10.

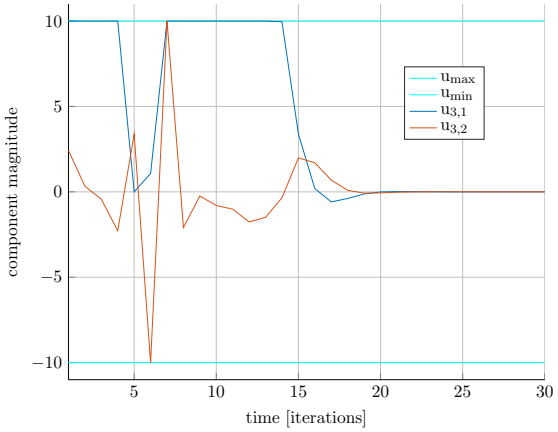

Figure B.26: The inputs signals directing agent 3 over time. Their value is constrained between −10 and 10.

B.4 Test case four: three agents – two obstacles

In this case the initial configurations of the three agents are $\mathbf{z}_1 = [-6, 3.5, 0]^\top$, $\mathbf{z}_2 = [-6, 2.3, 0]^\top$ and $\mathbf{z}_3 = [-6, 4.7, 0]^\top$. Their desired configurations in steady-state are $\mathbf{z}_{1,des} = [6, 3.5, 0]^\top$, $\mathbf{z}_{2,des} = [6, 2.3, 0]^\top$ and $\mathbf{z}_{3,des} = [6, 4.7, 0]^\top$. Obstacles o_1 and o_2 are placed between the two at

$[0, 2.0]^\top$ and $[0, 5.5]^\top$ respectively. The penalty matrices $\boldsymbol{Q}$, $\boldsymbol{R}$, $\boldsymbol{P}$ were set to $\boldsymbol{Q} = 0.5(I_3 + 0.05\dagger_3)$, $\boldsymbol{R} = 0.005 I_2$ and $\boldsymbol{P} = 0.5(I_3 + 0.05\dagger_3)$, where $\dagger_N$ is a $N \times N$ matrix whose elements are chosen at random between the values 0.0 and 1.0.

In subsection B.4.1, frames of the evolution of the trajectories of the three agents are depicted. Subsections B.4.2 and B.4.4 illustrate the evolution of the error states and the input signals of the three agents respectively. Subsection B.4.3 features the figures relating to the evolution of the distance between the three agents along with that between them and the two obstacles.

B.4.1 Trajectories in 2D

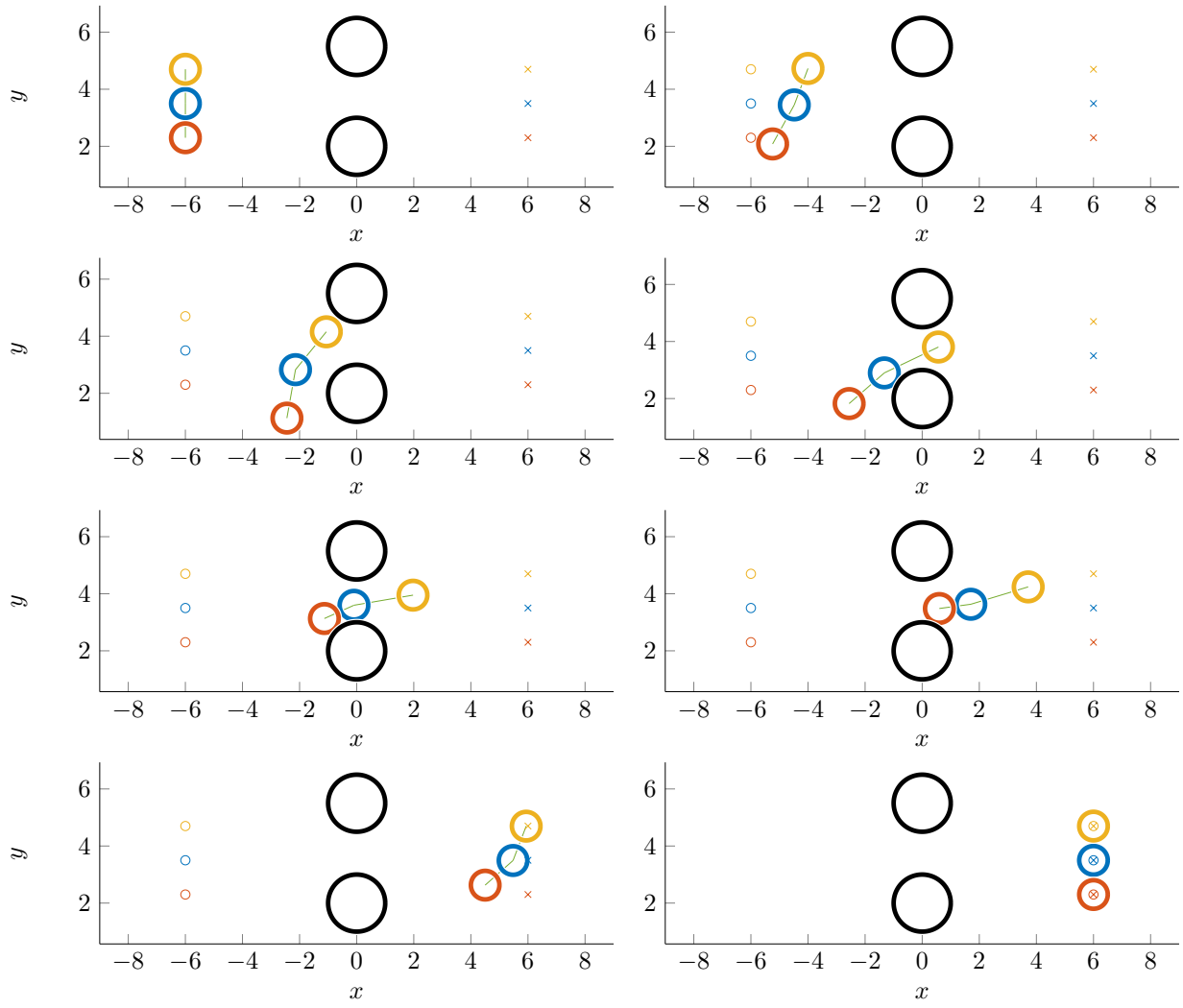

Figure B.27: The trajectories of the three agents in the $x-y$ plane. Agent 1 is with blue, agent 2 with red and agent 3 with yellow. The obstacles are black. Mark O denotes equilibrium configurations. Mark X marks desired configurations.

B.4.2 State errors

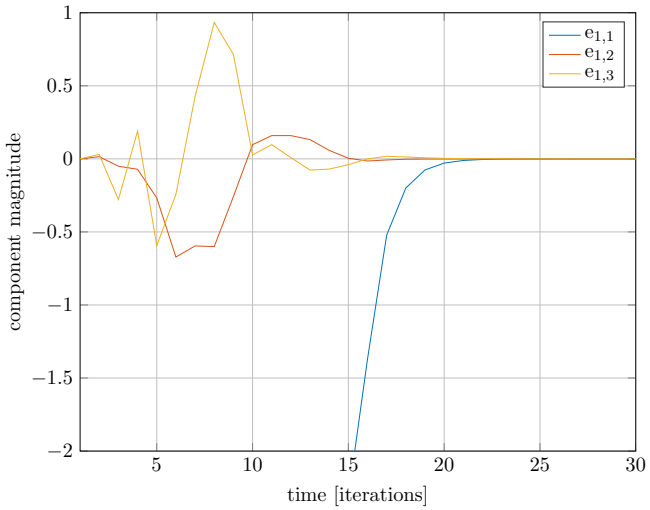

Figure B.28: The evolution of the error states of agent 1 over time.

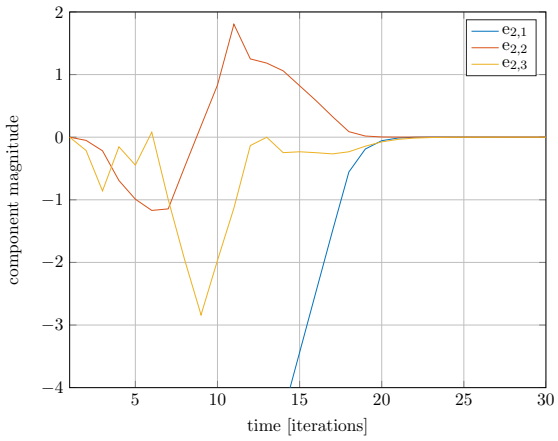

Figure B.29: The evolution of the error states of agent 2 over time.

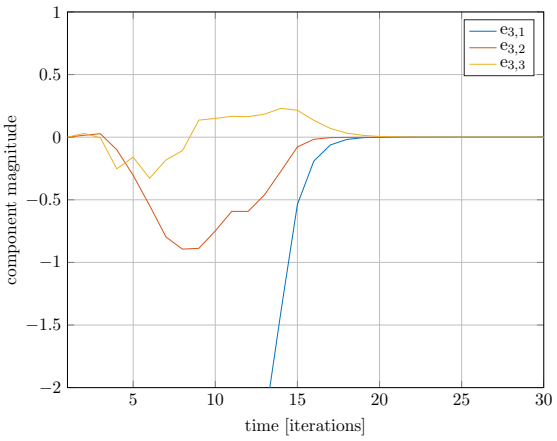

Figure B.30: The evolution of the error states of agent 3 over time.

B.4.3 Distances between actors

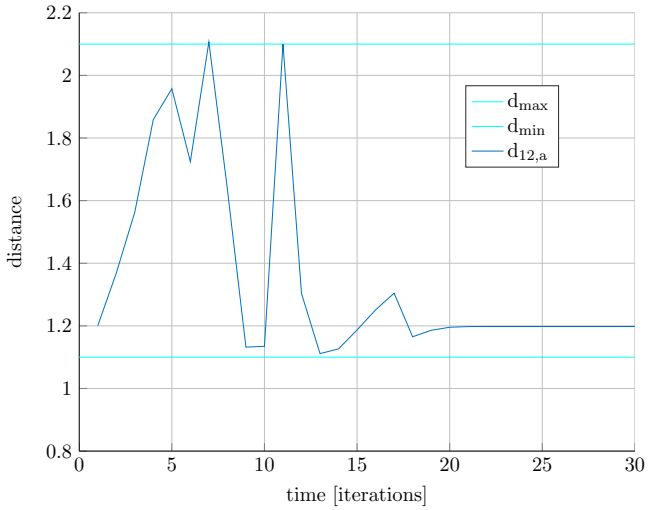

Figure B.31: The distance between agents 1 and 2 over time. The maximum allowed distance has a value of 2.1 and the minimum allowed distance a value of 1.1.

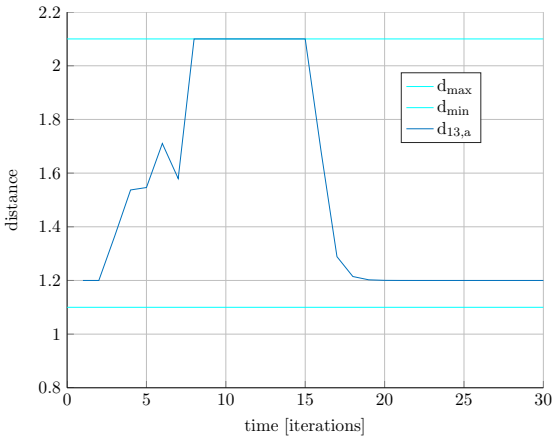

Figure B.32: The distance between agents 1 and 3 over time. The maximum allowed distance has a value of 2.1 and the minimum allowed distance a value of 1.1.

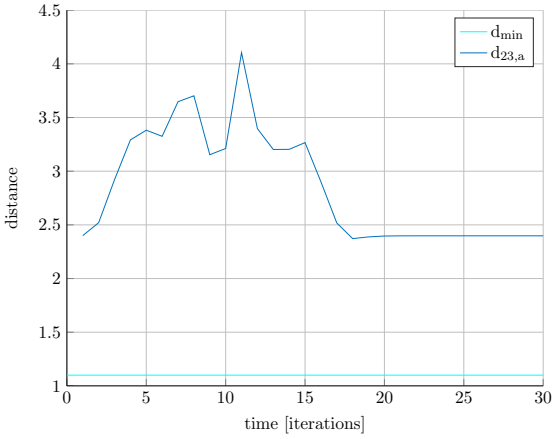

Figure B.33: The distance between agents 2 and 3 over time. The minimum allowed distance a value of 1.1.

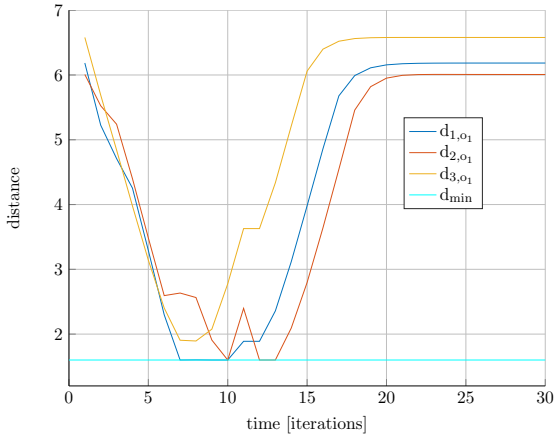

Figure B.34: The distance between each agent and obstacle 1 over time. The minimum allowed distance has a value of 1.6.

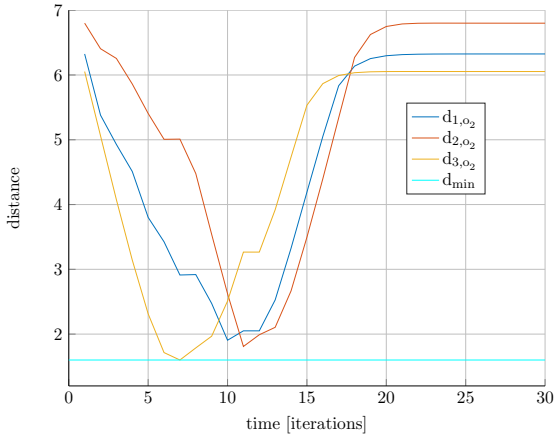

Figure B.35: The distance between each agent and obstacle 2 over time. The minimum allowed distance has a value of 1.6.

B.4.4 Input signals

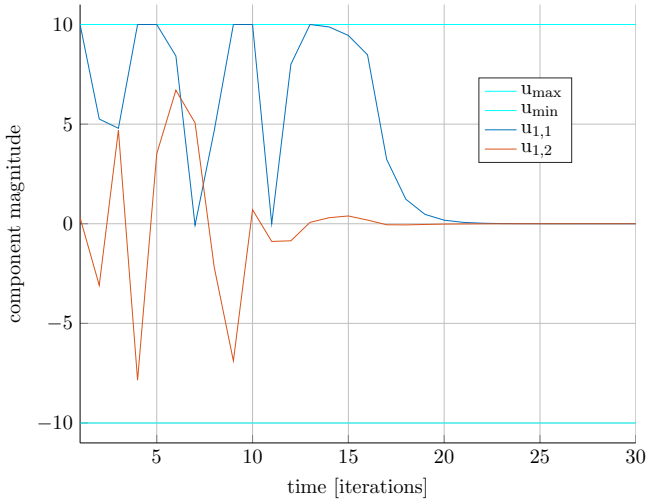

Figure B.36: The inputs signals directing agent 1 over time. Their value is constrained between -10 and 10.

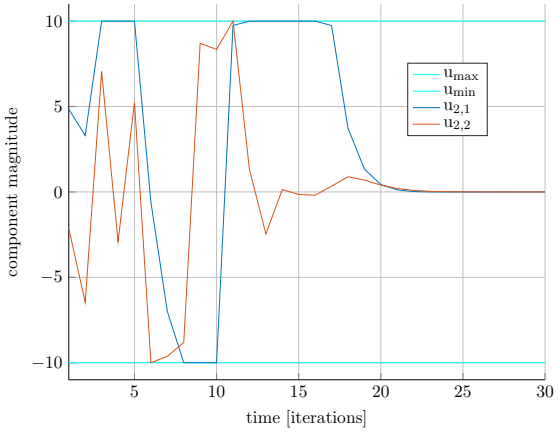

Figure B.37: The inputs signals directing agent 2 over time. Their value is constrained between −10 and 10.

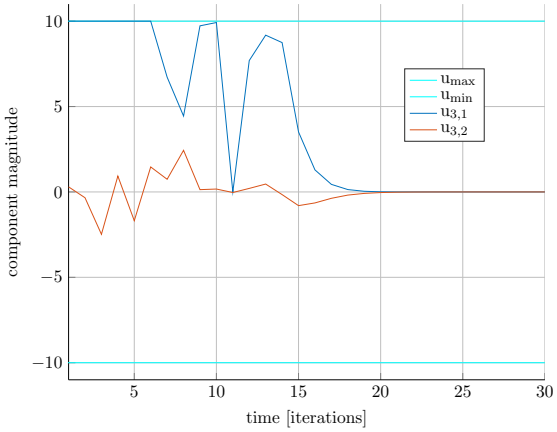

Figure B.38: The inputs signals directing agent 3 over time. Their value is constrained between −10 and 10.

C

Simulation figures – disturbances present

The section with the agents' trajectories is omitted here, as there is nothing interestingly different compared to those in the case where disturbances were absent.

C.1 Test case one: two agents – one obstacle

In this case the initial configurations of the two agents are $\mathbf{z}_1 = [-6, 3.5, 0]^\top$ and $\mathbf{z}_2 = [-6, 2.3, 0]^\top$. Their desired configurations in steady-state are $\mathbf{z}_{1,des} = [6, 3.5, 0]^\top$ and $\mathbf{z}_{2,des} = [6, 2.3, 0]^\top$. The related constants concerned with the execution of this simulation are as follows: $L_{g_i} = 9.073$, $L_{V_i} = 0.0942$, $\varepsilon_{\Psi_i} = 0.0649$ and $\varepsilon_{\Omega_i} = 0.0071$ for all $i \in \mathcal{V}$. The obstacle is placed between the two, at $[0, 2.9]^\top$. The penalty matrices $\boldsymbol{Q}$, $\boldsymbol{R}$, $\boldsymbol{P}$ were set to $\boldsymbol{Q} = 0.5(I_3 + 0.5\dagger_3)$, $\boldsymbol{R} = 0.005 I_2$ and $\boldsymbol{P} = I_3 + 0.5\dagger_3$, where $\dagger_N$ is a $N \times N$ matrix whose elements are chosen at random between the values 0.0 and 1.0.

Subsections C.1.1 and C.1.3 illustrate the evolution of the error states and the input signals of the two agents respectively. Subsection C.1.2 features the figures relating to the evolution of the distance between the two agents along with that between them and the obstacle. Subsection C.1.4 features the evolution of the quadratic function $\mathbf{e}^\top \boldsymbol{P}\mathbf{e}$ through time for all three agents.

C.1.1 State errors

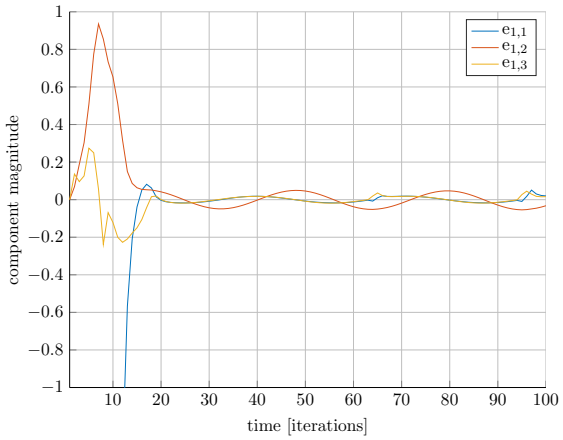

Figure C.1: The evolution of the error states of agent 1 over time.

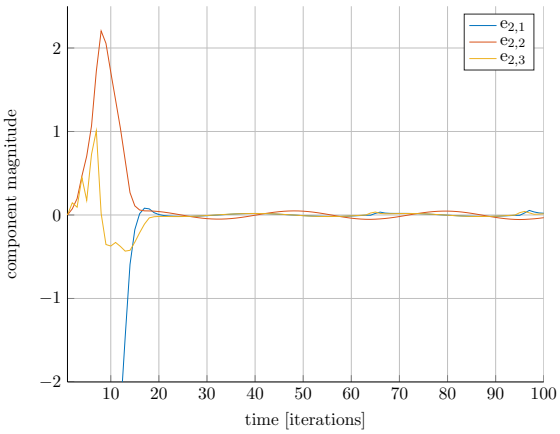

Figure C.2: The evolution of the error states of agent 2 over time.

C.1.2 Distances between actors

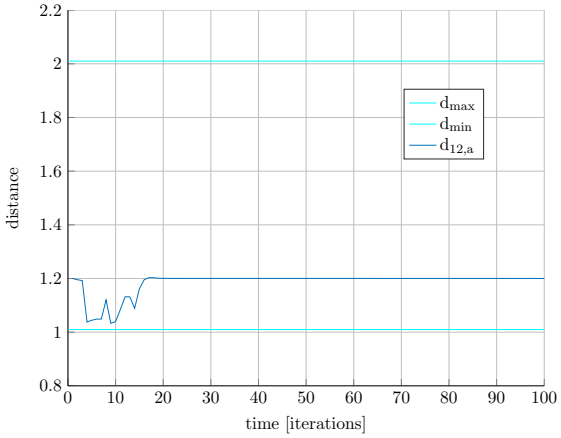

Figure C.3: The distance between the two agents over time. The maximum allowed distance has a value of 2.01 and the minimum allowed distance a value of 1.01.

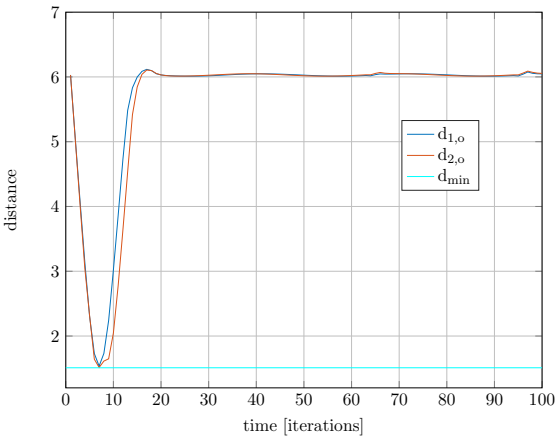

Figure C.4: The distance between each agent and the obstacle over time. The minimum allowed distance has a value of 1.51.

C.1.3 Input signals

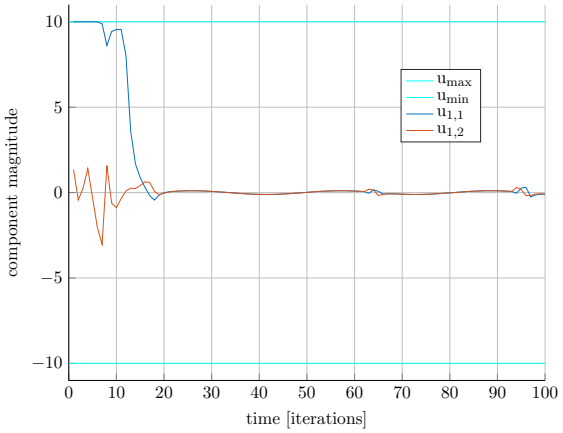

Figure C.5: The inputs signals directing agent 1 over time. Their value is constrained between −10 and 10.

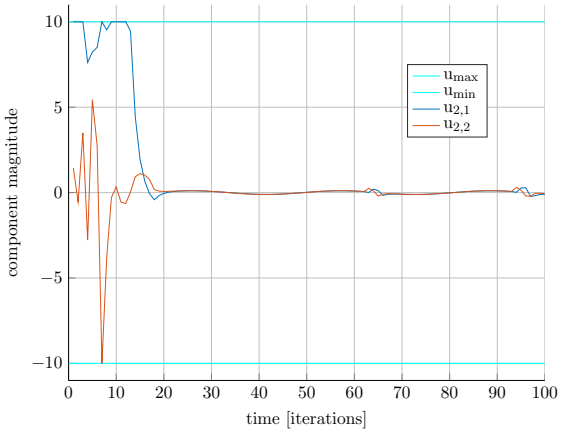

Figure C.6: The inputs signals directing agent 2 over time. Their value is constrained between −10 and 10.

C.1.4 Energy of the system

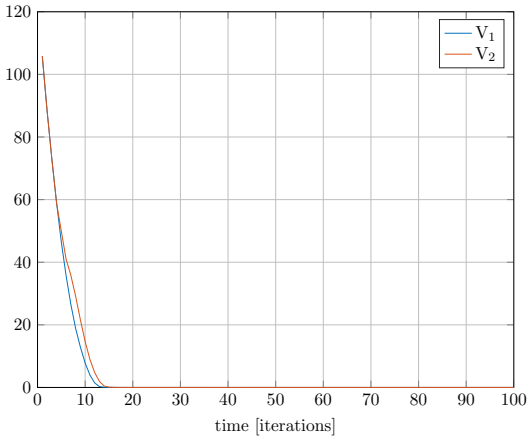

Figure C.7: The $\boldsymbol{P}-$norms of the errors of the three agents through time.

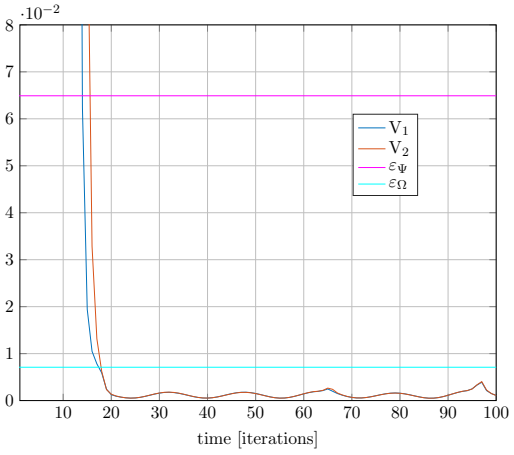

Figure C.8: The $\boldsymbol{P}-$norms of the errors of the three agents through time, focused. The colour magenta is used to illustrate the threshold ε_Ψ, while cyan is used for ε_Ω.

C.2 Test case two: two agents – two obstacles

In this case the initial configurations of the two agents are $\mathbf{z}_1 = [-6, 2.75, 0]^\top$ and $\mathbf{z}_2 = [-6, 4.25, 0]^\top$. Their desired configurations in steady-state are $\mathbf{z}_{1,des} = [6, 2.75, 0]^\top$ and $\mathbf{z}_{2,des} = [6, 4.25, 0]^\top$. Obstacles o_1, 0_2 are placed between the two, at $[0, 1.85]^\top$ and $[0, 5.15]^\top$ respectively. The penalty matrices $\boldsymbol{Q}$, $\boldsymbol{R}$, $\boldsymbol{P}$ were set to $\boldsymbol{Q} = 0.5(I_3 + 0.1\dagger_3)$, $\boldsymbol{R} = 0.005I_2$ and $\boldsymbol{P} = 0.5(I_3 + 0.1\dagger_3)$, where $\dagger_N$ is a $N \times N$ matrix whose elements are chosen at random between the values 0.0 and 1.0. The related constants concerned with the execution of this simulation are as follows: $L_{g_i} = 10.265$, $L_{V_i} = 0.6685$, $\varepsilon_{\Psi_i} = 0.7117$ and $\varepsilon_{\Omega_i} = 0.0035$ for all $i \in \mathcal{V}$.

Subsections C.2.1 and C.2.3 illustrate the evolution of the error states and the input signals of the two agents respectively. Subsection C.2.2 features the figures relating to the evolution of the distance between the two agents along with that between them and the two obstacles. Subsection C.2.4 features the evolution of the quadratic function $\mathbf{e}^\top \boldsymbol{P}\mathbf{e}$ through time for all three agents.

C.2.1 State errors

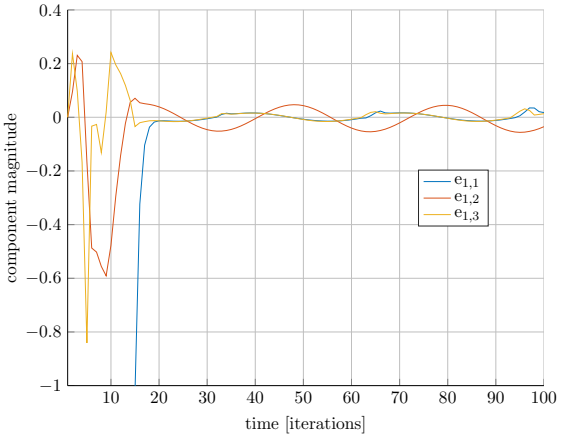

Figure C.9: The evolution of the error states of agent 1 over time.

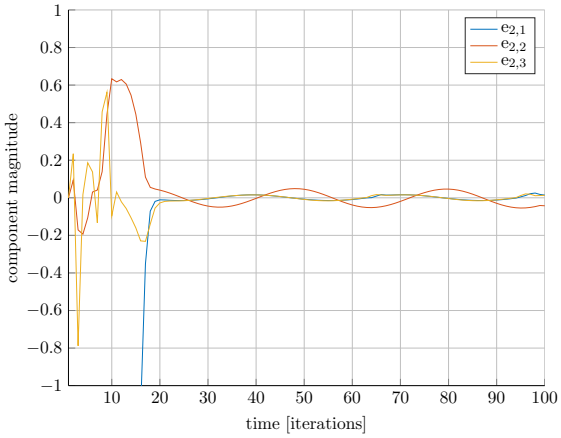

Figure C.10: The evolution of the error states of agent 2 over time.

C.2.2 Distances between actors

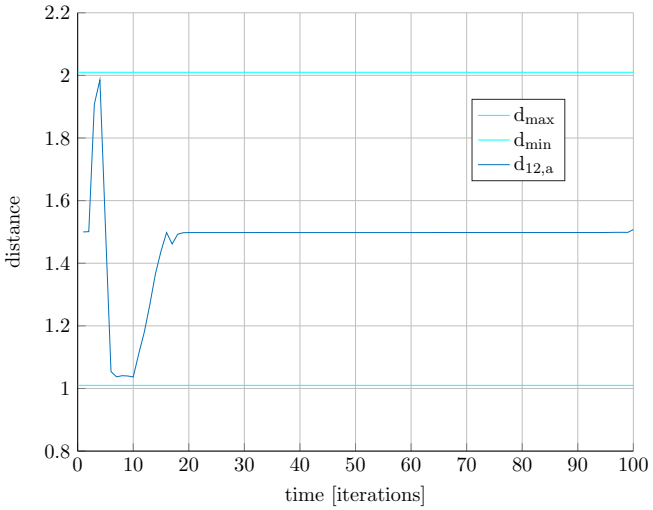

Figure C.11: The distance between the two agents over time. The maximum allowed distance has a value of 2.01 and the minimum allowed distance a value of 1.01.

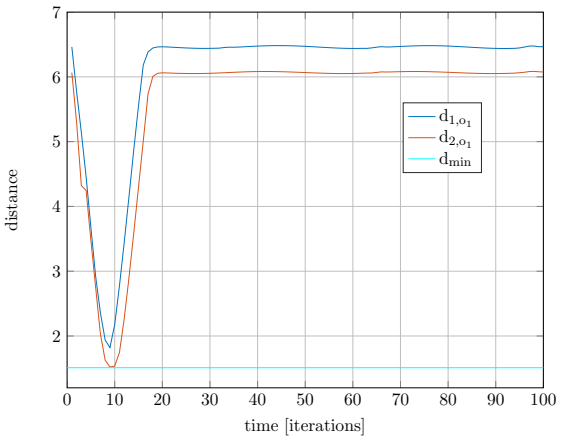

Figure C.12: The distance between each agent and obstacle 1 over time. The minimum allowed distance has a value of 1.51.

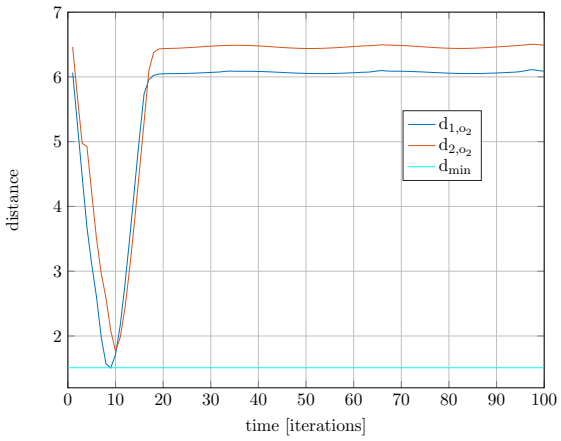

Figure C.13: The distance between each agent and obstacle 2 over time. The minimum allowed distance has a value of 1.51.

C.2.3 Input signals

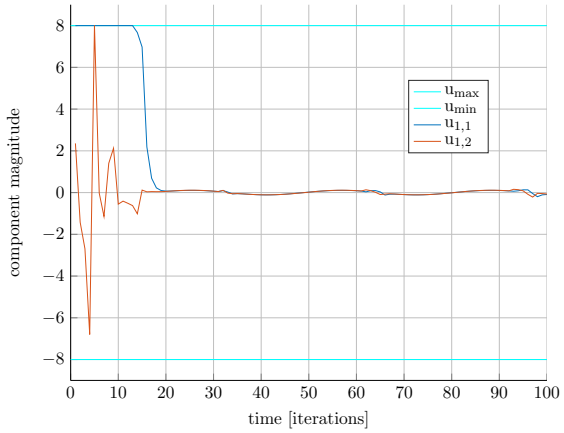

Figure C.14: The inputs signals directing agent 1 over time. Their value is constrained between -8 and 8.

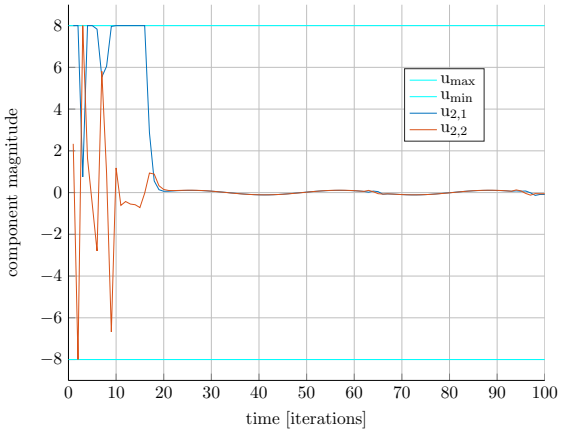

Figure C.15: The inputs signals directing agent 2 over time. Their value is constrained between -8 and 8.

C.2.4 Energy of the system

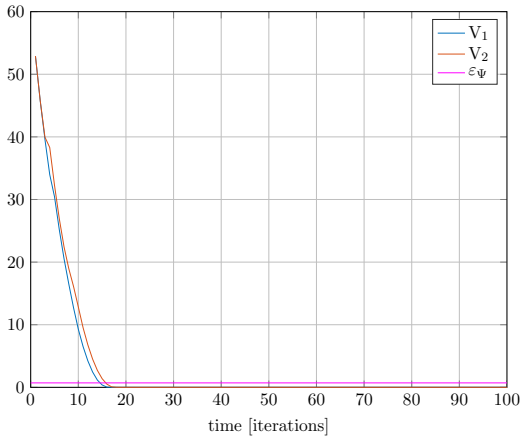

Figure C.16: The $\boldsymbol{P}-$norms of the errors of the three agents through time.

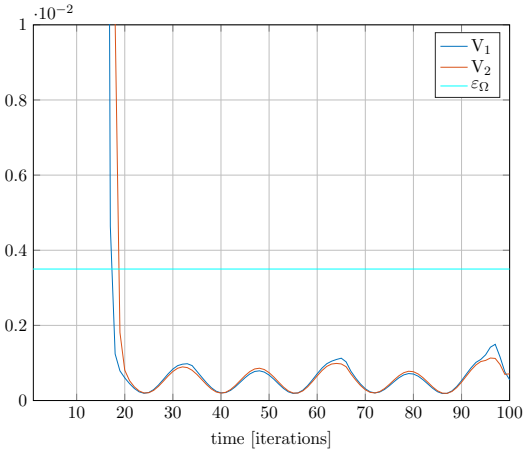

Figure C.17: The $\boldsymbol{P}-$norms of the errors of the three agents through time, focused. The colour cyan is used to illustrate the threshold ε_Ω.

C.3 Test case three: three agents – one obstacle

In this case the initial configurations of the three agents are $\mathbf{z}_1 = [-6, 3.5, 0]^\top$, $\mathbf{z}_2 = [-6, 2.3, 0]^\top$ and $\mathbf{z}_3 = [-6, 4.7, 0]^\top$. Their desired configurations in steady-state are $\mathbf{z}_{1,des} = [6, 3.5, 0]^\top$, $\mathbf{z}_{2,des} = [6, 2.3, 0]^\top$ and $\mathbf{z}_{3,des} = [6, 4.7, 0]^\top$. Obstacle o_1 is placed between the two at $[0, 3.5]^\top$.

The penalty matrices $\boldsymbol{Q}$, $\boldsymbol{R}$, $\boldsymbol{P}$ were set to $\boldsymbol{Q} = 0.5(I_3 + \dagger_3)$, $\boldsymbol{R} = 0.005 I_2$ and $\boldsymbol{P} = 0.5(I_3 + \dagger_3)$, where $\dagger_N$ is a $N \times N$ matrix whose elements are chosen at random between the values 0.0 and 1.0. The related constants concerned with the execution of this simulation are as follows: $L_{g_i} = 12.7758$, $L_{V_i} = 0.1401$, $\varepsilon_{\Psi_i} = 0.4809$ and $\varepsilon_{\Omega_i} = 0.0105$ for all $i \in \mathcal{V}$.

Subsections C.3.1 and C.3.3 illustrate the evolution of the error states and the input signals of the three agents respectively. Subsection C.3.2 features the figures relating to the evolution of the distance between the three agents along with that between them and the obstacle. Subsection C.3.4 features the evolution of the quadratic function $\mathbf{e}^\top \boldsymbol{P} \mathbf{e}$ through time for all three agents.

C.3.1 State errors

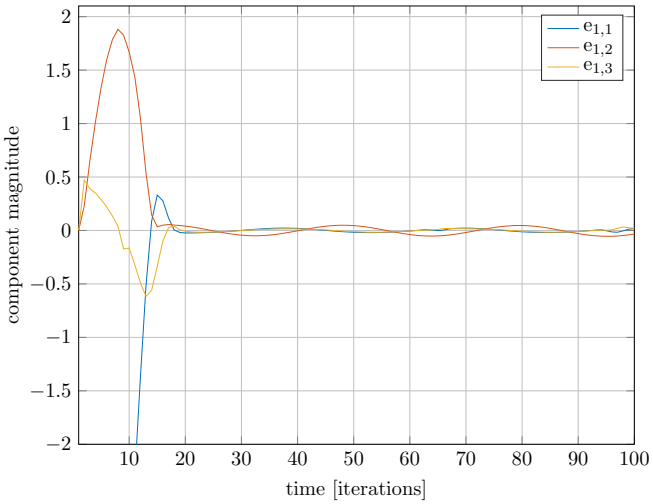

Figure C.18: The evolution of the error states of agent 1 over time.

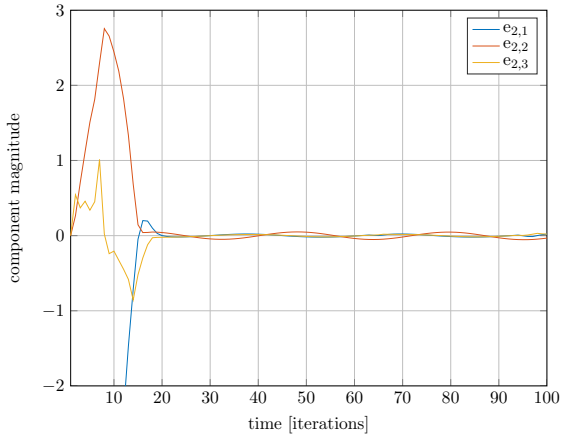

Figure C.19: The evolution of the error states of agent 2 over time.

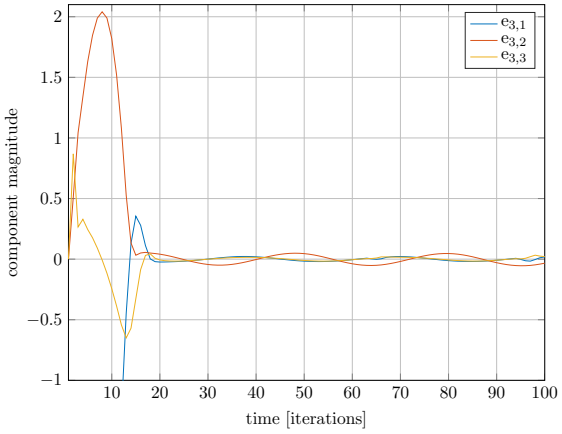

Figure C.20: The evolution of the error states of agent 3 over time.

C.3.2 Distances between actors

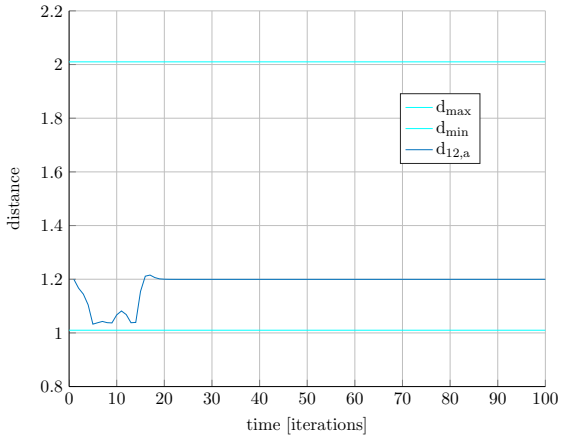

Figure C.21: The distance between agents 1 and 2 over time. The maximum allowed distance has a value of 2.01 and the minimum allowed distance a value of 1.01.

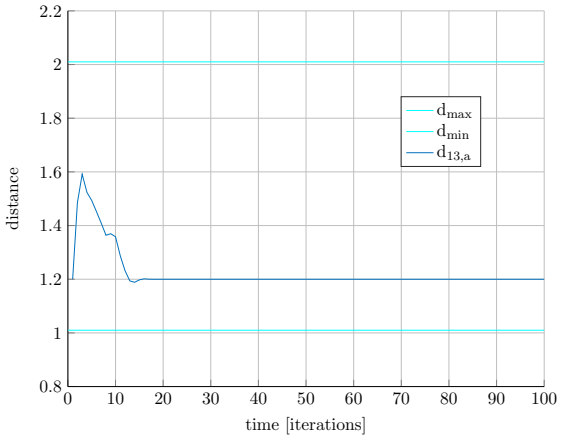

Figure C.22: The distance between agents 1 and 3 over time. The maximum allowed distance has a value of 2.01 and the minimum allowed distance a value of 1.01.

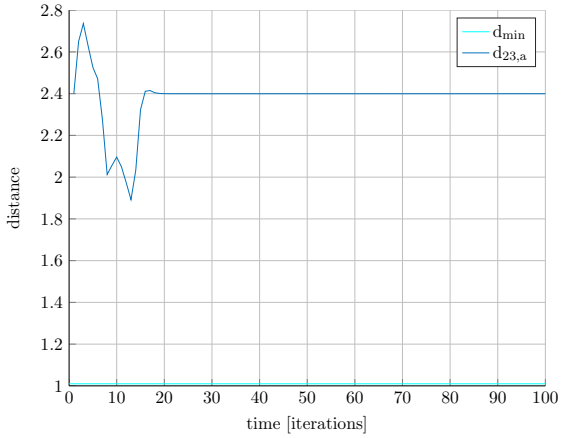

Figure C.23: The distance between agents 2 and 3 over time. The minimum allowed distance a value of 1.01.

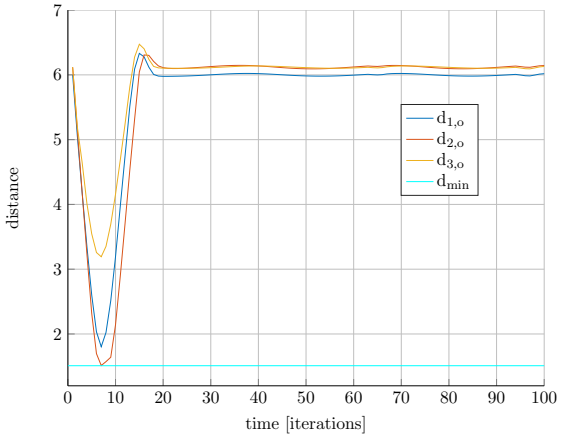

Figure C.24: The distance between each agent and the obstacle over time. The minimum allowed distance has a value of 1.51.

C.3.3 Input signals

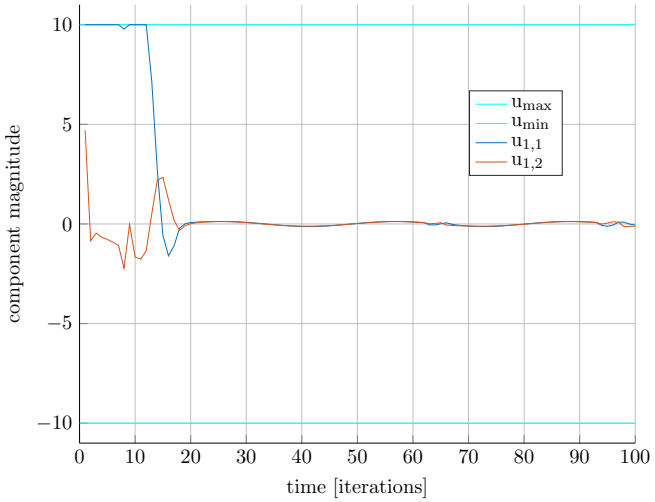

Figure C.25: The inputs signals directing agent 1 over time. Their value is constrained between −10 and 10.

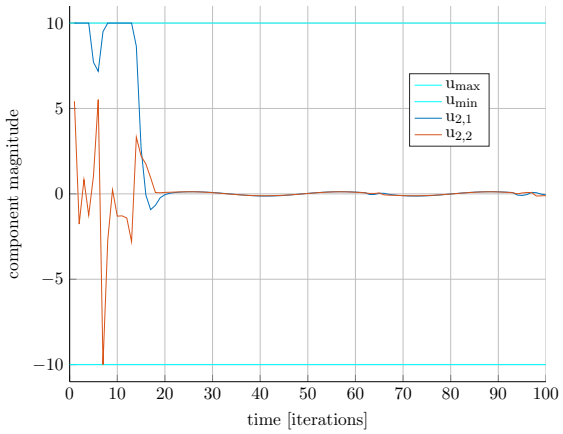

Figure C.26: The inputs signals directing agent 2 over time. Their value is constrained between −10 and 10.

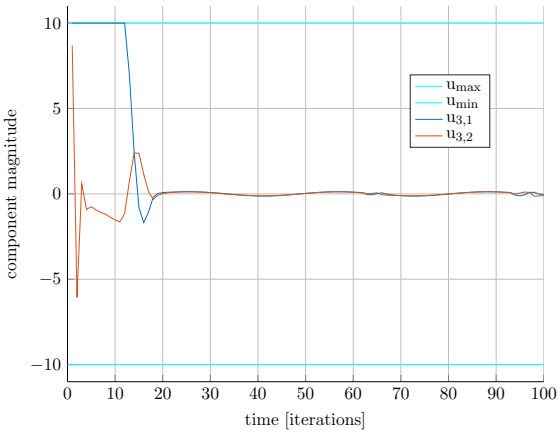

Figure C.27: The inputs signals directing agent 3 over time. Their value is constrained between −10 and 10.

C.3.4 Energy of the system

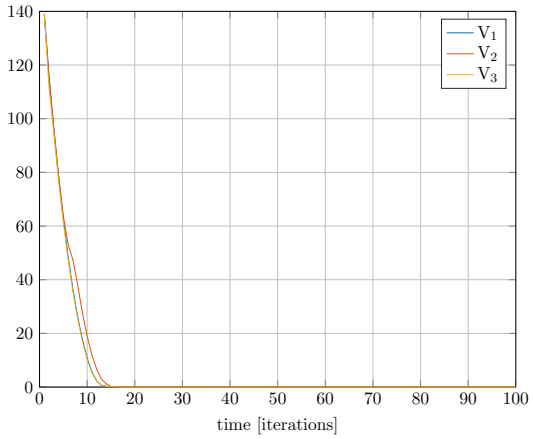

Figure C.28: The $\boldsymbol{P}-$norms of the errors of the three agents through time.

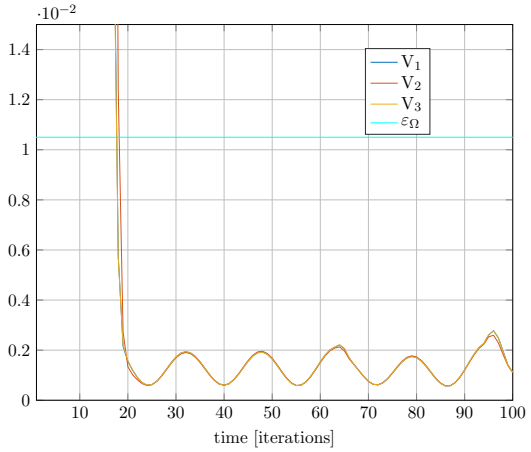

Figure C.29: The $\boldsymbol{P}-$norms of the errors of the three agents through time, focused. The colour cyan is used to illustrate the threshold ε_Ω.

C.4 Test case four: three agents – two obstacles

In this case the initial configurations of the three agents are $\mathbf{z}_1 = [-6, 3.5, 0]^\top$, $\mathbf{z}_2 = [-6, 2.3, 0]^\top$ and $\mathbf{z}_3 = [-6, 4.7, 0]^\top$. Their desired configurations in steady-state are $\mathbf{z}_{1,des} = [6, 3.5, 0]^\top$, $\mathbf{z}_{2,des} = [6, 2.3, 0]^\top$ and $\mathbf{z}_{3,des} = [6, 4.7, 0]^\top$. Obstacles o_1 and o_2 are placed between the two at $[0, 2.0]^\top$ and $[0, 5.5]^\top$ respectively. The penalty matrices $\boldsymbol{Q}$, $\boldsymbol{R}$, $\boldsymbol{P}$ were set to $\boldsymbol{Q} = 0.7(I_3 + 0.5\dagger_3)$, $\boldsymbol{R} = 0.005 I_2$ and $\boldsymbol{P} = 0.5(I_3 + 0.5\dagger_3)$, where $\dagger_N$ is a $N \times N$ matrix whose elements are chosen at random between the values 0.0 and 1.0. The related constants concerned with the execution of this simulation are as follows: $L_{g_i} = 10.7354$, $L_{V_i} = 0.0471$, $\varepsilon_{\Psi_i} = 0.0654$ and $\varepsilon_{\Omega_i} = 0.0035$ for all $i \in \mathcal{V}$.

Subsections C.4.1 and C.4.3 illustrate the evolution of the error states and the input signals of the three agents respectively. Subsection C.4.2 features the figures relating to the evolution of the distance between the three agents along with that between them and the two obstacles. Subsection C.4.4 features the evolution of the quadratic function $\mathbf{e}^\top \boldsymbol{P} \mathbf{e}$ through time for all three agents.

C.4.1 State errors

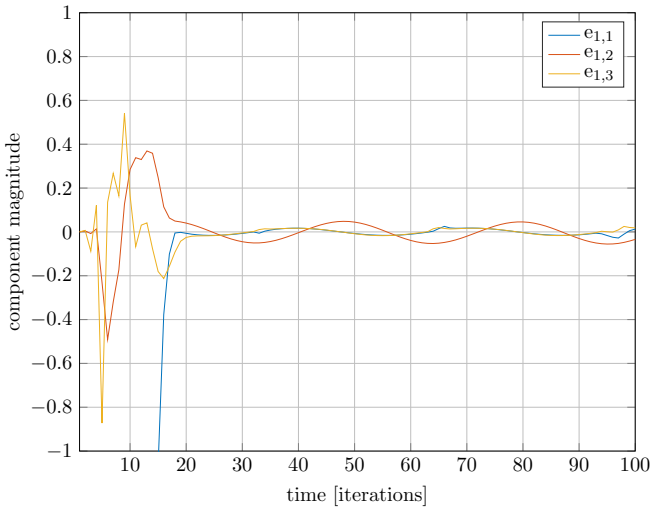

Figure C.30: The evolution of the error states of agent 1 over time.

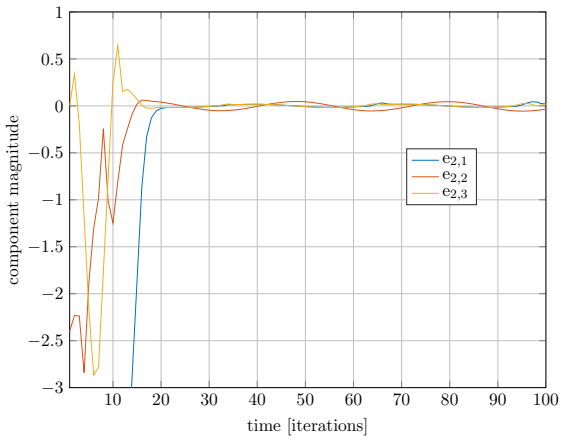

Figure C.31: The evolution of the error states of agent 2 over time.

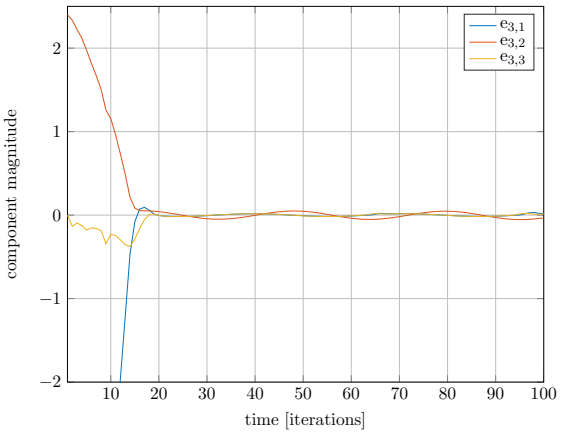

Figure C.32: The evolution of the error states of agent 3 over time.

C.4.2 Distances between actors

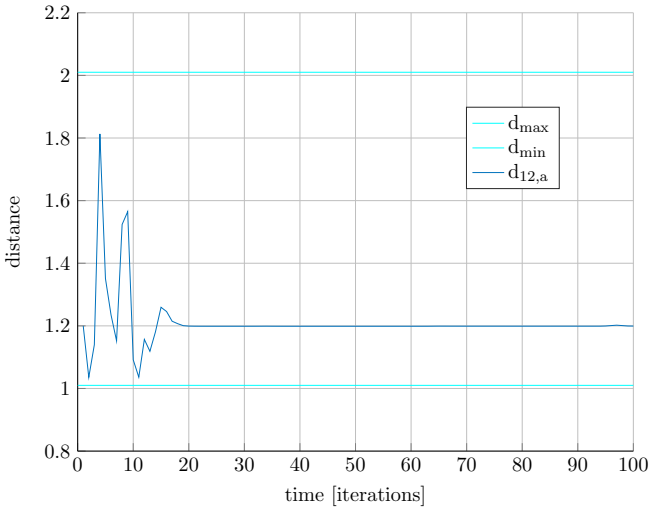

Figure C.33: The distance between agents 1 and 2 over time. The maximum allowed distance has a value of 2.01 and the minimum allowed distance a value of 1.01.

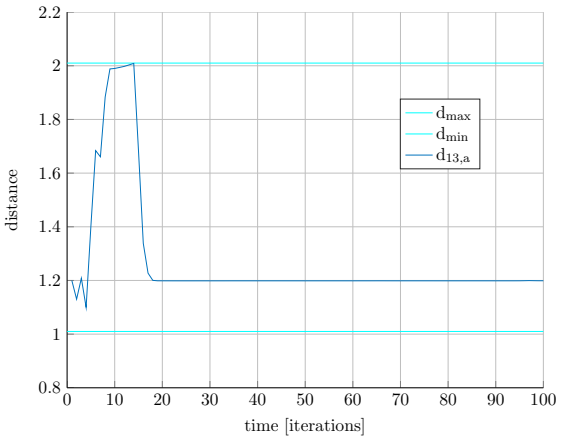

Figure C.34: The distance between agents 1 and 3 over time. The maximum allowed distance has a value of 2.01 and the minimum allowed distance a value of 1.01.

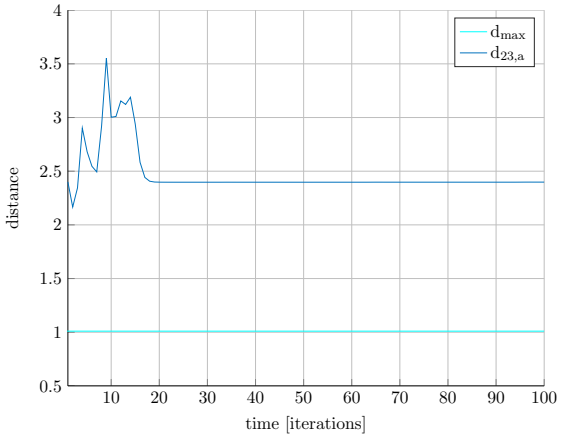

Figure C.35: The distance between agents 2 and 3 over time. The minimum allowed distance a value of 1.01.

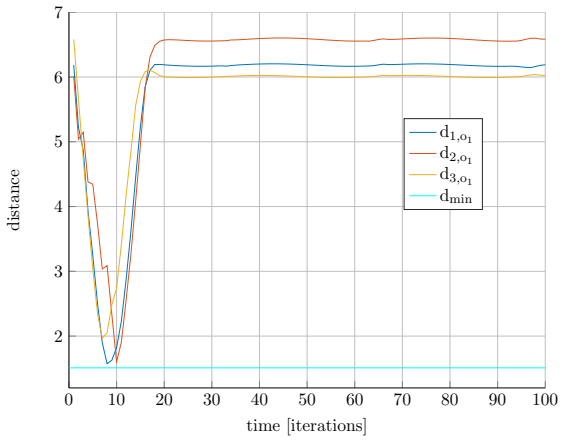

Figure C.36: The distance between each agent and obstacle 1 over time. The minimum allowed distance has a value of 1.51.

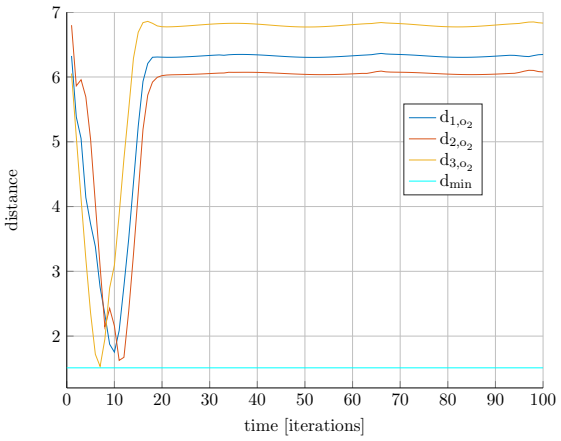

Figure C.37: The distance between each agent and obstacle 2 over time. The minimum allowed distance has a value of 1.51.

C.4.3 Input signals

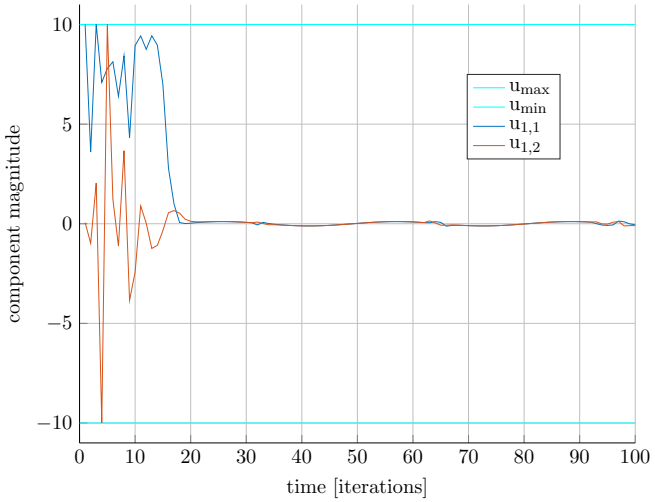

Figure C.38: The inputs signals directing agent 1 over time. Their value is constrained between -10 and 10.

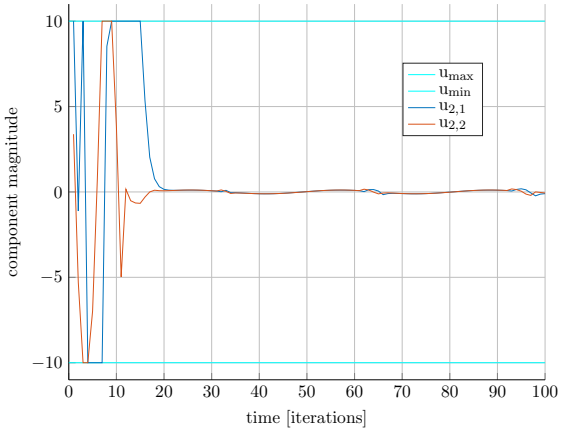

Figure C.39: The inputs signals directing agent 2 over time. Their value is constrained between −10 and 10.

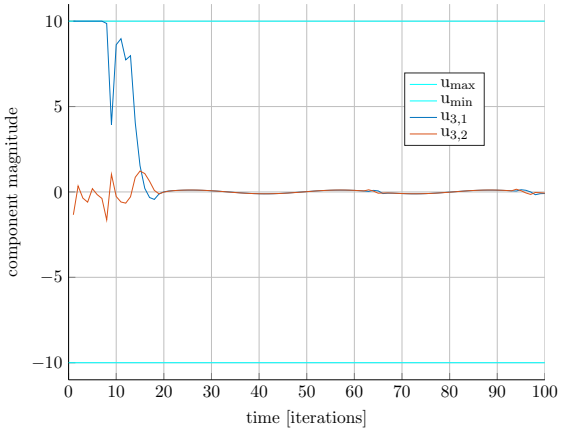

Figure C.40: The inputs signals directing agent 3 over time. Their value is constrained between −10 and 10.

C.4.4 Energy of the system

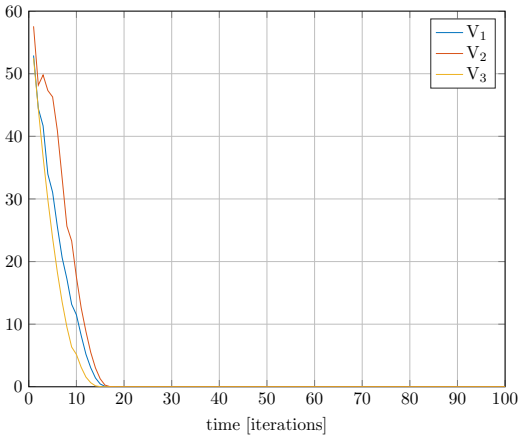

Figure C.41: The $\boldsymbol{P}-$norms of the errors of the three agents through time.

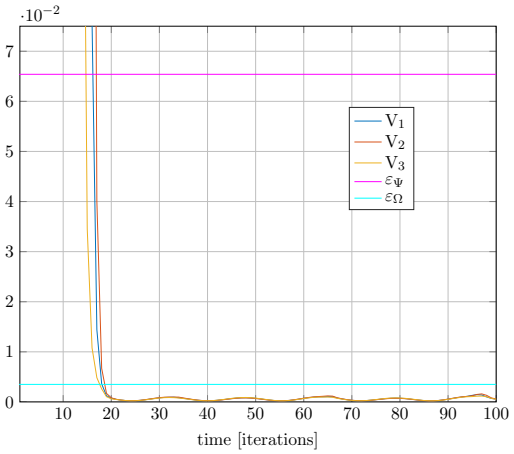

Figure C.42: The $\boldsymbol{P}-$norms of the errors of the three agents through time, focused. The colour magenta is used to illustrate the threshold ε_Ψ, while cyan is used for ε_Ω.

Bibliography

[1] E. Franco, L. Magni, T. Parisini, M. M. Polycarpou, and D. M. Raimondo, "Cooperative constrained control of distributed agents with nonlinear dynamics and delayed information exchange: A stabilizing receding-horizon approach," *IEEE Transactions on Automatic Control*, vol. 53, pp. 324–338, Feb 2008.

[2] "Project iswarm, http://microrobotics.ira.uka.de,"

[3] "Project micron, http://wwwipr.ira.uka.de/micron,"

[4] A. Richards and J. How, "Decentralized model predictive control of cooperating uavs," in *2004 43rd IEEE Conference on Decision and Control (CDC) (IEEE Cat. No.04CH37601)*, vol. 4, pp. 4286–4291 Vol.4, Dec 2004.

[5] W. B. Dunbar and R. M. Murray, "Distributed receding horizon control for multi-vehicle formation stabilization," *Automatica*, vol. 42, no. 4, pp. 549 – 558, 2006.

[6] T. Keviczky, F. Borrelli, K. Fregene, D. Godbole, and G. J. Balas, "Decentralized receding horizon control and coordination of autonomous vehicle formations," *IEEE Transactions on Control Systems Technology*, vol. 16, pp. 19–33, Jan 2008.

[7] D. V. Dimarogonas and K. J. Kyriakopoulos, "Decentralized stabilization and collision avoidance of multiple air vehicles with limited sensing capabilities," in *Proceedings of the 2005, American Control Conference, 2005.*, pp. 4667–4672 vol. 7, June 2005.

[8] R. Findeisen, L. Imsland, F. Allgower, and B. A. Foss, "State and output feedback nonlinear model predictive control: An overview," *European Journal of Control*, vol. 9, no. 2, pp. 190 – 206, 2003.

[9] H. Michalska and D. Q. Mayne, "Robust receding horizon control of constrained nonlinear systems," *IEEE Transactions on Automatic Control*, vol. 38, pp. 1623–1633, Nov 1993.

[10] L. Grüne and J. Pannek, *Nonlinear Model Predictive Control: Theory and Algorithms*. Communications and Control Engineering, Springer International Publishing, 2016.

[11] D. Mayne, J. Rawlings, C. Rao, and P. Scokaert, "Constrained model predictive control: Stability and optimality," *Automatica*, vol. 36, no. 6, pp. 789 – 814, 2000.

[12] D. V. Dimarogonas and K. J. Kyriakopoulos, "A feedback control scheme for multiple independent dynamic non-point agents," *International Journal of Control*, vol. 79, no. 12, pp. 1613–1623, 2006.

[13] S. M. LaValle, *Planning Algorithms*. Cambridge, U.K.: Cambridge University Press, 2006. Available at http://planning.cs.uiuc.edu/.

[14] T. Gustavi, D. V. Dimarogonas, M. Egerstedt, and X. Hu, "Sufficient conditions for connectivity maintenance and rendezvous in leaderfollower networks," *Automatica*, vol. 46, no. 1, pp. 133 – 139, 2010.

[15] A. Richards and J. How, "A decentralized algorithm for robust constrained model predictive control," in *Proceedings of the 2004 American Control Conference*, vol. 5, pp. 4261–4266 vol.5, June 2004.

[16] D. L. Marruedo, T. Alamo, and E. F. Camacho, "Input-to-state stable mpc for constrained discrete-time nonlinear systems with bounded additive uncertainties," in *Proceedings of the 41st IEEE Conference on Decision and Control, 2002.*, vol. 4, pp. 4619–4624 vol.4, Dec 2002.

[17] H. Khalil, *Noninear Systems*. Prentice-Hall, New Jersey, 1996.

[18] F. A. C. C. Fontes, L. Magni, and E. Gyurkovics, *Sampled-Data Model Predictive Control for Nonlinear Time-Varying Systems: Stability and Robustness*, pp. 115–129. Berlin, Heidelberg: Springer Berlin Heidelberg, 2007.

[19] H. Márquez, *Nonlinear Control Systems: Analysis and Design*. Wiley, 2003.

[20] L. Magni, D. M. Raimondo, and R. Scattolini, "Input-to-state stability for nonlinear model predictive control," in *Proceedings of the 45th IEEE Conference on Decision and Control*, pp. 4836–4841, Dec 2006.

[21] I. Kolmanovsky and E. G. Gilbert, "Theory and computation of disturbance invariant sets for discrete-time linear systems," *Mathematical Problems in Engineering*, vol. 4, no. 4, pp. 317–367, 1998.

[22] R. Schneider, *Minkowski addition*, pp. 139–207. Encyclopedia of Mathematics and its Applications, Cambridge University Press, 2013.

TRITA - EE 2017:055
ISSN 1653-5146